

ELECTRON TRANSFER DISSOCIATION

MASS SPECTROMERTY STUDIES

OF PEPTIDES

by

CHANGGENG FENG

CAROLYN J. CASSADY, COMMITTEE CHAIR

GREGORY J. SZULCZEWSKI

LAURA S. BUSENLEHNER

STEPHEN A. WOSKI

YONGHYUN KIM

A DISSERTATION

Submitted in partial fulfillment of the requirements  
for the degree of Doctor of Philosophy  
in the Department of Chemistry  
in the Graduate School of  
The University of Alabama

TUSCALOOSA, ALABAMA

2014

Copyright Changgeng Feng 2014

ALL RIGHTS RESERVED

## ABSTRACT

Electron transfer dissociation (ETD) is an important tandem mass spectrometry technique in peptide and protein sequencing. In the past, ETD experiments have primarily involved basic peptides. A limitation of ETD is the requirement that analytes be at least doubly cationized by electrospray ionization (ESI). In this research, a method has been developed for enhancing protonation of acidic and neutral peptides. This has allowed doubly protonated ions,  $[M+2H]^{2+}$ , to be produced from peptides without basic residues and has enabled their study by ETD. This dissertation includes the first extensive study of non-basic peptides by ETD.

The effects of a basic residue on ETD were investigated using a series of heptapeptides with one lysine, histidine, or arginine residue. The spectra contain primarily  $c''$ - and  $z'$ -ions, which result from cleavage of  $N-C_\alpha$  bonds along the backbone. Almost all of product ions include the basic residue. Enhanced fragmentation occurs on the C-terminal side of the basic residue. Also,  $c_{n-1}''$  formation is enhanced, where  $n$  is the number of residues in the peptide.

Addition of Cr(III) nitrate to a solution of the neutral peptide heptaalanine yields abundant  $[M+2H]^{2+}$  formation by ESI. Eleven metal ions were tested and Cr(III) gave by far the most intense supercharging of peptides. In contrast, Cr(III) does not increase protonation of proteins. Experiments were performed to explore the supercharging mechanism. Addition of Cr(III) to the sample solution was used to produce  $[M+2H]^{2+}$  in the remainder of this research.

Neutral peptides with alkyl side chains were studied by ETD and found to produce  $b$ - and  $c''$ -ions. Two mechanisms are proposed for  $b$ -ion formation, which involves cleavage of

backbone amide (O=C)-N bonds. The length of peptide chain affects ETD fragmentation, but the identity of the alkyl residue has minimal effect.

Acidic peptides with one or two aspartic or glutamic acid residues produce b-, c''- and z'-ions. The mechanism of b-ion formation is probably the same as that for neutral peptides, while c''- and z'-ions result from a radical mechanism involving oxygen atoms on the acidic side chains. For highly acidic heptapeptides, c''- and z'-ions are the major products, which supports a radical mechanism.



## DEDICATION

This thesis is dedicated to my parents, Jiaji Feng and Youmei Qin, and my sisters, Shuchu Feng and Liping Feng, for their love and unconditional support for me throughout my whole life. Without the help from all of them I could not have completed this dissertation.

## LIST OF ABBREVIATIONS AND SYMBOLS

AC	alternating current
ACN	acetonitrile
AI	absolute intensity
Ala	alanine (A)
Arg	arginine (R)
Asp	aspartic acid (D)
bar	unit of pressure
cal	calorie
CID	collision-induced dissociation
Da	Dalton
DC	direct current
DIC	1,3-diisopropylcarbodiimide
DMF	N,N-dimethylformamide
e <sup>-*</sup>	low energy electron
ECD	electron capture dissociation
EM	electron multiplier
ESI	electrospray ionization
ET	electron transfer
ETD	electron transfer dissociation
ETnoD	electron transfer no dissociation
eV	electron volt
FA	formic acid
Fmoc	9-fluorenylmethoxycarbonyl

FT	Fourier transform
g	grams
GB	gas-phase basicity
Glu	glutamic acid
Gly	glycine
H•	hydrogen radical
HCT	high capacity trap
His	histidine
Hobt	1-hydroxybenzotriazole hydrate
HPLC	high performance liquid chromatography
Hz	hertz
ICC	ion charge control
ICR	ion cyclotron resonance
IE	ionization energy
Ile	isoleucine (I)
IRMPD	infrared radiation multiphoton dissociation
J	joule
k	kilo (prefix)
KE	kinetic energy
L	liters
LC	liquid chromatography
Leu	leucine (L)
LMWCr	low-molecular-weight chromium-binding substance
Lys	lysine (K)
μ	micro (prefix)

m	milli (prefix)
m	meter
M	moles/liter (concentration)
MALDI	matrix-assisted laser desorption ionization
MeOH	methanol
Met	Metal
mol	mole(s)
MS	mass spectrometry
MS/MS	tandem mass spectrometry
MS <sup>n</sup>	tandem mass spectrometry
m/z	mass-to-charge ratio
n	nano (prefix)
nanoESI	nanoelectrospray ionization
nCI	negative chemical ionization
NMP	N-methyl-2-pyrrolidinone
-OMe	methyl ester (-OCH <sub>3</sub> )
p	pico (prefix)
pE	pyroglutamate
PIP	piperidine
PTM	Post-translational modification
QIT	quadrupole ion trap
RE	recombination energy
RF	radiofrequency
s	second
SPPS	solid phase peptide synthesis

t	time
TFA	trifluoroacetic acid
TIPS	triisopropyl silane
TOF	time-of-flight
UW	Utah-Washington
Val	valine (V)
V	volt
$\omega$	angular frequency

## ACKNOWLEDGEMENTS

I am pleased to have this opportunity to express my deepest appreciation to my research advisor Dr. Carolyn J. Cassady for her guidance in academics. I have also learned from her professional communication and behavior unique to American culture.

I would like to thank all of my current committee members, Drs. Gregory Szulczewski, Laura Busenlehner, Stephen Woski, and Yonghyun Kim and former committee member Dr. Perry Churchill for their valuable inspiring questions and advice on my academic progress. I would also like to thank Dr. John Vincent for providing me with different metal salts and for help in my research project. I am grateful for the assistance in instrumental electronics from Mr. Billy Atkins. I would like to thank Dr. Qiaoli Liang for training me in use and maintenance of the LC-MS in our department.

The financial support of the National Institutes of Health (grant number 1R15GM109401A) is gratefully acknowledged. Thanks to the National Science Foundation CRIF program for purchasing the Bruker HCTultra PTM discovery system (CHE 0639003).

I would like to thank the current and former group members of Dr. Cassady lab. I am grateful for some of the basic and acidic peptides they left. I enjoy the atmosphere in our office. I would especially thank Chelsea Plummer for checking my English writings and Juliette Commodore for help with the methyl esters experiments.

Finally, I would like to thank my family who never stopped encouraging me and gave me support when I was depressed. I also thank my friends for their help in my daily life. I really appreciate the people who helped me at the University of Alabama.

## TABLE OF CONTENTS

ABSTRACT .....	ii
DEDICATION.....	iv
LIST OF ABBREVIATIONS AND SYMBOLS .....	v
ACKNOWLEDGEMENTS.....	ix
LIST OF TABLES .....	xiv
LIST OF FIGURES .....	xv
CHAPTER 1 AN OVERVIEW OF THE DISSERTATION.....	1
References .....	7
CHAPTER 2 INSTRUMENTATION AND EXPERIMENTAL PROCEDURES .....	13
2.1 Electrospray Ionization/Nanoelectrospray Ionization .....	13
2.2 Quadrupole Ion Trap .....	17
2.3 Dissociation Techniques .....	22
2.3.1 Collision-Induced Dissociation .....	22
2.3.2 Electron Transfer Dissociation .....	23
2.4 Peptide Sequencing Nomenclature .....	26
2.5 Peptide Synthesis .....	27
2.6 Amino Acid Structure .....	30
References .....	34
CHAPTER 3 ELECTRON TRANSFER DISSOCIATION OF BASIC PEPTIDES .....	36
3.1 Introduction.....	36
3.2 Experimental .....	38
3.2.1 Peptides .....	38



3.2.2	Mass Spectrometry .....	39
3.3	Results and Discussion .....	40
3.3.1	Effect of Basic Residue Position on ETD .....	41
3.3.2	Effect of the Identity of the Basic Residue on ETD .....	46
3.3.3	Preferential Cleavages .....	49
3.4	Conclusions .....	53
	References .....	54
CHAPTER 4	THE USE OF CHROMIUM(III) TO SUPERCHARGE PEPTIDES BY PROTONATION AT THE PEPTIDE BACKBONE .....	59
4.1	Introduction .....	59
4.2	Experimental .....	62
4.2.1	Peptides and Reagents .....	62
4.2.2	Mass Spectrometry .....	63
4.3	Results and Discussion .....	64
4.3.1	Effects of Selected Metal Ions on Supercharging of A7 .....	64
4.3.2	Optimal Conditions for Supercharging A7 Using Cr(III) .....	67
4.3.3	Supercharging Other Peptides with Cr(III) .....	68
4.3.4	Comparison of Cr(III) to Organic Supercharging Reagents .....	74
4.3.5	Factors that May Contribute to the Ability of Cr(III) to Supercharge .....	75
4.3.6	The Role of Cr(III)-Peptide Interactions in Supercharging .....	80
4.4	Conclusions .....	83
	References .....	84
CHAPTER 5	ELECTRON TRANSFER DISSOCIATION OF NEUTRAL PEPTIDES WITH ALKYL SIDE CHAINS .....	92

5.1	Introduction.....	92
5.2	Experimental .....	95
5.2.1	Peptides .....	95
5.2.2	Mass Spectrometry .....	96
5.3	Results.....	96
5.4	Discussion .....	100
5.4.1	Effect of the Identity of the Neutral Residue with Alkyl Side Chain on ETD .....	100
5.4.2	Mechanism of b-Ion Formation in ETD of Neutral Peptides .....	100
5.4.3	Effect of Peptide Chain Length on b-Ion Formation .....	121
5.5	Conclusions .....	122
	References .....	124
CHAPTER 6	ELECTRON TRANSFER DISSOCIATION OF ACIDIC PEPTIDES WITHOUT BASIC AMINO ACID RESIDUES .....	129
6.1	Introduction.....	129
6.2	Experimental .....	131
6.2.1	Peptides .....	131
6.2.2	Mass Spectrometry .....	132
6.3	Results and Discussions.....	132
6.3.1	Effects of Glutamic Acid Residues on ETD .....	132
6.3.2	Effects of Aspartic Acid Residues on ETD .....	139
6.3.3	Effects of Overall Peptide Acidity on ETD .....	142
6.4	Conclusions .....	144
	References .....	145
CHAPTER 7	CONCLUDING REMARKS .....	149

## LIST OF TABLES

4.1	Absolute signal intensity for $[M+2H]^{2+}$ from heptaalanine (A7), pH of the solutions, and properties of the metal ions .....	65
5.1	Product ions produced by ETD on $[M+2H]^{2+}$ of peptides with alkyl side chains .....	98
6.1	Product ions produced by ETD on $[M+2H]^{2+}$ of peptides with acidic side chains .....	137

## LIST OF FIGURES

1.1	Peptide sequence nomenclature .....	2
2.1	Diagram of ESI source .....	15
2.2	Schematic depiction of an ESI source operated in positive ion mode .....	16
2.3	Ion transfer from ion source to ion trap. ....	19
2.4	Diagram of a QIT mass analyzer .....	19
2.5	Mathieu stability diagram .....	21
2.6	ETD reaction used to produce peptide fragmentation .....	25
2.7	ETD set-up .....	25
2.8	Fmoc-L-amino acid residue. ....	29
2.9	Peptide methyl esterification reaction .....	29
2.10	Basic amino acids. ....	30
2.11	Neutral amino acids and polar amino acids .....	31
2.12	Acidic amino acids .....	32
3.1	ETD mass spectra of $[M+2H]^{2+}$ from (a) RAAAAAA, (b) ARAAAAA, (c) AAARAAA, (d) AAAAARA, and (e) *AAAAAAR. The asterisk indicates that the N-terminal alanine residue has $^{13}C$ substitution at its methyl side chain .....	42
3.2	ETD mass spectra of $[M+2H]^{2+}$ from (a) K*AAAAAA, (b) AKAAAAA, (c) AAKAAAA, (d) AAAAACA, and (e) AAAAAAK. The asterisk indicates that the first alanine residue has $^{13}C$ substitution at its methyl side chain. ....	43
3.3	ETD mass spectra of $[M+2H]^{2+}$ from (a) HAAAAAA, (b) AHAAAAA, (c) AAHAAAA, (d) AAAAAHA, and (e) AAAAAAH .....	45
3.4	ETD mass spectrum of $[M+2H]^{2+}$ from AAKAAAA. ....	51
3.5	Scheme for $c_{n-1}''$ ion formation from basic peptides .....	52
4.1	ESI mass spectra of solutions containing a 10:1 molar ratio of metal:A7 for: (a) no metal, (b) Cr(III), (c) Zn(II), (d) La(III), and (e) Eu(III). For Figure 4.1(c), the low intensity peak below the arrow labelled “No $[M+2H]^{2+}$ ” is not the ion of interest, but a singly charged impurity.....	66

4.2	ESI mass spectra of the following peptides with Cr(III) added at a 10:1 molar ratio of metal ion to peptide: (a) AGGAAAA, (b) AAAAA (A5), and (c) AAAEAAA.....	69
4.3	ESI mass spectra of AHAAAAA with (a) no Cr(III) and (b) Cr(III) at a 10:1 molar ratio of Cr: AHAAAAA. ....	71
4.4	ESI mass spectra of EEEEGDD with (a) no Cr(III), (b) Cr(III) at a 10:1 molar ratio of Cr:EEEGDD, and (c) ETD on $[M+2H]^{2+}$ produced by addition of Cr(III). ....	73
4.5	The ball-and-stick model of Cr(III) and A7.....	82
5.1	The ETD spectra of $[M+2H]^{2+}$ from (a) AAAAAAA and (b) AAARAAA .....	97
5.2	The ETD spectra of $[M+2H]^{2+}$ from (a) AAIAAAA, (b) AALAAAA, and (c) AAVAAAA. ....	99
5.3	The ETD spectra of $[M+2H]^{2+}$ from (a) AGGAAAAAA, and (b) A14.....	101
5.4	The ETD spectrum of $[M+2H]^{2+}$ from GGAVAAA .....	102
5.5	The ETD spectrum of $[M+2H]^{2+}$ from A13.....	103
5.6	The CID spectrum of $[M+H]^+$ from A7.....	105
5.7	The CID spectra (MS/MS/MS) of $b_6$ produced by (a) ETD on $[M+2H]^{2+}$ on A7 and by (b) CID on $[M+H]^+$ on A7.....	106
5.8	The CID spectra (MS/MS/MS) of $b_4$ produced by (a) ETD on $[M+2H]^{2+}$ on A7 and by (b) CID on $[M+H]^+$ on A7.....	107
5.9	The CID spectra (MS/MS/MS) of $b_5$ produced by (a) ETD on $[M+2H]^{2+}$ on A7 and by (b) CID on $[M+H]^+$ on A7.....	108
5.10	(a) ETD spectrum of $[M+2H]^{2+}$ from AAAAAGA and (b) CID spectrum of $[M+H]^+$ from AAAAAGA.....	109
5.11	The CID spectra (MS/MS/MS) of $b_4$ produced by (a) ETD on $[M+2H]^{2+}$ on AAAAAGA and by (b) CID on $[M+H]^+$ on AAAAAGA. ....	110
5.12	The CID spectra (MS/MS/MS) of $b_5$ produced by (a) ETD on $[M+2H]^{2+}$ on AAAAAGA and by (b) CID on $[M+H]^+$ on AAAAAGA .....	111
5.13	(a) ETD spectrum of $[M+2H]^{2+}$ from AGGAAAA and (b) CID spectrum of $[M+H]^+$ from AGGAAAA .....	112
5.14	The CID spectra (MS/MS/MS) of $b_4$ produced by (a) ETD on $[M+2H]^{2+}$ on AGGAAAA and by (b) CID on $[M+H]^+$ on AGGAAAA .....	113

5.15	The CID spectra (MS/MS/MS) of $b_5$ produced by (a) ETD on $[M+2H]^{2+}$ on AGGAAAA and by (b) CID on $[M+H]^+$ on AGGAAAA .....	114
5.16	The CID spectra (MS/MS/MS) of $b_6$ produced by (a) ETD on $[M+2H]^{2+}$ on AGGAAAA and by (b) CID on $[M+H]^+$ on AGGAAAA .....	115
5.17	(a) ETD spectrum of $[M+2H]^{2+}$ from AGGAAAAA and (b) CID spectrum of $[M+H]^+$ from AGGAAAAA. ....	116
5.18	The CID spectra (MS/MS/MS) of $b_5$ produced by (a) ETD on $[M+2H]^{2+}$ on AGGAAAAA and by (b) CID on $[M+H]^+$ on AGGAAAAA .....	117
5.19	The CID spectra (MS/MS/MS) of $b_6$ produced by (a) ETD on $[M+2H]^{2+}$ on AGGAAAAA and by (b) CID on $[M+H]^+$ on AGGAAAAA .....	118
5.20	The CID spectra (MS/MS/MS) of $b_7$ produced by (a) ETD on $[M+2H]^{2+}$ on AGGAAAAA and by (b) CID on $[M+H]^+$ on AGGAAAAA .....	119
6.1	ETD mass spectra of $[M+2H]^{2+}$ from (a) EAAAEA, (b) AAARAAA, and (c) AAAAAAA.....	134
6.2	ETD mass spectrum of $[M+2H]^{2+}$ from EAAAAE.....	135
6.3	ETD mass spectrum of $[M+2H]^{2+}$ from AAEEAA.....	136
6.4	ETD mass spectra of $[M+2H]^{2+}$ from (a) EAAAAAA, (b) AAEEAAA, and (c) AAAAAAE.....	138
6.5	ETD mass spectra of $[M+2H]^{2+}$ from (a) DAAADA, and (b) AAAADD. ....	140
6.6	ETD mass spectra of $[M+2H]^{2+}$ from (a) DAAAAAA, (b) AAADAAA, and (c) AAAAAAD.....	141
6.7	ETD mass spectra of $[M+2H]^{2+}$ from (a) EEEEGDD, (b) DDDDDDD, and (c) EEEEEEE.....	143

## CHAPTER 1: AN OVERVIEW OF THE DISSERTATION

In September 2011, the Human Proteome Project was started with the aim of characterizing protein products of the human genome.<sup>1</sup> In order to understand protein structure and function, the initial step is to obtain sequence information. Mass spectrometry is a standard analytical tool in the Human Proteome Project to sequence peptides and proteins.<sup>1-6</sup> Tandem mass spectrometry techniques (MS/MS) such as collision-induced dissociation (CID),<sup>7,8</sup> electron capture dissociation (ECD),<sup>9-14</sup> and electron transfer dissociation (ETD)<sup>15-19</sup> are widely used in peptide sequencing of protonated molecular ions. The ability to use MS/MS to provide peptide and protein sequence information has been greatly benefited by fundamental studies of peptide fragmentation mechanisms.<sup>20-28</sup> A recent article in *Nature* reported that tandem mass spectrometry has identified around 84% of proteins from 20,687 annotated human protein coding-genes.<sup>29</sup> In May 2014, a draft of a mass spectrometry based human proteomics database called ProteomicsDB was established.<sup>30</sup>

Today, CID is the main method used in peptide and protein sequence analysis. Development of new dissociation methods is still greatly needed as many peptides are not identified by CID.<sup>31-35</sup> In a study of yeast peptides, only 26,815 peptides out of 162,000 compounds were identified from their MS and MS/MS spectra.<sup>34</sup> The recent development of ECD and ETD could change the situation. ETD is reported as an important method for increasing sequence coverage in the Human Proteome.<sup>29</sup> ECD and ETD provide peptide sequence information that is complementary to CID.<sup>13</sup> ECD and ETD produce c- and z-ions

while CID produces b- and y-ions. (See Figure 1.1 for cleavage nomenclature, which will be discussed in more detail in Chapter 2.) ECD and ETD preserve post-translational modifications (PTMs) by providing little vibrational heating during cleavage. The ETD and ECD processes are faster than CID processes and therefore result in more random non-ergodic cleavage.<sup>13</sup>

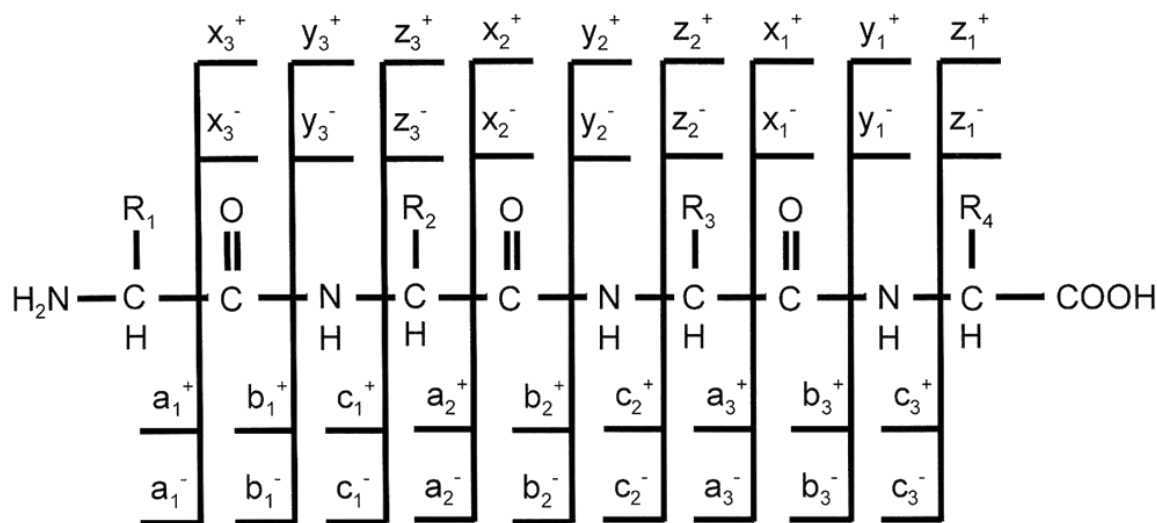


**Figure 1.1.** Peptide sequence nomenclature.

ETD and ECD are electron-based methods that produce primarily c- and z-type fragment ions by random backbone N-C<sub>α</sub> bond cleavages. Although the method with which the precursor ion obtains an electron differs for ECD and ETD, the fragmentation mechanisms and the resulting mass spectra are very similar.<sup>13</sup> ETD and ECD are very promising dissociation techniques in peptide sequencing, but also have limitations. The biggest issue is that ETD can only be used for basic peptides. Non-basic peptides generally do not produce a precursor ion with a charge of +2 or higher. In ETD or ECD, the addition of an electron to a singly positively



charged precursor ion makes the charge neutral and neutral species cannot be detected by mass spectrometry.

Basic residues play important roles in biological processes and in peptide fragmentation. In proteomics, trypsin is an important protease for cleaving protein chains into smaller basic peptides that contain arginine or lysine residues at the C-terminus.<sup>35</sup> These resulting tryptic peptides are mostly sequenced by ETD, ECD or CID.<sup>15,16,36-40</sup> Basic residues (lysine, histidine and arginine) can affect the protonation of a peptide and the fragmentation pathways observed.<sup>22,41-47</sup> The reason is that basic residues have high gas-phase basicities (GBs) and their side chains more readily sequester protons as compared to amide groups on the peptide backbone. Arginine is the most basic residue and therefore is the most able to retain a proton and limit fragmentation.<sup>48,49</sup> With arginine residues, additional energy may be needed to move the hydrogen ion to the peptide backbone and induce dissociation.<sup>42</sup>

The analysis of peptides without basic residues is very important because many peptides with predominately neutral or acidic side chains exist in nature.<sup>50-53</sup> For example, numerous peptides in biological processes such as neurology,<sup>50,54,55</sup> blood coagulation,<sup>51,56</sup> and HIV infection<sup>57</sup> are acidic. In addition, some acidic peptides have been studied to treat HIV<sup>52,53</sup> and malaria.<sup>58</sup> In proteomics, *staphylococcus aureus* V8 protease is widely used to cleave proteins bonds to produce smaller peptides that contain aspartic acid or glutamic acid residues at the C-terminus, while asp-N-protease digests proteins into peptides with aspartic acid or glutamic acid at the N-terminus.<sup>59</sup> Peptides containing acidic residues readily donate protons and are difficult to multiply protonate in the positive ion mode by electrospray ionization (ESI). Therefore these peptides are often limited to analysis by negative ion mode ESI, which is not compatible with ETD because negative ions do not readily accept an electron due to charge repulsion.<sup>60,61</sup>

In peptide and protein sequence analysis using mass spectrometry, it is very important to protonate a molecule in ESI.<sup>62</sup> ESI can produce multiply charged ions that have advantages in the sequencing of peptides and proteins by MS/MS.<sup>2-4</sup> Multiple charging can shift the mass-to-charge ratio ( $m/z$ ) of ions to a range of the spectrum where resolution is optimal<sup>63</sup> and can increase the ion intensity for mass spectrometers in which the signal detected is proportional to charge.<sup>64,65</sup> In addition, for peptides and proteins, higher charge state ions generally require less energy to initiate dissociation and provide more sequence-informative product ions than lower charge state ions.<sup>39,66-68</sup>

Enhanced production of  $[M+2H]^{2+}$  is greatly needed for peptide sequencing by MS/MS. First, ETD and ECD can only be performed for at least doubly protonated ions. Enhanced protonation provides an opportunity to study non-basic peptides by ETD and ECD. Second, for CID,  $[M+2H]^{2+}$  precursor ions produce more structurally-informative product ions than singly protonated ions,  $[M+H]^+$ . This is why the majority of CID studies for peptide sequencing involve  $[M+2H]^{2+}$ .<sup>69,70</sup> Finally, enhanced  $[M+2H]^{2+}$  precursor ion intensity would result in a corresponding increase in the signal-to-noise ratio (S/N) of the MS/MS spectra. In a noisy mass spectrum with low S/N, automated data processing routines have difficulty deciding if a peak corresponds to a real peptide ion. This difficulty in peak recognition becomes a limiting factor in bioinformatics work and may result in a false positive identification for peptides.<sup>71,72</sup>

The studies presented in the dissertation are focused on use of the ETD to obtain sequence information for peptides. This includes work on the mechanism of ETD for basic peptides, the supercharging of non-basic peptides, and extension of the applications of ETD for non-basic peptides (i.e., peptides without arginine, histidine, or lysine residues). The objective

of this research is to enhance the understanding of peptide fragmentation by ETD and expand the applications of ETD to neutral and acidic peptides.

Chapter 2 describes the instrumentation and experimental procedures employed in the research project: (1) electrospray ionization (ESI), (2) nanospray ionization (nanoESI), (3) quadrupole ion trap (QIT) mass analyzer, (4) collision-induced dissociation (CID), (5) electron transfer dissociation (ETD), (6) peptide sequencing nomenclature, (7) peptide synthesis, and (8) structures of amino acids used in this work.

Chapter 3 discusses the effects of basic residue identity and position on the ETD spectra of small peptides. ETD on  $[M+2H]^{2+}$  produces almost exclusively  $c''$  and  $z'$ -ions. Almost all the ETD products ions contain the basic residue, suggesting that the side chains of lysine, histidine, and arginine contain a charge site. Specific side chain cleavages from arginine residues may be useful in identifying arginine residues in peptides. A characteristic of histidine residues is formation of an electron transfer without dissociation product. In general, basic residues promote enhanced cleavage at neighboring N- terminal or C-terminal residues. When a basic residue is located at the N-terminus, a whole series of  $c''$ -ions is produced that may be very useful for peptide sequencing.

Chapter 4 explores the addition of metal salts to solutions of small peptides undergoing ESI. The purpose was to find the optimal conditions for increasing both charge and ion intensity of protonated peptides; this process is known as “supercharging.” The addition of Cr(III) nitrate to peptide solutions in ESI dramatically increases  $[M+2H]^{2+}$  intensity for neutral and acidic peptides that normally produce only  $[M+H]^+$ . For some basic peptides that produce  $[M+2H]^{2+}$  in low abundance, Cr(III) can greatly enhance the signal intensity of  $[M+2H]^{2+}$  and the number of

ions being protonated. The ability of Cr(III) to supercharge small peptides by ESI may prove to be highly useful in peptide analysis and sequencing.

Sequencing and analysis of neutral peptides is important because a large number of peptides are neutral in nature.<sup>39</sup> In proteomics, chymotrypsin protease is widely used to digest proteins into smaller peptides that contain tryptophan, tyrosine or phenylalanine residues at the C-terminus.<sup>59</sup> These resulting peptides are non-basic and difficult to sequence by electron-induced dissociation techniques. In Chapter 5, Cr(III) nitrate is applied to neutral peptide solutions produced by ESI, which allows these peptides to be studied by ETD. Compared to basic peptides, ETD of neutral peptides cleaves at backbone C-N amide bonds to produce b-ions. Two explanations are used to discuss b-ion formation. In addition, peptide chain length can change the fragmentation pathways, but the identity of the alkyl residue has minimal effect on ETD. An understanding of mechanisms for ETD of neutral peptides could extend the use of ETD and provide guidance in peptide sequencing.

In Chapter 6, Cr(III) nitrate is added to solutions of acidic peptides in order to produce  $[M+2H]^{2+}$  for study by ETD. These experiments represent the first investigation of ETD on acidic peptides without basic residues. Small peptides with one or two acidic residues were analyzed in ETD and mainly produce b-, c- and z-series ions. The c- and z-series are produced like basic peptides and b-ion series are produced like neutral peptides. The identity and location of the glutamic acid and aspartic acid residues has minimal effect on ETD. For highly acidic peptides, ETD product ions changed to primarily members of the c- and z-series. These results show that ETD provides abundant sequence information for acidic peptides.

Chapter 7 summarizes the most important aspects of this dissertation work and discusses potential future work.

## References

1. The Call of the Human Proteome. *Nat. Methods* **2010**, 7, 661.
2. Nilsson, T.; Mann, M.; Aebersold, R.; Yates, J. R.; Bairoch, A.; Bergeron, J. J. M. Mass Spectrometry in High-throughput Proteomics: Ready for the Big Time. *Nat. Methods* **2010**, 7, 681-685.
3. Vestal, M. L. The Future of Biological Mass Spectrometry. *J. Am. Soc. Mass Spectrom.* **2011**, 22, 953-959.
4. Kollipara, S.; Agarwal, N.; Varshney, B.; Paliwal, J. Technological Advancements in Mass Spectrometry and Its Impact on Proteomics. *Anal. Lett.* **2011**, 44, 1498-1520.
5. Bogdanov, B.; Smith, R. D. Proteomics by FTICR Mass Spectrometry: Top Down and Bottom Up. *Mass Spectrom. Rev.* **2005**, 24, 168-200.
6. Yates, J. R.; Osterman, A. L. Introduction: Advances in Genomics and Proteomics. *Chem. Rev.* **2007**, 108, 3363-3366.
7. Biemann, K.; Martin, S. A. Mass Spectrometric Determination of the Amino Acid Sequence of Peptides and Proteins. *Mass Spectrom. Rev.* **1987**, 6, 1-76.
8. Papayannopoulos, I. A. The Interpretation of Collision-induced Dissociation Tandem Mass Spectra of Peptides. *Mass Spectrom. Rev.* **1995**, 14, 49-73.
9. McLafferty, F. W.; Horn, D. M.; Breuker, K.; Ge, Y.; Lewis, M. A.; Cerda, B. A.; Zubarev, R. A.; Carpenter, B. K. Electron Capture Dissociation of Gaseous Multiply Charged Ions by Fourier Transform ion Cyclotron Resonance. *J. Am. Soc. Mass Spectrom.* **2001**, 12, 245-249.
10. Zubarev, R. A.; Horn, D. M.; Fridriksson, E. K.; Kelleher, N. L.; Kruger, N. A.; Lewis, M. A.; Carpenter, B. K.; McLafferty, F. W. Electron Capture Dissociation for Structural Characterization of Multiply Charged Protein Cations. *Anal. Chem.* **2000**, 72, 563-573.
11. Zubarev, R. A.; Haselmann, K. F.; Budnik, B.; Kjeldsen, F.; Jensen, F. Towards an Understanding of the Mechanism of Electron-capture Dissociation: A Historical Perspective and Modern Ideas. *Eur. J. Mass Spectrom.* **2002**, 8, 337-349.
12. Yang, H.; Fung, Y. M. E.; Zubarev, A. R.; Zubarev, R. A. The Use of ECD for Proteomics-wide Identification and Quantification of iso-Asp Residues. *Mol. Cell. Proteomics* **2009**, S13-S13.
13. Zubarev, R. A.; Zubarev, A. R.; Savitski, M. M. Electron Capture/Transfer versus Collisionally Activated/Induced Dissociations: Solo or Duet? *J. Am. Soc. Mass Spectrom.* **2008**, 19, 753-761.

14. Liu, H.; Håkansson, K. Abundant b-Type Ions Produced in Electron Capture Dissociation of Peptides Without Basic Amino Acid Residues. *J. Am. Soc. Mass Spectrom.* **2007**, *18*, 2007-2013.
15. Syka, J. E. P.; Coon, J. J.; Schroeder, M. J.; Shabanowitz, J.; Hunt, D. F. Peptide and Protein Sequence Analysis by Electron Transfer Dissociation Mass Spectrometry. *Proc. Natl. Acad. Sci. USA* **2004**, *101*, 9528-9533.
16. Coon, J. J. Collisions or Electrons? Protein Sequence Analysis in the 21st Century. *Anal. Chem.* **2009**, *81*, 3208-3215.
17. Good, D. M.; Wirtala, M.; McAlister, G. C.; Coon, J. J. Performance Characteristics of Electron Transfer Dissociation Mass Spectrometry. *Mol. Cell. Proteomics* **2007**, *6*, 1942-1951.
18. Tureček, F.; Chung, T. W.; Moss, C. L.; Wyer, J. A.; Ehlerding, A.; Holm, A. I. S.; Zettergren, H.; Nielsen, S. B.; Hvelplund, P.; Chamot-Rooke, J.; Bythell, B.; Paizs, B. The Histidine Effect. Electron Transfer and Capture Cause Different Dissociations and Rearrangements of Histidine Peptide Cation-Radicals. *J. Am. Chem. Soc.* **2010**, *132*, 10728-10740.
19. Gunawardena, H. P.; Gorenstein, L.; Erickson, D. E.; Xia, Y.; McLuckey, S. A. Electron Transfer Dissociation of Multiply Protonated and Fixed Charge Disulfide Linked Polypeptides. *Int. J. Mass Spectrom.* **2007**, *265*, 130-138.
20. Wysocki, V. H.; Tsaprailis, G.; Smith, L. L.; Brei, L. A. Special Feature: Commentary - Mobile and Localized Protons: A Framework for Understanding Peptide Dissociation. *J. Mass Spectrom.* **2000**, *35*, 1399-1406.
21. Paizs, B.; Suhai, S. Fragmentation Pathways of Protonated Peptides. *Mass Spectrom. Rev.* **2005**, *24*, 508-548.
22. Tang, X.; Thibault, P.; Boyd, R. K. Fragmentation Reactions of Multiply-Protonated Peptides and Implications for Sequencing by Tandem Mass Spectrometry with Low-Energy Collision-Induced Dissociation. *Anal. Chem.* **1993**, *65*, 2824-2834.
23. Johnson, R. S.; Martin, S. A.; Biemann, K. Collision-induced Fragmentation of (M+H)<sup>+</sup> Ions of Peptides. Side Chain Specific Sequence Ions. *Int. J. Mass Spectrom. Ion Proc.* **1988**, *86*, 137-154.
24. Sullivan, A. G.; Brancia, F. L.; Tyldesley, R.; Bateman, R.; Sidhu, K.; Hubbard, S. J.; Oliver, S. G.; Gaskell, S. J. The Exploitation of Selective Cleavage of Singly Protonated Peptide Ions Adjacent to Aspartic Acid Residues Using a Quadrupole Orthogonal Time-of-Flight Mass Spectrometer Equipped with a Matrix-assisted Laser Desorption/Ionization Source. *Int. J. Mass Spectrom.* **2001**, *210/211*, 665-676.

25. Polce, M. J.; Ren, D.; Wesdemiotis, C. Dissociation of the Peptide Bond in Protonated Peptides. *J. Mass Spectrom.* **2000**, *35*, 1391-1398.
26. Chawner, R.; Eyers, C. E.; Gaskell, S. J. The influence of a C-terminal basic residue on peptide fragmentation pathways. *Int. J. Mass Spectrom.* **2012**, *316–318*, 284-291.
27. Boyd, R.; Somogyi, Á. The Mobile Proton Hypothesis in Fragmentation of Protonated Peptides: A Perspective. *J. Am. Soc. Mass Spectrom.* **2010**, *21*, 1275-1278.
28. Laskin, J.; Yang, Z.; Song, T.; Lam, C.; Chu, I. K. Effect of the Basic Residue on the Energetics, Dynamics, and Mechanisms of Gas-phase Fragmentation of Protonated Peptides. *J. Am. Chem. Soc.* **2010**, *132*, 16006-16016.
29. Kim, M.; Pinto, S. M.; Getnet, D.; Nirujogi, R. S.; Manda, S. S.; Chaerkady, R.; Madugundu, A. K.; Kelkar, D. S.; Isserlin, R.; Jain, S.; Thomas, J. K.; Muthusamy, B.; Leal-Rojas, P.; Kumar, P.; Sahasrabudhe, N. A.; Balakrishnan, L.; Advani, J.; George, B.; Renuse, S.; Selvan, L. D. N.; Patil, A. H.; Nanjappa, V.; Radhakrishnan, A.; Prasad, S.; Subbannayya, T.; Raju, R.; Kumar, M.; Sreenivasamurthy, S. K.; Marimuthu, A.; Sathe, G. J.; Chavan, S.; Datta, K. K.; Subbannayya, Y.; Sahu, A.; Yelamanchi, S. D.; Jayaram, S.; Rajagopalan, P.; Sharma, J.; Murthy, K. R.; Syed, N.; Goel, R.; Khan, A. A.; Ahmad, S.; Dey, G.; Mudgal, K.; Chatterjee, A.; Huang, T.; Zhong, J.; Wu, X.; Shaw, P. G.; Freed, D.; Zahari, M. S.; Mukherjee, K. K.; Shankar, S.; Mahadevan, A.; Lam, H.; Mitchell, C. J.; Shankar, S. K.; Satishchandra, P.; Schroeder, J. T.; Sirdeshmukh, R.; Maitra, A.; Leach, S. D.; Drake, C. G.; Halushka, M. K.; Prasad, T. S. K.; Hruban, R. H.; Kerr, C. L.; Bader, G. D.; Iacobuzio-Donahue, C.; Gowda, H.; Pandey, A. A Draft Map of the Human Proteome. *Nature* **2014**, *509*, 575-581.
30. Wilhelm, M.; Schlegl, J.; Hahne, H.; Gholami, A. M.; Lieberenz, M.; Savitski, M. M.; Ziegler, E.; Butzmann, L.; Gessulat, S.; Marx, H.; Mathieson, T.; Lemeer, S.; Schnatbaum, K.; Reimer, U.; Wenschuh, H.; Mollenhauer, M.; Slotta-Huspenina, J.; Boese, J.; Bantscheff, M.; Gerstmair, A.; Faerber, F.; Kuster, B. Mass-spectrometry-based Draft of the Human Proteome. *Nature* **2014**, *509*, 582-587.
31. McLuckey, S. A.; Mentinova, M. Ion/neutral, Ion/electron, Ion/photon, and Ion/ion Interactions in Tandem Mass Spectrometry: Do We Need Them All? Are They Enough? *J. Am. Soc. Mass Spectrom.* **2011**, *22*, 3-12.
32. Lubec, G.; Afjehi-Sadat, L. Limitations and Pitfalls in Protein Identification by Mass Spectrometry. *Chem. Rev.* **2007**, *107*, 3568-3584.
33. Cottingham, K. Name that Peptide. *Anal. Chem.* **2004**, *76*, 95A.
34. Peng, J.; Elias, J. E.; Thoreen, C. C.; Licklider, L. J.; Gygi, S. P. Evaluation of Multidimensional Chromatography Coupled with Tandem Mass Spectrometry (LC/LC-MS/MS) for Large-Scale Protein Analysis: The Yeast Proteome. *J. Proteome Res.* **2003**, *2*, 43-50.

35. Tabb, D. L.; Huang, Y.; Wysocki, V. H.; Yates, J. R. Influence of Basic Residue Content on Fragment Ion Peak Intensities in Low-energy Collision-induced Dissociation Spectra of Peptides. *Anal. Chem.* **2004**, *76*, 1243-1248.
36. Bensadek, D.; Monigatti, F.; Steen, J. A. J.; Steen, H. Why b, y's? Sodiation-induced Tryptic Peptide-like Fragmentation of Non-tryptic Peptides. *Int. J. Mass Spectrom.* **2007**, *268*, 181-189.
37. Sun, R.; Dong, M.; Song, C.; Chi, H.; Yang, B.; Xiu, L.; Tao, L.; Jing, Z.; Liu, C.; Wang, L.; Fu, Y.; He, S. Improved Peptide Identification for Proteomic Analysis Based on Comprehensive Characterization of Electron Transfer Dissociation Spectra. *J. Proteome Res.* **2010**, *9*, 6354-6367.
38. Kalli, A.; Håkansson, K. Electron Capture Dissociation of Highly Charged Proteolytic Peptides from Lys N, Lys C and Glu C Digestion. *Mol. BioSyst.* **2010**, *6*, 1668-1681.
39. Kjeldsen, F.; Giessing, A. M. B.; Ingrell, C. R.; Jensen, O. N. Peptide Sequencing and Characterization of Post-Translational Modifications by Enhanced Ion-Charging and Liquid Chromatography Electron-Transfer Dissociation Tandem Mass Spectrometry. *Anal. Chem.* **2007**, *79*, 9243-9252.
40. Coon, J. J.; Syka, J. E. P.; Shabanowitz, J.; Hunt, D. F. Tandem Mass Spectrometry for Peptide and Protein Sequence Analysis. *BioTechniques* **2005**, *38*, 519-523.
41. Vachet, R. W.; Asam, M. R.; Glish, G. L. Secondary Interactions Affecting the Dissociation Patterns of Arginine-Containing Peptide Ions. *J. Am. Chem. Soc.* **1996**, *118*, 6252-6256.
42. Wysocki, V. H.; Tsapralis, G.; Smith, L. L.; Brexi, L. A. Mobile and Localized Protons: A Framework for Understanding Peptide Dissociation. *J. Mass Spectrom.* **2000**, *35*, 1399-1406.
43. Tureček, F.; Chung, T. W.; Moss, C. L.; Wyer, J. A.; Ehlerding, A.; Holm, A. I. S.; Zettergren, H.; Nielsen, S. B.; Hvelplund, P.; Chamot-Rooke, J.; Bythell, B.; Paizs, B. The Histidine Effect. Electron Transfer and Capture Cause Different Dissociations and Rearrangements of Histidine Peptide Cation-Radicals. *J. Am. Chem. Soc.* **2010**, *132*, 10728-10740.
44. Tsybin, Y. O.; Haselmann, K. F.; Emmett, M. R.; Hendrickson, C. L.; Marshall, A. G. Charge Location Directs Electron Capture Dissociation of Peptide Dications. *J. Am. Soc. Mass Spectrom.* **2006**, *17*, 1704-1711.
45. Pu, D.; Clipston, N. L.; Cassady, C. J. A Comparison of Positive and Negative Ion Collision-induced Dissociation for Model Heptapeptides with One Basic Residue. *J. Mass Spectrom.* **2010**, *45*, 297-305.
46. Summerfield, S. G.; Gaskell, S. J. Fragmentation Efficiencies of Peptide Ions Following Low Energy Collisional Activation. *Int. J. Mass Spectrom. Ion Proc.* **1997**, *165*, 509-521.



47. Zhang, X.; Jai-Nhuknan, J.; Cassady, C. J. Collision-induced Dissociation and Post-source Decay of Model Dodecapeptide Ions Containing Lysine and Glycine. *Int. J. Mass Spectrom.* **1997**, *171*, 135-145.
48. Chen, X.; Tureček, F. The Arginine Anomaly: Arginine Radicals are Poor Hydrogen Atom Donors in Electron Transfer Induced Dissociations. *J. Am. Chem. Soc.* **2006**, *128*, 12520-12530.
49. Xia, Y.; Gunawardena, H. P.; Erickson, D. E.; McLuckey, S. A. Effects of Cation Charge-Site Identity and Position on Electron-Transfer Dissociation of Polypeptide Cations. *J. Am. Chem. Soc.* **2007**, *129*, 12232-12243.
50. Pierotti, A. R.; Prat, A.; Chesneau, V.; Gaudoux, F.; Leseney, A. M.; Foulon, T.; Cohen, P. N-Arginine Dibasic Convertase, a Metalloendopeptidase as a Prototype of a Class of Processing Enzymes. *Proc. Natl. Acad. Sci. USA* **1994**, *91*, 6078-6082.
51. Ebert, R. F.; Bell, W. R. Assay of Human Fibrinopeptides by High-Performance Liquid Chromatography. *Anal. Biochem.* **1985**, *148*, 70-78.
52. Nara, P. L.; Hwang, K. M.; Rausch, D. M.; Lifso, J. D.; Eiden, L. E. CD4 Antigen-based Antireceptor Peptides Inhibit Infectivity of Human Immunodeficiency Virus In Vitro at Multiple Stages of the Viral Life Cycle. *Proc. Natl. Acad. Sci. USA* **1989**, *86*, 7139-7143.
53. Lifson, J. D.; Hwang, K. M.; Nara, P. L.; Fraser, B.; Padgett, M.; Dunlop, N. M.; Eiden, L. E. Synthetic CD4 Peptide Derivatives that Inhibit HIV Infection and Cytopathicity. *Science* **1988**, *241*, 712-716.
54. Lemaire, S.; Yamashiro, D.; Rao, A. J.; Li, C. H. Synthesis and Biological Activity of beta-Melanotropins and Analogs. *J. Med. Chem.* **1977**, *20*, 155-158.
55. Tatemoto, K. Neuropeptide Y: Complete Amino Acid Sequence of the Brain Peptide. *Proc. Natl. Acad. Sci. USA* **1982**, *79*, 5485-5489.
56. Voet, D.; Voet, J. G. *Biochemistry*; John Wiley & Sons: New York, 1995.
57. Chan, D. C.; Kim, P. S. HIV Entry and Its Inhibition. *Cell* **1998**, *93*, 681-684.
58. Chougnet, C.; Troye-Blomberg, M.; Deloron, P.; Kabilan, L.; Lepers, J. P.; Savel, J.; Perlmann, P. Human Immune Response in Plasmodium Falciparum Malaria. Synthetic Peptides Corresponding to Known Epitopes of the Pf155/RESA Antigen Induce Production of Parasite-specific Antibodies in Vitro. *J. Immunol.* **1991**, *147*, 2295-2301.
59. Nelson, D. L.; Cox, M. M., Eds. In *Lehninger Principles of Biochemistry*; W. H. Freeman: New York, 2004.

60. Madsen, J. A.; Kaoud, T. S.; Dalby, K. N.; Brodbelt, J. S. 193-nm Photodissociation of Dingly and Multiply Vharged Peptide Anions for Acidic Proteome Characterization. *Proteomics* **2011**, *11*, 1329-1334.
61. Ewing, N. P.; Cassady, C. J. Dissociation of Multiply-charged Negative Ions for Hirudin (54-65), Fibrinopeptide B, and Insulin A (Oxidized). *J. Am. Soc. Mass Spectrom.* **2001**, *12*, 105-116.
62. Fenn, J. B.; Mann, M.; Meng, C. K.; Wong, S. F. Electrospray Ionization--Principles and Practice. *Mass Spectrom. Rev.* **1990**, *9*, 37-70.
63. Marshall, A. G.; Hendrickson, C. L. Charge Reduction Lowers Mass Resolving Power for Isotopically Resolved Electrospray ionization Fourier Transform Ion Cyclotron Resonance Mass Spectra. *Rapid Commun. Mass Spectrom.* **2001**, *15*, 232-235.
64. Marshall, A. G.; Hendrickson, C. L. High-Resolution Mass Spectrometers. *Ann. Rev. Anal. Chem.* **2008**, *1*, 579-599.
65. Perry, R. H.; Cooks, R. G.; Noll, R. J. Orbitrap Nass Spectrometry: Instrumentation, Ion Motion and Applications. *Mass Spectrom. Rev.* **2008**, *27*, 661-699.
66. Dongre, A. R.; Jones, J. L.; Somogyi, A.; Wysocki, V. H. Influence of Peptide Composition, Gas-Phase Basicity, and Chemical Modification on Fragmentation Efficiency: Evidence for the Mobile Proton Model. *J. Am. Chem. Soc.* **1996**, *118*, 8365-8374.
67. Wells, J. M.; Stephenson Jr., J. L.; McLuckey, S. A. Charge Dependence of Protonated Insulin Decompositions. *Int. J. Mass Spectrom.* **2000**, *203*, A1-A9.
68. Madsen, J. A.; Brodbelt, J. S. Comparison of Infrared Multiphoton Dissociation and Collision-Induced Dissociation of Supercharged Peptides in Ion Traps. *J. Am. Soc. Mass Spectrom.* **2009**, *20*, 349-358.
69. Savitski, M. M.; Faelth, M.; Fung, Y. M. E.; Adams, C. M.; Zubarev, R. A. Bifurcating Fragmentation Behavior of Gas-Phase Tryptic Peptide Dications in Collisional Activation. *J. Am. Soc. Mass Spectrom.* **2008**, *19*, 1755-1763.
70. Faelth, M.; Savitski, M. M.; Nielsen, M. L.; Kjeldsen, F.; Andren, P. E.; Zubarev, R. A. SwedCAD, a Database of Annotated High-Mass Accuracy MS/MS Spectra of Tryptic Peptides. *J. Proteome Res.* **2007**, *6*, 4063-4067.
71. Aebersold, R.; Mann, M. Mass Spectrometry-based Proteomics. *Nature* **2003**, *422*, 198-207.
72. Michalski, A.; Cox, J.; Mann, M. More than 100,000 Detectable Peptide Species Elute in Single Shotgun Proteomics Runs but the Majority is Inaccessible to Data-Dependent LC-MS/MS. *J. Proteome Res.* **2011**, *10*, 1785-1793.

## CHAPTER 2: INSTRUMENTATION AND EXPERIMENTAL PROCEDURES

All mass spectra in this dissertation were acquired by a Bruker (Billerica, MA, USA) HCTultra PTM Discovery System equipped with ESI. This chapter will discuss the general principles of the mass spectrometry used in this work: ionization techniques, quadrupole ion trap, and dissociation techniques. Then, solid phase peptide synthesis, structures of the amino acid residues under study, and peptide sequencing nomenclature will be described.

### 2.1 Electrospray Ionization/Nanoelectrospray Ionization

Mass spectrometry analyses are based on gas-phase ions, which is due to the fact that mass-to-charge ( $m/z$ ) analysis only works for charged particles. The movement of ions is easy to control experimentally. Varying the electric and magnetic fields can control the energy and velocity of ions, which in turn provides separation by  $m/z$  and detection. There are many different gas-phase ionization techniques. Electrospray ionization (ESI) is a very important ionization technique for characterization of large biomolecules.<sup>1</sup> ESI was first used by Malcom Dole<sup>2</sup> in 1968, and later developed by John Fenn<sup>3,4</sup> in the 1980s. Fenn won the Nobel Prize in Chemistry in 2002 for the development of ESI. ESI is a very soft ionization technique because it gives negligible fragmentation. The most important feature of ESI is the production of multiply charged ions,  $[M+nH]^{n+}$  or  $[M-nH]^{n-}$ , from large molecules. Positive multiply charged ions are especially useful in electron transfer dissociation (ETD) studies.

Electrospray ionization (ESI) is a process involving a fine spray of charged droplets in the presence of a strong electric field. The solvent is evaporated to allow the charged drops to convert into gas-phase ions. A sample is dissolved in a solvent that usually consists of a mixture of water, acetonitrile, or methanol. Depending on the desired ionization polarity, 0.1-2% (v/v) of additives such as acetic acid, formic acid, salts, or ammonium hydroxide may be added to assist in ion formation. Acids and salts help to protonate or cationize samples, while bases deprotonate samples. The concentration is varied depending upon the sample properties but the sensitivity of ESI can be as low as the attomole ( $1 \times 10^{-15}$  M) range. The sample concentration used in this work is around 0.1-20  $\mu$ M.

Sample solutions were infused into a stainless steel needle at a flow rate of 50-250  $\mu$ L/h using a syringe pump. A simplified diagram is illustrated in Figure 2.1. In the Bruker instrument, the needle tip is kept at ground voltage, while the capillary cap, endplate, and capillary entrance are held at a high potential (3 to 4 kV). For some instruments from other manufacturers, the high voltage is applied to the needle tip while keep capillary cap region is at ground voltage. No matter where the voltage is applied, there is a potential difference (around 3.5 kV) between the needle tip and capillary cap region. The high potential difference produces an electrostatic field to disperse the sample solution into a fine spray of charged droplets. To nebulize the sample, a flow of heated nitrogen is introduced in the same direction as the needle. A drying gas of nitrogen flows in the opposite direction to evaporate the charged droplets. In this dissertation work, the drying gas and nebulizer gas are both nitrogen. The drying gas has a temperature of 250-350°C and a flow rate of 5-10 L/min. The pressure of the nebulizer gas was optimized between 5.0-10.0 psi to obtain the best ESI signal.

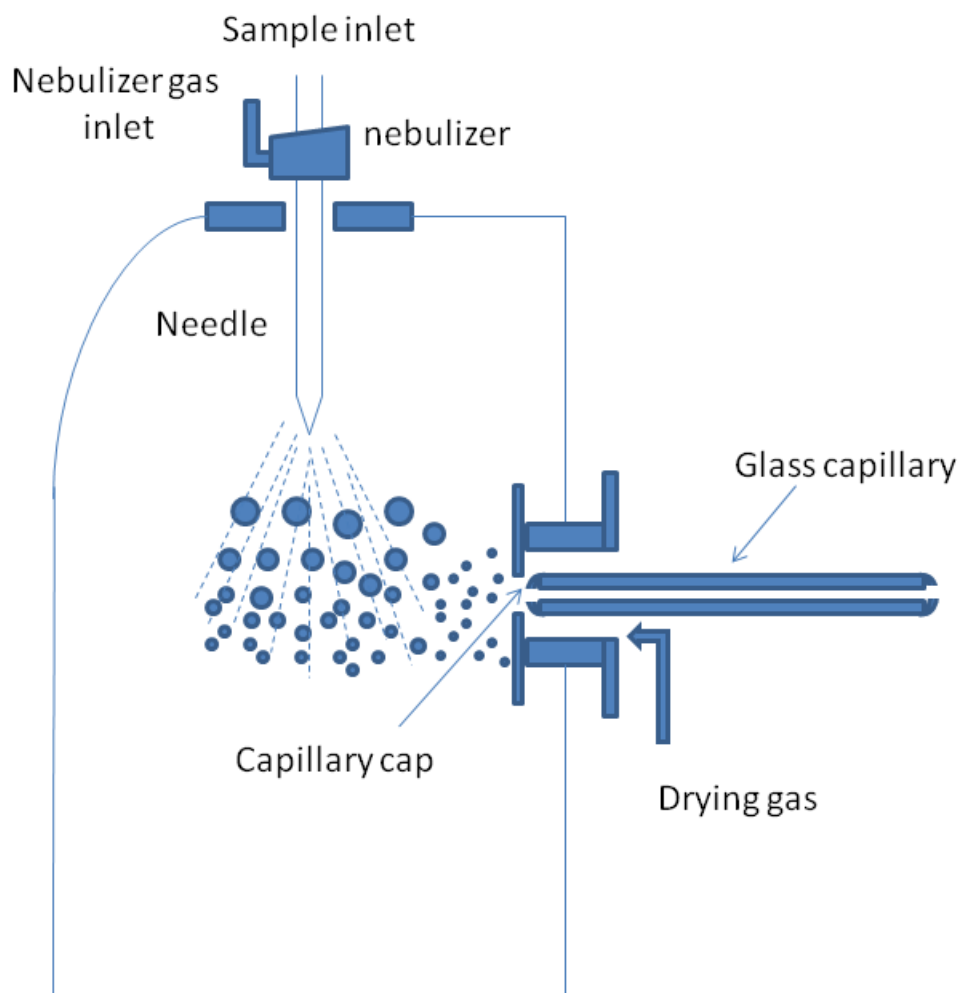


**Figure 2.1.** Diagram of ESI source.

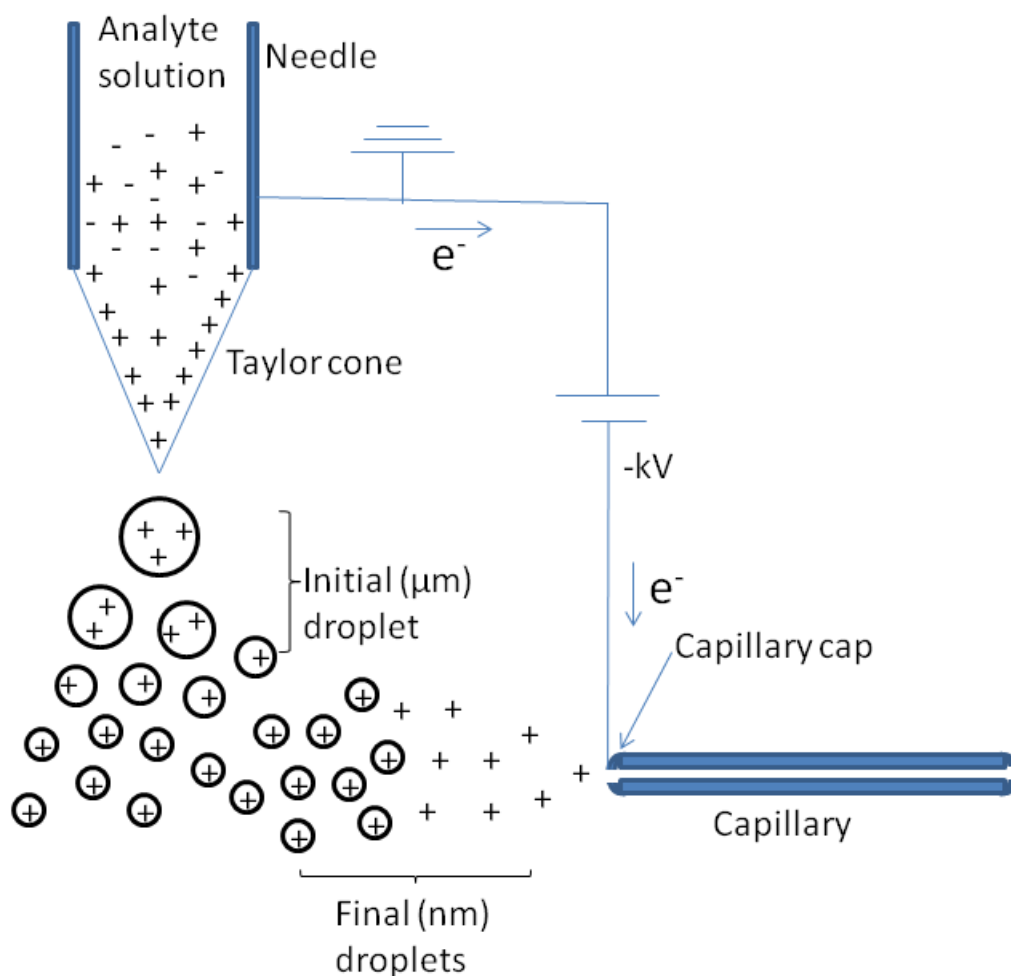


**Figure 2.2.** Schematic depiction of an ESI source operated in positive ion mode.

Electrospray ionization (ESI) occurs in three steps: droplet formation, droplet shrinkage, and desorption of gaseous ions.<sup>5</sup> Figure 2.2 is a schematic depiction of the ESI process in positive mode.<sup>6</sup> Initially, the electrostatic force on the analyte solution causes a partial separation of the charges. Cations move to the tip of the spray needle and anions move in the opposite direction. A Taylor cone forms at the tip of the needle, where the movement of the cations is compensated by the surface tension of the analyte solution. If the applied electric force is strong enough, a fine mist of droplets is emitted from the Taylor cone.

The rapid solvent evaporation by heating leads to droplet shrinkage. As the size of droplets decreases, the charge density on the surface of the droplets increases. Finally, when the force of the Coulomb repulsion is equal to the surface tension of the droplet (the Rayleigh limit), a Coulombic explosion breaks the droplets into even smaller and highly charged droplets. This droplet shrinkage and explosion process is repeated. In the end, quasi-molecular ions,  $[M+nH]^{n+}$ , are produced. These ions are then transported through two stages of pumping from the atmospheric pressure region into a high vacuum region containing the mass analyzer.

Nanoelectrospray ionization (nanoESI), which was introduced by Wilm and Mann,<sup>7,8</sup> is designed to operate at low flow rates (50-500 nL/min). NanoESI is a miniaturized version of ESI but has some differences. First, the sprayer needle tip in nanoESI is 10-15  $\mu\text{m}$  in diameter, while for standard ESI the sprayer needle tip diameter is around 100  $\mu\text{m}$ . Second, the nebulizing gas in nanoESI is not needed because the initial droplets are very small. Third, after the needle is installed on the nanoESI device, the three dimensional (3D) position of the needle needs to be adjusted correctly to obtain a good spectrum. The operation of the nanoESI is more complicated than for standard ESI. In this research, nanoESI was occasionally used because this technique has a lower sample flow rate into the source and a greater tolerance for salt impurities than ESI. Low flow rates have been reported to increase ion intensity.<sup>9</sup> NanoESI was employed to test whether lower flow rates could increase the supercharging of peptides, which is discussed in Chapter 4.

## 2.2 Quadrupole Ion Trap

The quadrupole ion trap (QIT), with the original name Paul trap, is a 3D ion trap where ions are held in a quadrupolar electric field. The QIT was introduced by Wolfgang Paul in 1958.

He won the 1989 Nobel Prize in Physics for its development.<sup>10</sup> The QIT is a trapping mass analyzer that can store ions for milliseconds to seconds. One important feature of a QIT is that it can trap positive and negative ions at the same time, which is especially useful for ETD experiments. Multiple stages of MS ( $MS^n$ ) can be performed within a single QIT analyzer.

Ions entering the QIT were produced in the ESI source and introduced into the trap by electrostatic focusing using a combination of two octopole ion guides and electrostatic lenses, as shown in Figure 2.3. The 3D quadrupole consists of a two dome-shaped end cap electrodes and a central ring electrode. One of the end cap electrodes has a small aperture to allow the ion beam to be gated periodically into the trap. The other end cap electrode has a small hole to allow ions to be ejected to a detector (see Figure 2.4). The ions are trapped in the QIT by applying a radiofrequency (RF) potential to the ring electrode while the end cap electrodes are kept at ground potential. This results in an oscillating electric field to trap the ions. Helium buffer gas, at a pressure of  $\sim 10^{-3}$  mbar, is used to damp the motion of trapped ions and concentrate ions in the center of the trap.

Ions in the QIT move in an oscillating motion around the center of the trap. The motion of the ions can be described by solutions of the Mathieu equation.<sup>11</sup> The canonical form of the Mathieu equation is:

$$\frac{d^2u}{d\xi^2} + (a_u - 2q_u \cos 2\xi) u = 0 \quad 2.1$$

where  $u$  represents the direction of motion as radial (x, y) or axial (z),  $\xi$  is a dimensionless parameter equal to  $\Omega t/2$  where  $\Omega$  is the frequency of the RF potential and  $t$  is time, and  $a_u$  and  $q_u$  are trapping parameters.



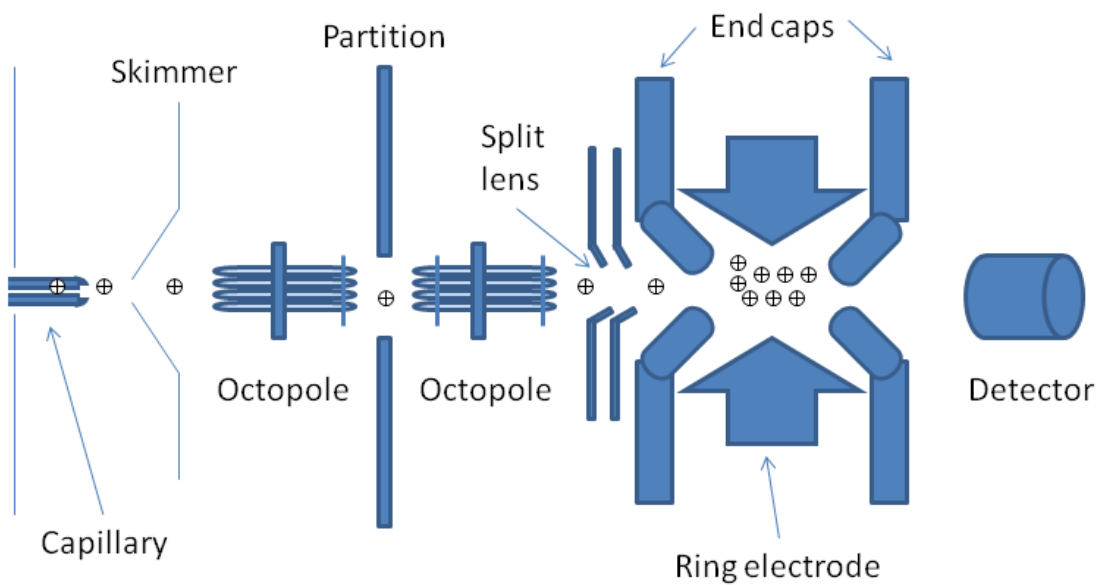


**Figure 2.3.** Ion transfer from ion source to ion trap.

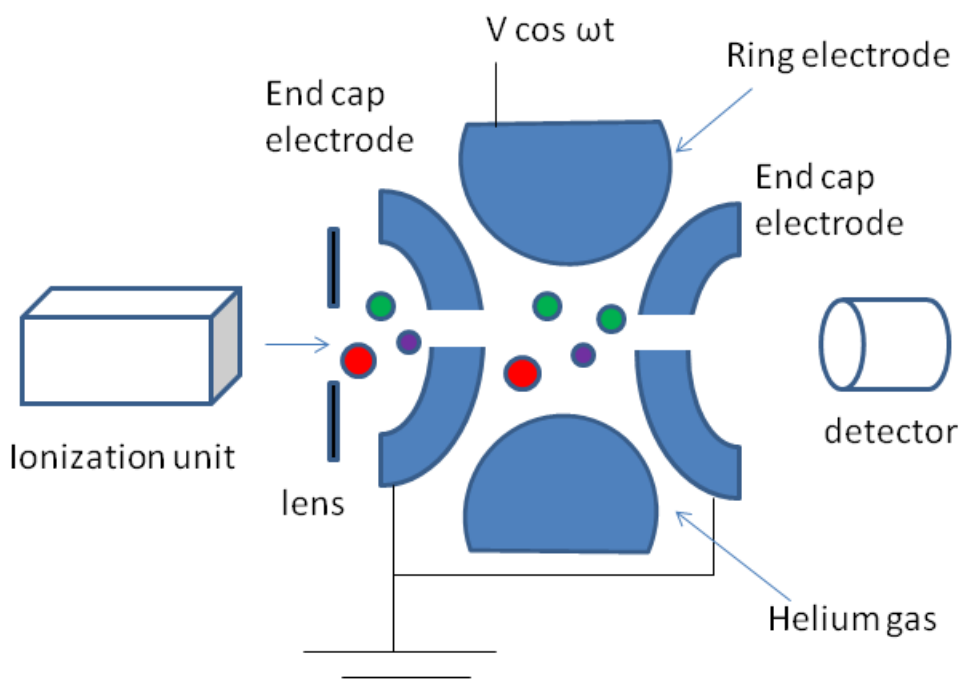


**Figure 2.4.** Diagram of a QIT mass analyzer.

After much substitution and rearrangement, the following trapping parameter expressions are obtained:

$$a_x = \frac{8zeU}{mr_0^2\Omega^2} \quad 2.2$$

$$q_x = -\frac{4zeU}{mr_0^2\Omega^2} \quad 2.3$$

$$a_z = -\frac{8zeU}{mr_0^2\Omega^2} \quad 2.4$$

$$q_z = \frac{4zeV}{mr_0^2\Omega^2} \quad 2.5$$

where  $U$  is the amplitude of the DC voltage,  $V$  is the amplitude of the AC voltage,  $r$  is the radius of the ring electrode,  $m$  is the mass of the ion,  $z$  is the charge of ion, and  $e$  is the charge of an electron.

The solutions to the Mathieu equation can be interpreted in terms of trajectory stability in radial ( $x$ ,  $y$ ) and axial ( $z$ ) directions. The Mathieu stability diagram in Figure 2.5 shows stable regions where ions of a certain  $m/z$  range can be stored in the QIT. In most commercial instruments, the mass selective instability mode is used. This mode, which is simple and is the most popular mode in mass analysis, only applies an RF voltage to the ring electrode and maintains the end cap electrode at ground potential ( $U$  and  $a_z$  are 0). The ions in this mode are in an oscillating electric field. At a given value of  $V$ , all ions above a certain  $m/z$  value are trapped in the QIT. The relationship of the cut-off  $m/z$  and  $V$  is given by:

$$\frac{m}{z} = \frac{4eV}{q_{\max}\Omega^2 r_0^2} \quad 2.6$$

where  $q_{\max}$  is maximum value of  $q_z$ , usually at 0.908. The peak-to-peak magnitude of  $V$  in these experiments was 30 kV (15 kV zero-to-peak).

The ions move in an oscillating mode in the trap and each  $m/z$  has a characteristic secular frequency. When an exterior voltage with this same frequency is applied to the end cap

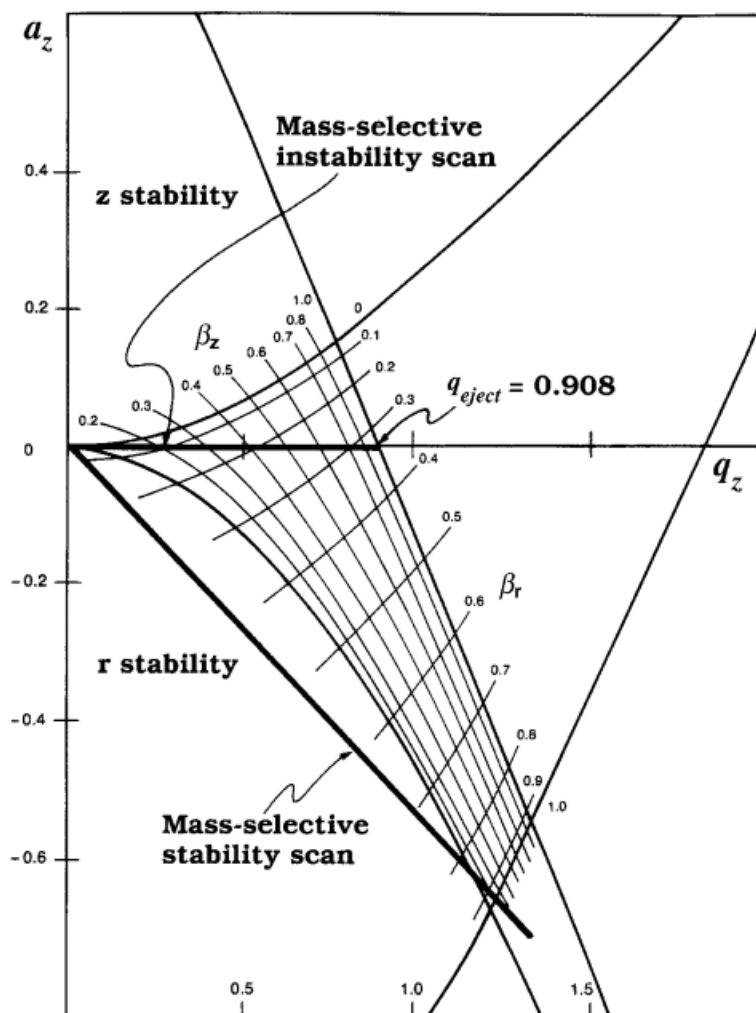


**Figure 2.5.** Mathieu stability diagram (used with permission from Reference 10).

electrode, ions are brought into resonance, which increases their orbital radius and velocity. The energy absorbed by an ion in resonance moves the ion away from the center of the trap. As the RF voltage (V) is increased, ions of increasing  $m/z$  expand their range of motion and are ejected out of the trap and detected by a Daly detector system.

The Daly system<sup>12</sup> is currently the most common detector in mass spectrometry and has the advantage of a long lifetime because ions and neutrals do not come into contact with the

electron amplification dynodes. After the ions exit the ion trap, an electrostatic lens is used to focus the ions on a conversion dynode, which produces a photon beam. Photons pass through a glass seal and hit another dynode, which produces an electron beam. The electron beam is multiplied using an electron multiplier (EM), which is a horn-shaped assembly made of a funnel of glass where the inner surface is coated with a copper-beryllium alloy that readily expels electrons upon bombardment with particles (including electrons). The emitted electrons continuously strike to the opposite surface until the exit is reached and the resulting electrical current is measured at an anode. The electrons are multiplied with a gain of  $10^6$  to  $10^7$ . The HCTultra PTM Discovery System used in this research contains a high capacity spherical ion trap (HCT).<sup>13</sup>

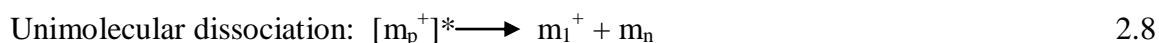
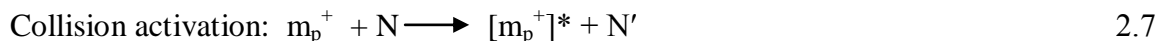
The HCT is not bigger than a QIT but contains more ions because its design and the method of applying voltages forces ions to bunch together in the center of the trap in a spherical shape. The main difference between an HCT and a conventional QIT is that a RF potential is applied to all three electrodes on the HCT to mimic the electric field of a hexapole. This gives the HCT better control of ion motion and interactions and greatly increases sensitivity.

## **2.3 Dissociation Techniques**

### **2.3.1 Collision-Induced Dissociation**

Collision-induced dissociation (CID) is also known as collision-activated dissociation (CAD). CID was first introduced in 1968<sup>14</sup> and is now the most widely used method in tandem mass spectrometry (MS/MS and MS<sup>n</sup>).<sup>15-17</sup> The CID process occurs in two steps: collision activation and unimolecular dissociation. The precursor ions, selected by resonance frequency techniques, are accelerated and collide with an inert gas (helium in the QIT), which excites the

ions excited to higher energy states. In the collision process, part of the translational energy of the precursor ion is converted into internal energy to cause the precursor ion to fragment by unimolecular dissociation. For peptides, CID breaks N-C amide backbone bonds to produce primarily b- and y-ions. (b- and y-Ions will be discussed in Section 2.4.) The processes involved are:



where  $m_p^+$  is the precursor ion, N is the inert gas, N' is the inert gas after collision, and  $m_1^+$  and  $m_n$  are fragments of the analyte ion.

There are two types of CID: high energy CID and low energy CID. High energy CID is mainly used in magnetic sector and TOF mass analyzers and the ions have translational energies between 3 and 10 keV.<sup>5</sup> The collision results in higher energy excited electronic states and vibrational states. High energy CID has more fragmentation than low energy CID. Low energy CID is primarily used in quadrupole and ion trap based tandem mass spectrometry. The ions are given collision energies below 100 eV. The low energy collisions excite ions only to upper vibrational states. In this dissertation, low energy CID is performed within the QIT of the Bruker HCTultra PTM Discovery System.

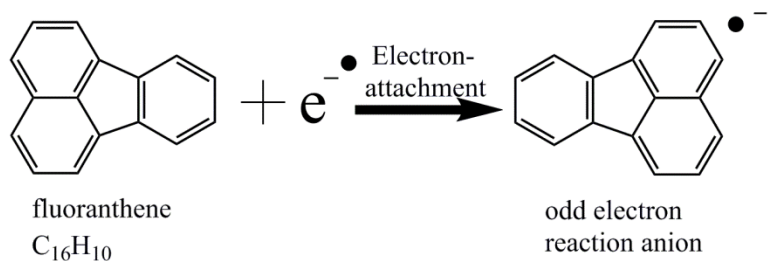
### 2.3.2 Electron Transfer Dissociation

Electron transfer dissociation (ETD) was developed by Hunt and coworkers<sup>18</sup> in 2004 and is an important new technique for peptide sequencing.<sup>19-22</sup> The ETD process uses an ion/ion reaction to transfer a low energy electron to a peptide ion and initiate dissociation as shown in Figure 2.6. The generation of low energy electrons is a multi-step process. First,

higher energy electrons are generated by an electron ionization (EI) filament source, where the electrons are accelerated with a potential of ~75 eV. In a negative chemical ionization (nCI) process, these electrons collide with methane gas and the resulting plasma generates very low energy electrons. The low energy electrons are captured by an ETD reagent gas with a low electron affinity. Fluoranthene, azobenzene and anthracene are common ETD reagents; fluoranthene was used in this work. The fluoranthene reagent anion is moved by electrostatic focusing into the QIT. Inside the QIT, the reagent anion and a m/z-selected precursor ion undergo an ion/ion reaction. The result is a reduced ion,  $[M+nH]^{(n-1)+\bullet}$ , that cleaves at the N-C $_{\alpha}$  backbone to produce c- and z-ions. (c- and z-Ions will be discussed in Section 2.4.) Peptides should be at least doubly protonated in ESI to perform ETD experiments. Otherwise, the addition of an electron to a singly charged precursor ion makes the charge neutral and undetectable by mass spectrometry. The ETD process is similar to the tandem mass spectrometry technique of electron capture dissociation (ECD)<sup>23</sup> except that an electron is captured by a multiply charged peptide ion in ECD. ECD is primarily used in Fourier transform ion cyclotron resonance (FT-ICR) mass spectrometry instruments.

All ETD experiments in this research were performed using a Bruker HCTultra PTM Discovery System equipped with ESI. The ETD source is shown in Figure 2.7. The nCI ionization source is located outside of the QIT. The fluoranthene anions produced by nCI and multiply charged peptide ions produced by ESI are transported into the trap using the same octopole. After the peptide cations are introduced into the ion trap, the ion transmission device is switched in polarity to accumulate fluoranthene anions. The peptide cations and reagent anions are then trapped together for a time in the range of 40-100 ms.

## Generation of reactant anion in the nCI source:



## ETD process within the ion trap:

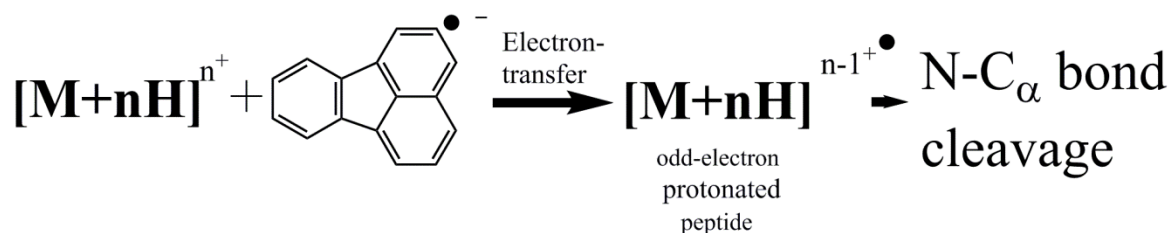


**Figure 2.6.** ETD reaction used to produce peptide fragmentation.

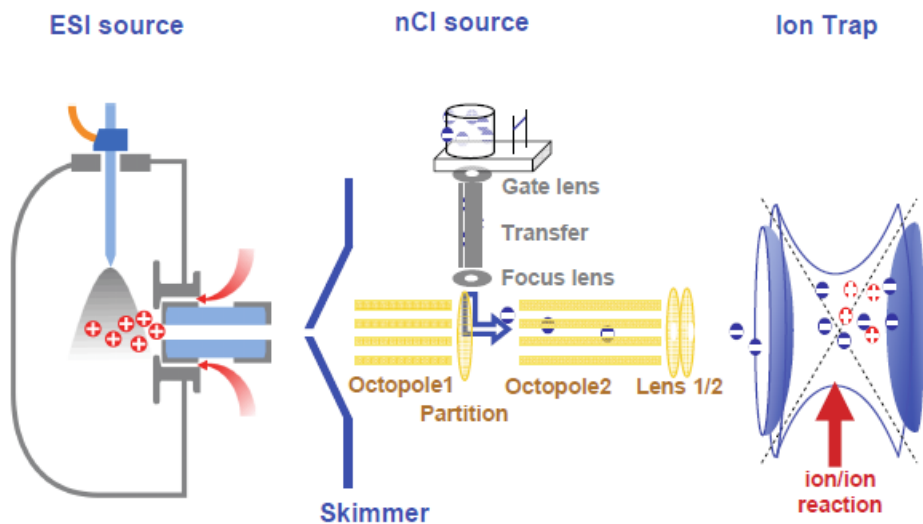


**Figure 2.7.** ETD set-up (used with permission from Reference 13).

Although the method with which the multiply charged peptide ion obtains an electron differs for ECD and ETD, the fragmentation mechanisms and the resulting mass spectra are very similar. ETD and ECD both produce primarily c- and z-type fragment ions by random backbone N-C $\alpha$  bond cleavages. The Corneliussen mechanism<sup>23</sup> and Utah-Washington mechanism<sup>24</sup> are used to explain the c- and z-ion formation. These mechanisms will be discussed in detail in Chapter 3. ETD and ECD are widely used in peptide and protein sequencing.<sup>18,19,21,22,25-30</sup>

## 2.4 Peptide Sequencing Nomenclature

The standard peptide fragment ion nomenclature<sup>31</sup> by Roepstorff and Fohlman is used throughout this dissertation for describing ions in the CID and ETD spectra. Figure 1.1 in Chapter 1 illustrates the nomenclature for peptide fragmentation. When a protonated or deprotonated peptide ion cleavages, the charge is retained on one side of the peptide. If the charge is retained near the N-terminus, a, b, and c are used to describe the ions. If the charge stays near the C-terminus, x, y, and z are used. The subscript number refers to the cleavage site, which is numbered from the terminus that retains the charge. Prime symbols on the right mean the addition of hydrogens. For example, c<sub>n</sub>' stands for [c<sub>n</sub>+H]<sup>+</sup> and c<sub>n</sub>'' stands for [c<sub>n</sub>+2H]<sup>+</sup>. Prime symbols on the left denote the subtraction of hydrogens. In 2002, Zubarev and coworkers developed a modified nomenclature<sup>32</sup> to denote for radical products in ETD in which the major ETD product ions are referred to as c' and z'. The c' of Zubarev nomenclature is c'' for Roepstorff and Fohlman nomenclature and z' is z'. To better keep track of additional hydrogens, Roepstorff and Fohlman nomenclature is used throughout this dissertation.



## 2.5 Peptide Synthesis

In order to meet specific research requirements in the projects of the dissertation, some custom synthesized peptides were needed. Most of these peptides were synthesized using standard Fmoc solid phase peptide synthesis (SPPS) protocol on an Advanced ChemTech Model 90 peptide synthesizer (Louisville, KY, USA) in our laboratory. In some cases, further modification of peptides via methyl esterification was used to eliminate the C-terminal carboxylic acid group.

Solid phase peptide synthesis was developed by Merrifield<sup>33</sup> in 1963 to help scientists synthesize peptides in their laboratory. Peptides are synthesized from the C-terminus to N-terminus on an insoluble support resin. An Fmoc (9-fluorenylmethoxycarbonyl) group is attached to an amino acid residue to protect the reactive amino group, as shown in Figure 2.8. The Fmoc-amino acid residue used for the C-terminus is attached to a resin, which is traditionally an insoluble polystyrene bead. The Fmoc-amino acid and Fmoc-amino acid residue can be purchased commercially. In these experiments, the Fmoc-amino acids and Fmoc-amino acid Wang resins (a standard resin in peptide synthesis) were purchased from Advanced ChemTech.

To synthesize a peptide, the desired resin was put into a reaction vial that was attached to the peptide synthesizer. The resin was first washed with dimethylformamide (DMF), methanol (MeOH) and then DMF again. A PIP solution of 20% piperidine (v:v) in DMF solvent was introduced into the reaction vial to remove the Fmoc group. The resulting amino acid resin was washed again using the same wash steps. 1-Hydroxybenzotriazole hydrate (Hobt), which is a coupling additive to reduce racemization, was dissolved in N-methyl-2-pyrrolidinone (NMP) to prepare a 0.5 M Hobt solution. The Hobt solution was used to make a 0.5 M Fmoc amino acid

residue solution. The prepared Fmoc amino acid residue solution along with 0.5 M solution of 1,3-diisopropylcarbodiimide (DIC) in NMP was added to the reaction vial to start coupling steps. The DIC was used to activate the carboxyl group of the Fmoc amino acid. After the coupling step was complete, another round of wash steps was performed. These wash-deprotect-couple-wash steps were automated by writing a program for the peptide synthesizer. The cycles were repeated to add other amino acid residues.

When all the residues were added, the C-terminal resin was cleaved from the resin to generate the synthesized peptide. A cleavage solution of 9.5 ml trifluoroacetic acid (TFA), 0.3 ml triisopropylsilane (TIPS), 0.5 ml deionized (DI) water was used to cleave the ester linkage between peptide and resin. The mixture was filtered to remove the resin, and then diethyl ether (which had been cooled to -78 °C in a bath of dry ice) and acetone were added to precipitate the peptide. The solution was centrifuged and the diethyl ether was decanted. The remaining gel was the peptide of interest, which was put in a desiccator to dry.

After drying, the synthesized peptide can be directly used for mass analysis. Sometimes, peptides needed to be further modified. For example, in Chapter 4, some peptides were converted to methyl esters to test if the carboxylic acid groups are involved in supercharging with Cr(III). Solution-phase chemistry<sup>34</sup> was used here to make methyl esterified peptides. Figure 2.9 illustrates the methyl esterification process. In these experiments, 5 µL of acetic anhydride, 6 µL of 12 M hydrochloric acid, and 69 µL of dry methanol were mixed for 5 minutes and then 1.2 mg of solid peptide was added. The resulting solution contained the peptide methyl ester.

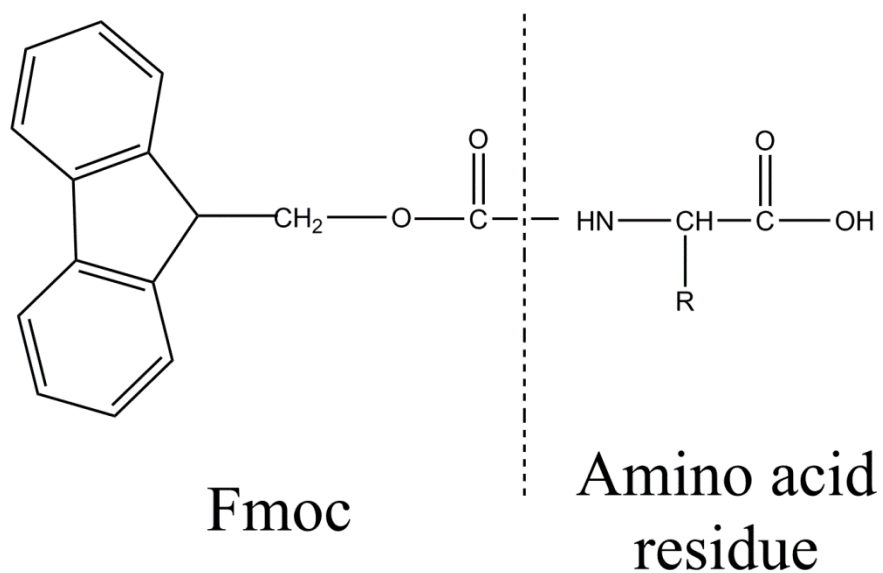


**Figure 2.8.** Fmoc-L-amino acid residue.

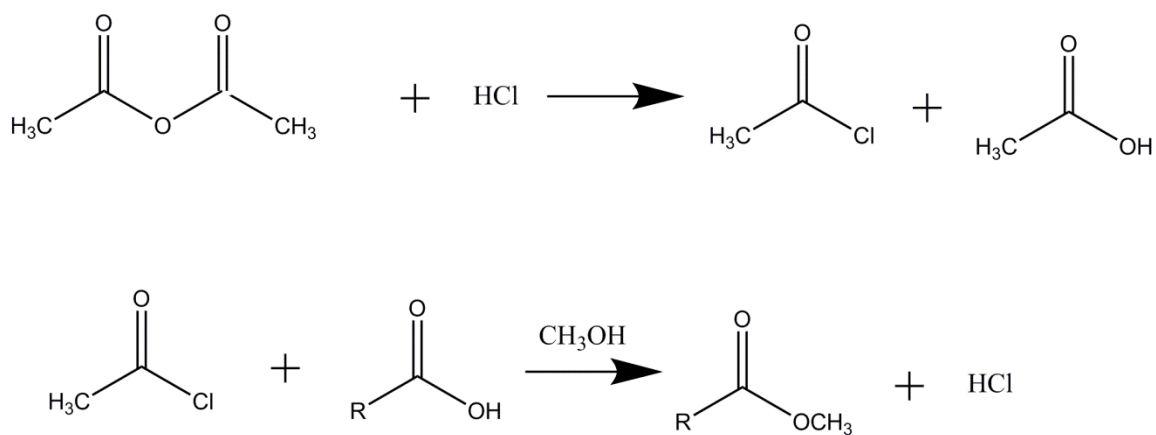


**Figure 2.9.** Peptide methyl esterification reaction.

## 2.6 Amino Acid Structure

The basic, neutral, and acid peptides used in these experiments are composed of different amino acid residues. Figure 2.10, 2.11, and 2.12 show the basic, neutral and acid amino acids, respectively, that are involved in this work.

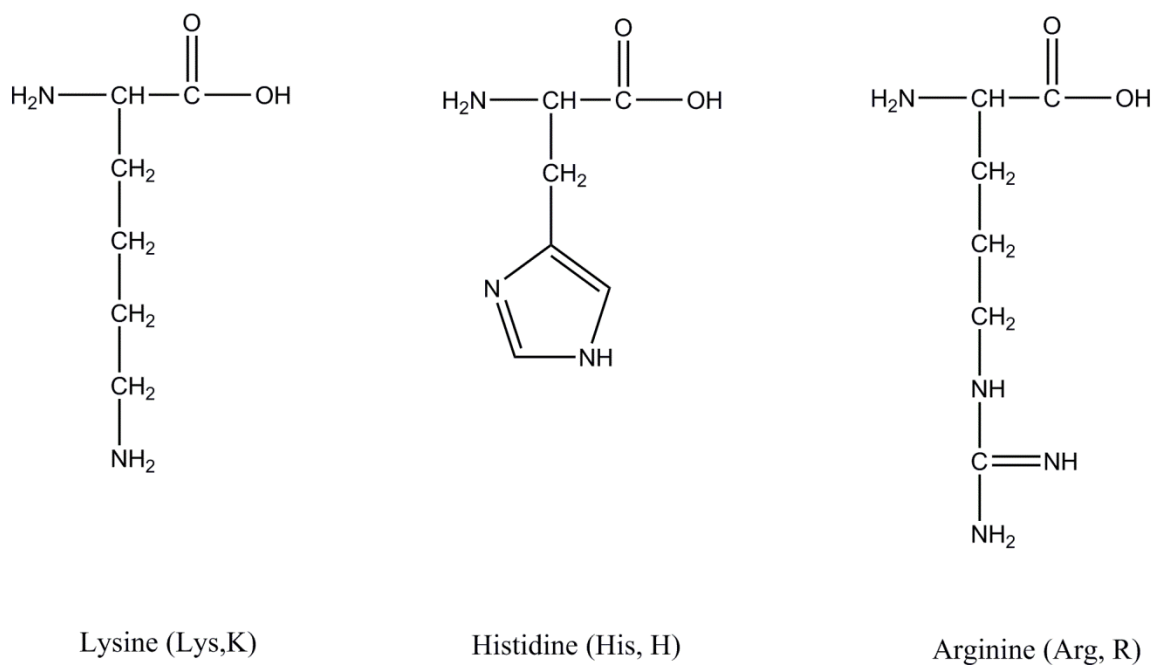
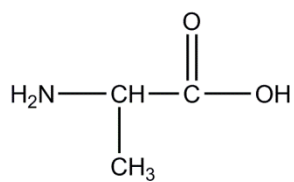
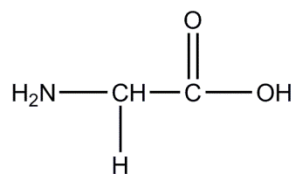


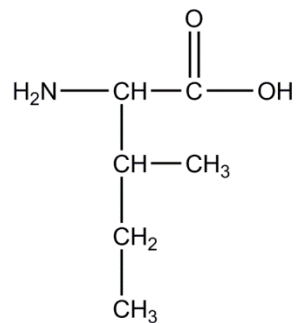
**Figure 2.10.** Basic amino acids.



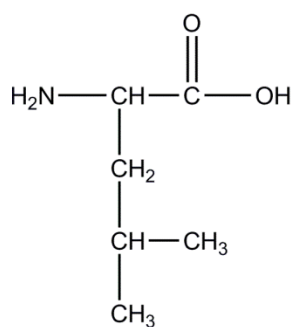
Alanine (Ala, A)



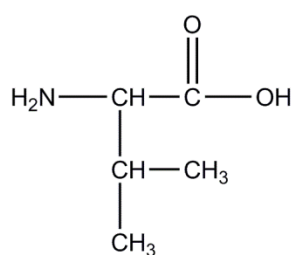
Glycine (Gly, G)



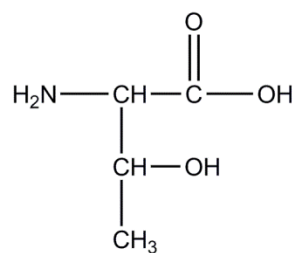
isoleucine (Ile, I)



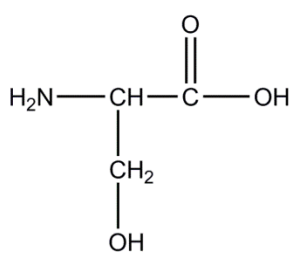
Leucine (Leu, L)



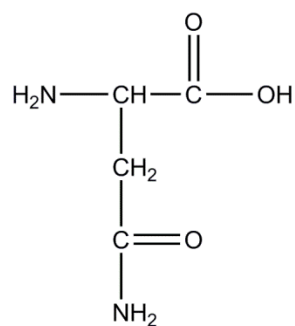
Valine (Val, V)



Threonine (Thr, T)

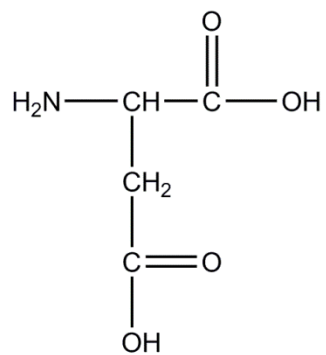


Serine (Ser, S)

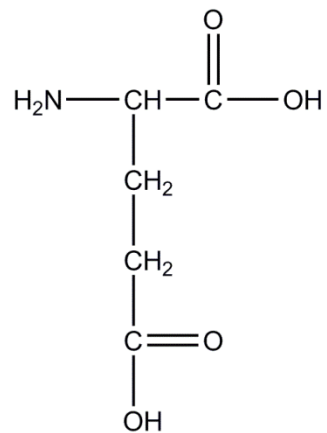


Asparagine (Asp, N)

**Figure 2.11.** Neutral amino acids and polar amino acids.



Aspartic acid (Asp, D)



Glutamic acid (Glu, E)

**Figure 2.12.** Acidic amino acids.

## References

1. Smith, R. D.; Loo, J. A.; Loo, R. R. O.; Busman, M.; Udseth, H. R. Principles and Practice of Electrospray Ionization - Mass-Spectrometry for Large Polypeptides and Proteins. *Mass Spectrom. Rev.* **1991**, *10*, 359-451.
2. Dole, M.; Mack, L. L.; Hines, R. L. Molecular Beams of Macroions. *J. Chem. Phys.* **1968**, *49*, 2240.
3. Fenn, J. B.; Mann, M.; Meng, C. K.; Wong, S. F.; Whitehouse, C. M. Electrospray Ionization for Mass Spectrometry of Large Biomolecules. *Science*. **1989**, *246*, 64-71.
4. Fenn, J. B.; Mann, M.; Meng, C. K.; Wong, S. F. Electrospray Ionization--Principles and Practice. *Mass Spectrom. Rev.* **1990**, *9*, 37-70.
5. Chhabil, D. *Fundamentals of Contemporary Mass Spectrometry*; John Wiley & Sons, Inc.: New Jersey, 2007.
6. Konermann, L.; Ahadi, E.; Rodriguez, A. D.; Vahidi, S. Unraveling the Mechanism of Electrospray Ionization. *Anal. Chem.* **2013**, *85*, 2-9.
7. Wilm, M. S.; Mann, M. Electrospray and Taylor-Cone Theory, Does Beam of Macromolecules at Last. *Int. J. Mass Spectrom.* **1994**, *136*, 167-180.
8. Wilm, M.; Mann, M. Analytical Properties of the Nanoelectrospray Ion Source. *Anal. Chem.* **1996**, *68*, 1-8.
9. Reschke, B.; Timperman, A. A Study of Electrospray Ionization Emitters with Differing Geometries with Respect to Flow Rate and Electrospray Voltage. *J. Am. Soc. Mass Spectrom.* **2011**, *22*, 2115-2124.
10. Paul, W. Electromagnetic Traps for Charged and Neutral Particles. *Rev. Mod. Phys.* **1990**, *62*, 531-540.
11. March, R. E. An Introduction to Quadrupole Ion Trap Mass Spectrometry. *J. Mass Spectrom.* **1997**, *32*, 351-369.
12. Exelis product page. <http://www.exelis-ps.com/product.cfm?prod=7596> (Accessed Aug 09, 2014).
13. Bruker Daltonics *HCTultra PTM Discovery System User Manual*; Billerica, MA, 2006.
14. Jennings, K. R. Collision-induced Decompositions of Aromatic Molecular Ions. *Int. J. Mass Spectrom. Ion Phys.* **1968**, *1*, 227-235.

15. Papayannopoulos, I. A. The Interpretation of Collision-Induced Dissociation Tandem Mass Spectra of Peptides. *Mass Spectrom. Rev.* **1995**, *14*, 49-73.
16. Biemann, K.; Martin, S. A. Mass Spectrometric Determination of the Amino Acid Sequence of Peptides and Proteins. *Mass Spectrom. Rev.* **1987**, *6*, 1-76.
17. Loo, J. A.; Edmonds, C. G.; Udseth, H. R.; Smith, R. D. Collisional Activation and Dissociation of Large Multiply Charged Proteins Produced by Electrospray Ionization. *Anal. Chim. Acta* **1990**, *241*, 167-173.
18. Syka, J. E. P.; Coon, J. J.; Schroeder, M. J.; Shabanowitz, J.; Hunt, D. F. Peptide and Protein Sequence Analysis by Electron Transfer Dissociation Mass Spectrometry. *Proc. Natl. Acad. Sci. USA* **2004**, *101*, 9528-9533.
19. Coon, J. J. Collisions or Electrons? Protein Sequence Analysis in the 21st Century. *Anal. Chem.* **2009**, *81*, 3208-3215.
20. Good, D. M.; Wirtala, M.; McAlister, G. C.; Coon, J. J. Performance Characteristics of Electron Transfer Dissociation Mass Spectrometry. *Mol. Cell Proteomics* **2007**, *6*, 1942-1951.
21. Tureček, F.; Chung, T. W.; Moss, C. L.; Wyer, J. A.; Ehlerding, A.; Holm, A. I. S.; Zettergren, H.; Nielsen, S. B.; Hvelplund, P.; Chamot-Rooke, J.; Bythell, B.; Paizs, B. The Histidine Effect. Electron Transfer and Capture Cause Different Dissociations and Rearrangements of Histidine Peptide Cation-Radicals. *J. Am. Chem. Soc.* **2010**, *132*, 10728-10740.
22. Gunawardena, H. P.; Gorenstein, L.; Erickson, D. E.; Xia, Y.; McLuckey, S. A. Electron Transfer Dissociation of Multiply Protonated and Fixed Charge Disulfide Linked Polypeptides. *Int. J. Mass Spectrom.* **2007**, *265*, 130-138.
23. Zubarev, R. A.; Kruger, N. A.; Fridriksson, E. K.; Lewis, M. A.; Horn, D. M.; Carpenter, B. K.; McLafferty, F. W. Electron Capture Dissociation of Gaseous Multiply-charged Proteins is Favored at Disulfide Bonds and Other Sites of High Hydrogen Atom Affinity. *J. Am. Chem. Soc.* **1999**, *121*, 2857-2862.
24. Chen, X.; Tureček, F. The Arginine Anomaly: Arginine Radicals Are Poor Hydrogen Atom Donors in Electron Transfer Induced Dissociations. *J. Am. Chem. Soc.* **2006**, *128*, 12520-12530.
25. McLafferty, F. W.; Horn, D. M.; Breuker, K.; Ge, Y.; Lewis, M. A.; Cerda, B. A.; Zubarev, R. A.; Carpenter, B. K. Electron Capture Dissociation of Gaseous Multiply Charged Ions by Fourier Transform ion Cyclotron Resonance. *J. Am. Soc. Mass Spectrom.* **2001**, *12*, 245-249.
26. Zubarev, R. A.; Horn, D. M.; Fridriksson, E. K.; Kelleher, N. L.; Kruger, N. A.; Lewis, M. A.; Carpenter, B. K.; McLafferty, F. W. Electron Capture Dissociation for Structural Characterization of Multiply Charged Protein Cations. *Anal. Chem.* **2000**, *72*, 563-573.



27. Zubarev, R. A.; Haselmann, K. F.; Budnik, B.; Kjeldsen, F.; Jensen, F. Towards an Understanding of the Mechanism of Electron-capture Dissociation: A Historical Perspective and Modern Ideas. *Eur. J. Mass Spectrom.* **2002**, 8, 337-349.
28. Yang, H.; Fung, Y. M. E.; Zubarev, A. R.; Zubarev, R. A. The Use of ECD for Proteomics-wide Identification and Quantification of iso-Asp Residues. *Mol. Cell. Proteomics* **2009**, S13-S13.
29. Zubarev, R. A.; Zubarev, A. R.; Savitski, M. M. Electron Capture/Transfer versus Collisionally Activated/Induced Dissociations: Solo or Duet? *J. Am. Soc. Mass Spectrom.* **2008**, 19, 753-761.
30. Good, D. M.; Wirtala, M.; McAlister, G. C.; Coon, J. J. Performance Characteristics of Electron Transfer Dissociation Mass Spectrometry. *Mol. Cell. Proteomics* **2007**, 6, 1942-1951.
31. Roepstorff, P.; Fohlman, J. Proposal for a Common Nomenclature for Sequence Ions in Mass Spectra of Peptides. *Biomed. Mass Spectrom.* **1984**, 11, 601.
32. Kjeldsen, F.; Haselmann, K. F.; Budnik, B. A.; Jensen, F.; Zubarev, R. A. Dissociative Capture of Hot (3–13 eV) Electrons by Polypeptide Polycations: an Efficient process Accompanied by Secondary Fragmentation. *Chem. Phys. Lett.* **2002**, 356, 201-206.
33. Merrifield, R. B. Solid Phase Peptide Synthesis. I. The Synthesis of a Tetrapeptide. *J. Am. Chem. Soc.* **1963**, 85, 2149-2154.
34. Greene, T. W.; Wuts, P. G. M., Eds.; In *Protective Groups in Organic Synthesis*; John Wiley & Sons, Inc.: New York, 1991.

## CHAPTER 3: ELECTRON TRANSFER DISSOCIATION OF BASIC PEPTIDES

### 3.1 Introduction

In proteomics, trypsin protease is widely used to digest proteins into smaller peptides that contain arginine or lysine residues at the C-terminus.<sup>1</sup> These resulting tryptic peptides are often sequenced by tandem mass spectrometry.<sup>2-9</sup> The presence of basic residues can affect both the location of protons in precursor ions and the fragmentation pathways observed.<sup>10-17</sup> Basic residues have high gas-phase basicities (GBs) and their side chains may sequester protons and limit fragmentation, especially for highly basic arginine residues.<sup>18,19</sup> Extra energy may be required to move the hydrogen ion to the peptide backbone and facilitate dissociation.<sup>12</sup> In collision-induced dissociation (CID) cleavage is favored at either the C-terminal or N-terminal sides of arginine residues.<sup>11</sup> In CID, many peptides exhibit preferential cleavage at the C-terminal side of histidine residues, including both adjacent to the histidine residue and two residues removed.<sup>12,20</sup>

In electron transfer dissociation (ETD) and electron capture dissociation (ECD), N-C $\alpha$  bond cleavage dominates the spectra of basic peptides.<sup>3,5,6,21-23</sup> Protonated peptides with lysine, histidine, or arginine participate in electron transfer to a similar degree.<sup>19</sup> Peptides with histidine residues show the highest degree of electron transfer without dissociation (ET no D).<sup>19</sup> Tureček and coworkers found that the ET no D products had undergone rearrangement and that proton migrations from peptide termini to the C-2' position of the reduced His-ring stabilized the undissociated radicals.<sup>13</sup> Basic peptides often generate ETD and ECD products that include side

chain losses, with such processes being particularly prominent for arginine residues.<sup>19,24-26</sup> Haag et al. found that for the pentapeptides KXXXX, XKXXX, and XXKXX (X = A or G), the product ions always contain lysine (Lys, K).<sup>27</sup> Marshall and coworkers reported that basic residues located at the N-terminus or C-terminus enhance the formation of a- and y-ions in ECD.<sup>14</sup> In contrast, Cooper found that lysine-containing peptides promote the formation of b-ions.<sup>28</sup> In addition, Liu and Håkansson observed in an ECD study that when histidine was adjacent to the N-terminal residue, b-ions were produced.<sup>29</sup>

ETD<sup>6</sup> and ECD<sup>30</sup> are electron-based methods that produce primarily c- and z-type fragment ions by random backbone N-C<sub>α</sub> bond cleavages.<sup>31</sup> Although the method with which the precursor ion obtains an electron differs for ECD and ETD, the fragmentation mechanisms and the resulting mass spectra are very similar.<sup>8</sup> The earliest mechanism proposed for ECD<sup>32</sup> is the Cornell mechanism by McLafferty and coworkers where an electron localized at a positively charged functional group (e.g., ammonium or guanidinium) captures a hydrogen atom to form an odd-electron ion that undergoes N-C<sub>α</sub> bond dissociations.<sup>33</sup> O'Connor and coworkers used a double resonance experiment to confirm the existence of a radical intermediate in ECD.<sup>34</sup> Zubarev and coworkers named the short lived radical intermediate the [c'+z<sup>•</sup>] or [c<sup>•</sup>+z'] complex.<sup>35</sup> The hydrogen atom is transferred to a carbonyl oxygen of an amide group; the result is N-C<sub>α</sub> bond cleavage that produces even-electron and radical product ions.<sup>35</sup> Most often, the product ions are members of the c- and z- series.<sup>6</sup> The non-ergodic N-C<sub>α</sub> bond dissociation process is affected by intramolecular solvation of protons at the side chains of basic residues.<sup>32</sup> However, this mechanism cannot explain N-C<sub>α</sub> bond dissociations that are remote to the basic residues.

Another mechanism to describe N-C $\alpha$  bond cleavage has been proposed by the Simons<sup>36</sup> and Tureček<sup>37</sup> groups independently and is known as Utah-Washington (UW) mechanism. In this mechanism, the electron in ECD or ETD is captured in a Coulomb stabilized amide  $\pi^*$  orbital that converts the amide bond into a superbase. The amide superbase can either abstract a proton from a nearby proton donor group, which triggers a backbone cleavage, or can undergo N-C $\alpha$  bond dissociation to form an enole-imidate anion, which then abstracts a proton to form c- and z-product ions.<sup>18</sup> The major difference between the UW and Cornell mechanisms is that the UW mechanism does not require the side chains of basic residues to participate in proton-coupled electron transfer.

In the present study, ETD was performed on doubly protonated ions,  $[M+2H]^{2+}$ , from fifteen model heptapeptides that contain one basic residue and six alanine residues. Because the methyl group comprising the side chain of alanine should not affect fragmentation, this allows determination of the effects of the identities and positions of basic residues on ETD.

## 3.2 Experimental

### 3.2.1 Peptides

The heptapeptides studied were XAAAAAA, AXAAAAA, AAAXAAA, AAAAAAXA and AAAAAAX, where X is arginine (R), lysine (K), or histidine (H) and A is alanine. The peptides were synthesized by standard Fmoc procedures<sup>38</sup> with an Advanced ChemTech (Louisville, KY, USA) model 90 automated peptide synthesizer, as discussed in Chapter 2. Peptides containing <sup>13</sup>C labeled alanine residues, K\*AAAAAA and \*AAAAAAR, were also synthesized and analyzed to further identify the product ion types. The asterisk indicates that the alanine residue, \*A, has <sup>13</sup>C substitution at its methyl side chain. In addition, the peptide

AAAKAAAA was purchased from Synthetic Biomolecules (San Diego, CA, USA). All reagents were used without further purification and were purchased from Advanced ChemTech or VWR (Radnor, PA, USA). Deionized and distilled water was produced with a Barnstead E-pure system (Dubuque, IA, USA).

To dissolve the basic peptides, they were first added to a solvent of methanol:water at 50:50 volume:volume ratio using a concentration of 1 mg peptide per mL of solvent. From this stock solution, solutions for analysis by ESI were dissolved to 10  $\mu$ M in acetonitrile:water:acetic acid at a volume ratio of 49.5:49.5:1.

### **3.2.2 Mass Spectrometry**

The peptides were analyzed on a Bruker (Billerica, MA, USA) HCTultra PTM Discovery System high capacity quadrupole ion trap mass spectrometer equipped with ESI as discussed in Chapter 2. The ESI end plate and capillary voltages were kept at  $\sim$ 4.0 kV and the capillary exit voltage was +103 V. The ESI drying and nebulizer gas was nitrogen heated to 250°C. Samples were infused at a flow rate of 1-2  $\mu$ L/min using a KD Scientific (Holliston, MA, USA) syringe pump.

Single stage mass spectra ( $m/z$  50-700) were acquired in standard enhanced positive ion mode and followed by ETD fragmentation experiments. The precursor cation target value was adjusted from 80,000 to 200,000 and a maximum accumulation time of 200 ms was used to regulate the number of ions entering the trap. Selection of the doubly protonated precursor ion,  $[M+2H]^{2+}$ , was optimized within an isolation window of 1.0- 4.0  $m/z$  in order to maximize precursor intensity while excluding nearby ions. Methane was used as the negative chemical ionization (nCI) reagent gas. Fluoranthene anions were generated within the nCI source and

were introduced into the trap, where they transferred electrons to the  $m/z$ -selected precursor ions in the ETD process. ETD was performed using Bruker's automatic smart decomposition,<sup>39,40</sup> which adjusted the anion/cation reaction times automatically in order to maximize fragmentation efficiency. Reaction times were in the range of 50-200 ms. The smart decomposition routine also applied a low energy resonance excitation pulse to the odd-electron protonated peptide ET no D ions,  $[M+2H]^{+*}$ . This essentially performed a very low energy collision-induced dissociation (CID) event on the ETD dissociation intermediate in order to break apart fragment clusters held together by non-covalent interactions, thus enhancing ETD fragmentation efficiency.<sup>39,40</sup> (Experiments were also performed without this additional CID activation and it was found that the pulse had negligible effects on the spectra presented here.) For ETD, the ion charge control (ICC) value was set to 50,000-400,000 to maximize dissociation efficiency. An initial lower end  $m/z$  cut-off of 140  $m/z$  was used to acquire ETD spectra. However, in order to observe lower  $m/z$  ETD product ions, cut-offs in the range of 50-140  $m/z$  were also employed. Reducing the lower  $m/z$  cut-off results in a somewhat reduced ETD efficiency because the corresponding ion trajectory changes lessen the overlap between the cationic and anionic ion clouds involved in ETD. All the spectra shown here were obtained from signal averaging of 200 scans.

### 3.3 Results and Discussion

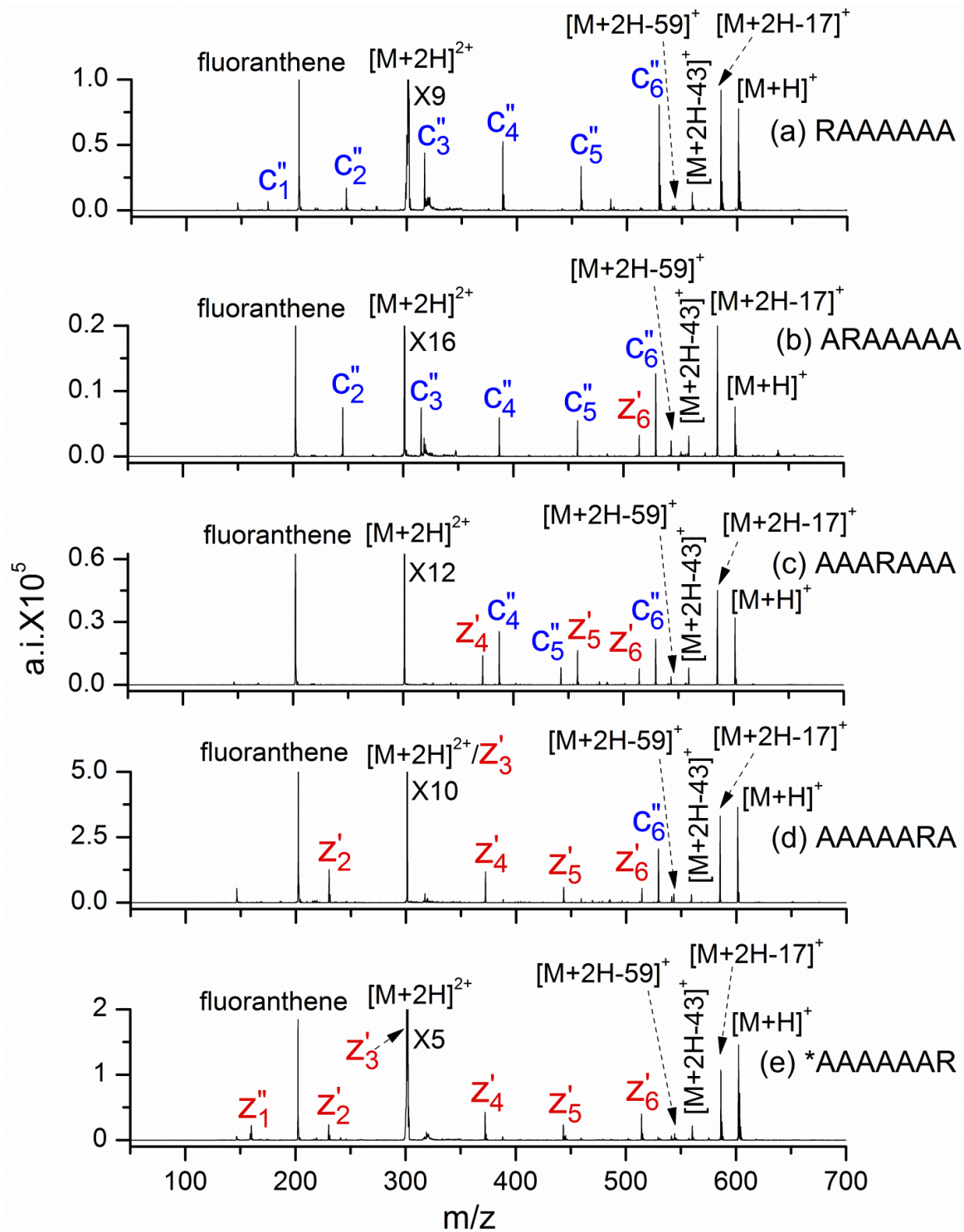
Doubly protonated heptapeptides XAAAAAA, AXAAAAA, AAAXAAA, AAAAAXA and AAAAAAX, where A is alanine and X is arginine (R), lysine (K), or histidine (H) residues, were dissociated by ETD. The standard peptide fragment nomenclature<sup>41</sup> by Roepstorff and

Fohlmann is used here for the ETD spectra. The nomenclature employed is discussed in Chapter 2.

### 3.3.1 Effect of Basic Residue Position on ETD

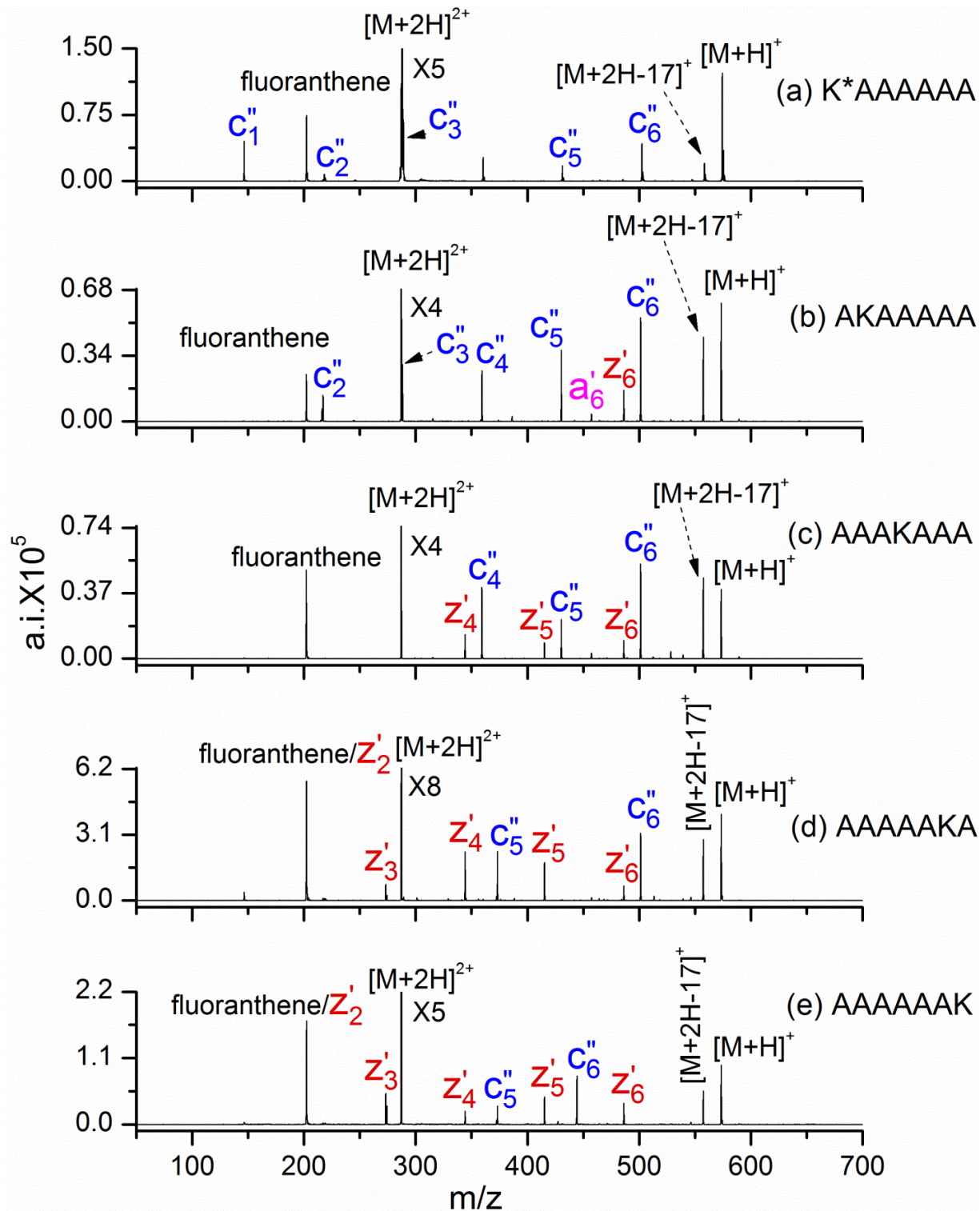
Figure 3.1 shows the ETD spectra of  $[M+2H]^{2+}$  from RAAAAAA, AAAAAA, AAARAAA, AAAAARA, and \*AAAAAAR. These peptides produce mainly c- and z-series ions with a few side chain losses. All of the ETD product ions contain an arginine residue. Figure 3.1(a) gives the spectrum for arginine at the N-terminus where a complete series of  $c_n''$ ,  $n = 1-6$  is produced. When arginine is located at the second position of the heptapeptide in Figure 3.1(b),  $c_n''$ ,  $n = 2-6$ , and  $z_6'$ , are produced. Figure 3.1(c) has arginine at the fourth position, where  $c_n''$ ,  $n = 4-6$ , and  $z_n'$ ,  $n = 4-6$ , form. Arginine at the sixth position in Figure 3.1(d) yields  $c_6''$  and  $z_n'$ ,  $n = 2-6$ . When arginine is located at the C-terminus in Figure 3.1(e),  $z_1''$  and  $z_n'$ ,  $n = 2-6$ , are produced. The isotopically labeled peptide \*AAAAAAR, with a  $^{13}C$  on the methyl group of the N-terminal residue, was used to distinguish the  $z_1''$  from  $c_2''$  and  $z_n'$  from  $c_{n+1}'$ , because these ion series have the same nominal  $m/z$ . When the position of arginine residue changes from the N-terminus to the C-terminus, the fragment ions change from a complete  $c_n''$  series to a complete  $z_n'$  series.

Figure 3.2 contains the ETD spectra of  $[M+2H]^{2+}$  from K\*AAAAAA, AKAAAAA, AAKAAA, AAAAKA and AAAAAK. The product ions are again primarily members of the  $c''$ -and  $z'$ -series, along with some ammonia loss species. The majority of the ETD product ions contain a lysine residue. When lysine is at the N-terminus in Figure 3.2(a), a complete series of  $c_n''$ ,  $n = 1-6$ , is produced. Lysine at the second position, in Figure 3.2(b), yields  $c_n''$ ,  $n = 2-6$ ,  $a_6'$  and  $z_6'$ . When lysine is located at the fourth position in Figure 3.2(c),  $c_n''$ ,  $n = 4-6$ , and



**Figure 3.1.** ETD mass spectra of  $[M+2H]^{2+}$  from (a) RAAAAAA, (b) ARAAAAA, (c) AAARAAA, (d) AAAAARA, and (e) \*AAAAAAR. The asterisk indicates that the N-terminal alanine residue has  $^{13}\text{C}$  substitution at its methyl side chain





**Figure 3.2.** ETD mass spectra of  $[M+2H]^{2+}$  from (a) K\*AAAAAA, (b) AKAAAAA, (c) AAKAAAA, (d) AAAAAKA, and (e) AAAAAAK. The asterisk indicates that the first alanine residue has  $^{13}\text{C}$  substitution at its methyl side chain.

$z_n'$ ,  $n = 4-6$ , form. Lysine is the sixth residue in Figure 3.2(d), where  $c_5''$ ,  $c_6''$  and  $z_n'$ ,  $n = 2-6$ , form. When lysine is located at the C-terminus in Figure 3.2(e),  $c_5''$ ,  $c_6''$  and  $z_n'$ ,  $n = 2-6$ , are produced. When the lysine residue is changed from the N-terminus to the C-terminus, the ETD product ions again change from the  $c_n''$  series to an almost complete  $z_n'$  series.  $^{13}\text{C}$ -labeled  $\text{K}^*\text{AAAAAA}$  was used to confirm the identity of product ions due to  $m/z$ -overlap of  $c_n''$  with  $z_{n+1}''$ ,  $n=1-5$ .

Figure 3.3 shows the ETD spectra of  $[\text{M}+2\text{H}]^{2+}$  from HAAAAAA, AHAAAAA, AAAHAAA, AAAAAHA, and AAAAAAH. The product ions are mainly  $c''$  and  $z'$  ions, and some ammonia loss is also observed. Histidine at the N-terminus, in Figure 3.3(a), produces a series of  $c_n''$ ,  $n = 2-6$  and also  $c_1'$ . Histidine at the second position of the heptapeptide in Figure 3.3(b), yields  $c_n''$ ,  $n = 2-6$ , and  $z_6'$ . When histidine is located at the fourth position in Figure 3.3(c),  $c_n''$ ,  $n = 4-6$ , and  $z_n'$ ,  $n = 4-6$ , are produced. Histidine is the sixth residue, in Figure 3.3(d), generates  $c_5''$ ,  $c_6''$ ,  $z_n'$ ,  $n = 2-6$ . In Figure 3.3(e), when histidine is at the C-terminus,  $c_5''$ ,  $c_6''$  and  $z_n'$ ,  $n = 2-6$ , are produced. With of the histidine residue is changed from the N-terminus to C-terminus, the ETD product ions are also changed from  $c_n''$  to primarily  $z_n'$ . The majority of the product ions contain the histidine residue; the only products without a histidine residue are  $c_5''$  from AAAAAHA [Figure 3.3(d)] and  $c_5''$  and  $c_6''$  from AAAAAAH [Figure 3.3(e)].

Heptapeptides with the basic residue in the second position were investigated because Liu and Håkansson suggested that a histidine in this position might enhance b-ion formation.<sup>29</sup> These researchers found that the hexapeptide WHWLQL produced abundant b-ions in ECD. They suggested that Coulombic repulsion would result in one proton being located near the N-terminus in the precursor ion (at either W or H) and that the second proton resided along the



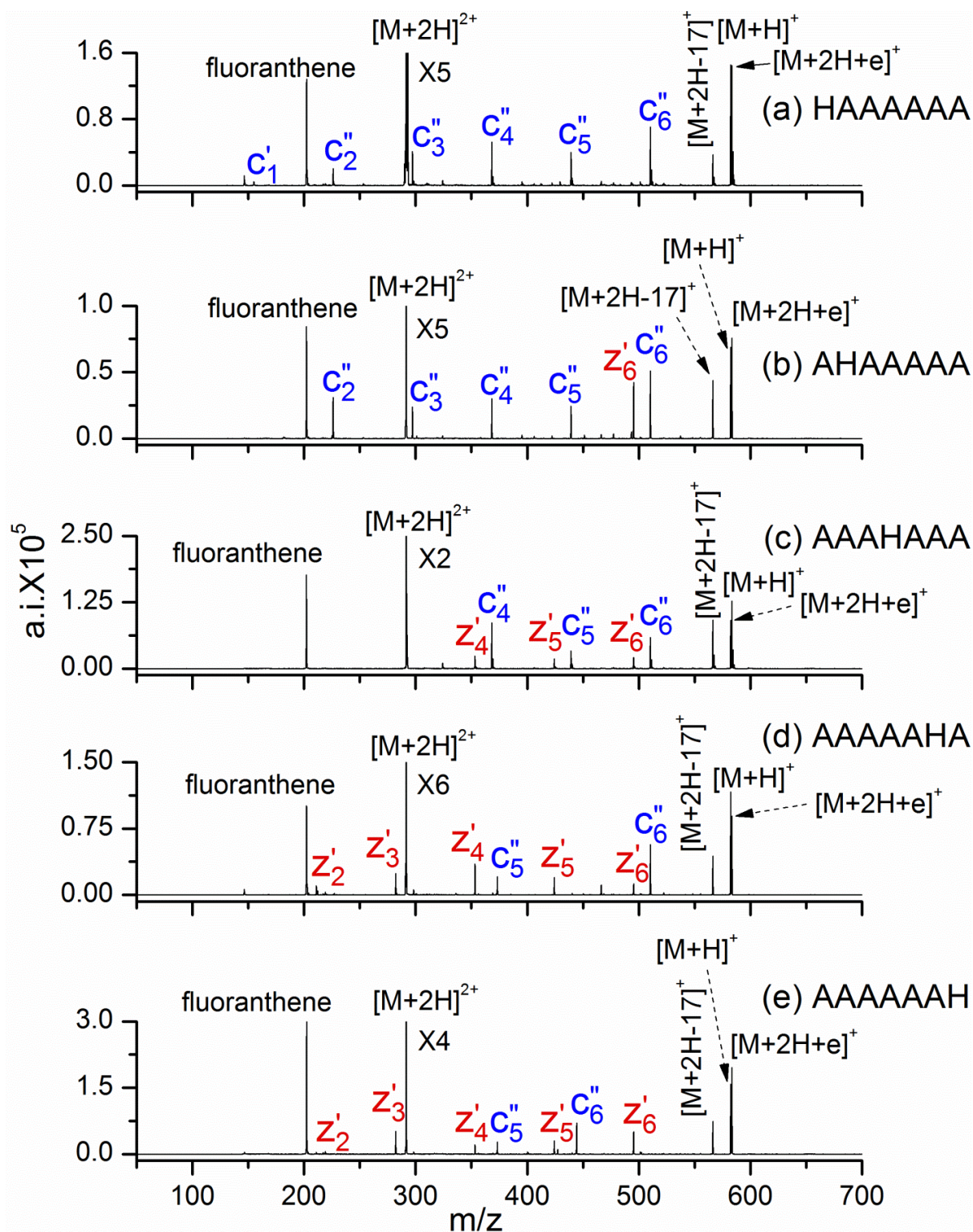


**Figure 3.3.** ETD mass spectra of  $[M+2H]^{2+}$  from (a) HAAAAAA, (b) AHAAAAA, (c) AAAHAAA, (d) AAAAAHA, and (e) AAAAAAH.

peptide backbone and facilitated the production of b- and y-ions.<sup>42</sup> However, in Figure 3.3(b), all the backbone cleavage products are c- and z-ions. Therefore, the histidine residue does not promote b-ion production in the peptide AHAAAAA.

For all of the basic model peptides, ETD produces extensive c'' and z' ions. As the basic residue's position moves from the N-terminus to the C-terminus, fewer c-ions are produced and more z-ions are formed. The presence of some high intensity a-, b-, and y-ions in the ECD spectra of basic peptides has been reported.<sup>29,43,44</sup> In our present ETD study, no b- and y-ions were observed and there was only one low intensity ion that might be a member of the a-series [a<sub>6</sub>' from AKAAAAA shown in Figure 3.2(b)] . This suggests that the formation of a-, b-, and y-ions in ETD and ECD may not only relate to the basic residue's identity and position, but also to the overall composition of amino acid residues in the peptide.

### **3.3.2 Effect of the Identity of the Basic Residue on ETD**

When a peptide contains a highly basic arginine residue, all of the ETD product ions include the arginine residue. For peptides with lysine and histidine residues, most (but not all) product ions contain the basic residue. In an ECD study, Cederquist and coworkers<sup>27</sup> also found that for model pentapeptides containing alanine, glycine, and lysine residues, each product ion contains a lysine residue. The reason is undoubtedly that lysine residues have a higher GB than alanine and glycine residues. Peptides with lysine and histidine residues show very similar fragmentation by ETD, which may be due to the nearly identical GBs for these amino acids. The GB for arginine is 240.58 kcal/mol, histidine is 227.1 kcal/mol and lysine is 227.3 kcal/mol.<sup>45-47</sup> The ETD spectra of our model heptapeptides with N-terminal basic residues contain the entire c<sub>1-6</sub>'' product ion distribution, which is especially useful for sequencing.

In our experiments, arginine-containing peptides produce only c- and z-ions and all ETD backbone cleavage products contain the arginine residue. Cooper and coworkers pointed out that peptides containing only one basic residue and no nitrotyrosine residue will follow the Cornell<sup>32</sup> or UW<sup>36,37</sup> mechanisms for electron-induced fragmentation.<sup>48</sup> According to the calculations of Tureček and coworkers, the guanidinium group of arginine more readily abstracts a hydrogen atom as opposed to serving as a hydrogen atom donor.<sup>18</sup> There is a large energy barrier for hydrogen atom transfer from the guanidinium group of arginine to a backbone carbonyl oxygen to form an aminoketyl intermediate. The initial step of the Cornell mechanism is this hydrogen atom transfer, which cannot occur for arginine because of the large energy barrier. Therefore, the Cornell mechanism does not apply to peptides with arginine residues and such peptides most likely obey the UW mechanism. In the UW mechanism, an electron is captured in a Coulomb stabilized amide  $\pi^*$  orbital and a mobile hydrogen atom migration from the C $_{\alpha}$  position of the peptide backbone to the guanidyl group of arginine occurs.<sup>18</sup> The radical intermediate formed will initiate hydrogen abstraction from the  $\alpha$ -carbon<sup>49</sup> and a free radical reaction cascade will occur.<sup>50</sup> Under the UW mechanism, arginine residues are charge carriers (i.e., protonated) and this could explain why all of the ETD product ions contain arginine.

For peptides with lysine and histidine residues, backbone cleavage may be under the Cornell<sup>32</sup> or UW<sup>36,37</sup> mechanisms. In our experiments, almost all of the product ions contain a basic residue. In the UW mechanism, basic amino residues are protonated and, consequently, ETD backbone cleavage ions should preferentially contain basic residues. In the Cornell mechanism, an electron is captured by the amide side chain of lysine. The resulting hydrogen atom is transferred to backbone carbonyl oxygen to initiate backbone cleavage. A similar process occurs with histidine (but not arginine). In the Cornell mechanism, the lysine and

histidine side chains do not need to be protonated. Therefore, the Cornell mechanism may result in the formation of a few product ions that do not contain lysine or histidine. In our spectra, the following product ions that do not contain the basic residue are observed:  $c_5''$  from AAAAAHA, AAAAAAH, AAAAAKA, and AAAAAAK;  $c_6''$  from AAAAAAH and AAAAAAK.

All of our spectra show elimination of ammonia,  $\text{NH}_3$  (17 Da). From our data, it cannot be determined if the ammonia originates from the N-terminal amino group or the side chains of the basic residues. Liu and Håkansson found that the ECD spectra of peptides without basic residues exhibit products with ammonia loss.<sup>29</sup> For the peptide SDKPDMAEIEKFDK, Coon and coworkers found that ammonia elimination occurs when the N-terminus is unprotected but not when the N-terminus is acetylated.<sup>24</sup> This provides evidence that the ammonia molecule can originate from the N-terminal amino group.

Arginine residues exhibit prominent neutral molecule loss from the side chain, with the elimination of  $\text{CH}_5\text{N}_3$  (59 Da) and  $\text{CH}_3\text{N}_2^\bullet$  (43 Da) occurring from the doubly protonated precursor ions. No characteristic side chain loss was observed for histidine and lysine residues. McLuckey and coworkers observed similar results for peptides containing the three basic residues.<sup>19</sup> In an ECD study, two different groups, Marshall and coworkers<sup>26</sup> as well as Chan and coworkers<sup>51</sup> found that arginine residues had side chain losses of  $\text{C}_4\text{H}_{11}\text{N}_3$  (101.093Da),  $\text{CH}_5\text{N}_3$  (59.045 Da),  $\text{CH}_4\text{N}_2$  (44.033 Da), and  $\text{CH}_3\text{N}_2^\bullet$  (43.029Da), histidine residues underwent a side chain loss of  $\text{C}_4\text{H}_6\text{N}_2$  (82.053), while lysine residues had a side chain loss of  $\text{C}_4\text{H}_{11}\text{N}$  (73.089). Tureček and coworkers calculated the energy for hydrogen transfer from the side chains of arginine, lysine, and histidine to the backbone amide carbonyl group.<sup>13,18,52</sup> Their calculations show that arginine has an inverse migration for a hydrogen atom from the peptide backbone to the side chain; this process increases the likelihood of side chain cleavage. Their calculations

also indicate that hydrogen atom transfer for the lysine side chain to the backbone is very facile, which decreases the possibility of lysine undergoing a side chain cleavage. Histidine has a stable imidazole group on the side chain that is difficult to cleave. The side chain losses of arginine that are present in the ETD spectra are useful in determining if arginine residues are present in a peptide sequence.

For peptides containing histidine residues, an electron transfer without dissociation (ET no D) product forms,  $[M+2H+e]^{++}$ . This process was not observed for peptides with lysine or arginine residues. McLuckey and coworkers have suggested that the ET no D product of histidine may be due to stability of the methylimidazolium side chain, which could delocalize the nearby radical.<sup>19</sup> Tureček and coworkers<sup>53</sup> have further pointed out that the relative intensity of  $[M+2H+e]^+$  depends on the peptide sequence and the number of histidine residues.

### 3.3.3 Preferential Cleavages

Most of the peptides studied here have previously been studied in our laboratory by low energy CID using a Fourier transform ion cyclotron resonance mass spectrometer (FT-ICR MS).<sup>15</sup> While the vast majority of the ETD product ions contain the basic residues, this is not the case in CID. For these peptides, CID produces a mixture of a-, b-, and y-ions both with and without the basic residue. In addition, for CID cleavage is favored adjacent to the basic residue at either the C-terminal or N-terminal side, with this effect being most pronounced for the highly basic arginine residues. While not as prominent, the ETD spectra show an increased intensity of cleavage adjacent to basic residues; for example, the enhanced abundance of  $c_4''$  from  $[M+2H]^{2+}$  of AAARAAA [Figure 3.1(c)], AAKKAAA [Figure 3.2(c)], and AAHHAAA [Figure 3.3(c)]. This enhancement may be explained by the inhibition of the mobile proton by the side chain of the basic residue.<sup>11,16,17</sup>

For several of the peptides, a relatively intense  $c_6''$  occurs in the ETD spectra that is independent of the position and identity of the basic residue. For example, enhanced  $c_6''$  is produced from RAAAAAA, ARAAAAA, AAAAARA, HAAAAAA, AHAAAAA, AAAAAHA, AAAAAAH, AKAAAAA and AAAAAKA. This is not an order of magnitude intensity enhancement as observed in the CID spectra,<sup>15</sup> but the intensity of  $c_6''$  is generally about 50-100 % greater than expected based on other ion intensities in the ETD spectra. In order to determine if the size of the neutral ETD product influences  $c_6''$  formation, the length of the peptide was increased. Figure 3.4 shows the ETD spectrum of  $[M+2H]^{2+}$  for the octapeptide AAKAAAA; the most intense peak is  $c_7''$ . Thus,  $c_6''$  formation is not specifically enhanced, but instead there is an increased production of  $c_{n-1}''$ , where n is the number of residues in the peptide. Because the stability of radical species generally increases as the size of the molecule increases,<sup>54</sup> it is unlikely that enhanced  $c_{n-1}''$  is a result of an increased stability of the neutral product, which in this case is  $C_3H_5O_2\bullet$ . Instead, the preferential formation of  $c_{n-1}''$  may be due to a slightly greater ability of a C-terminal residue to coordinate to the basic site and initiate c-ion formation. Figure 3.5 shows the mechanism for c-ion formation first proposed by McLafferty and co-workers.<sup>32</sup> An electron is captured on the side chain of a basic residue and, via interaction with a carbonyl oxygen, a hydrogen atom is transferred to the oxygen. A greater conformational flexibility of the C-terminal residue may result in a slight preference for coordination to the terminal carbonyl group.



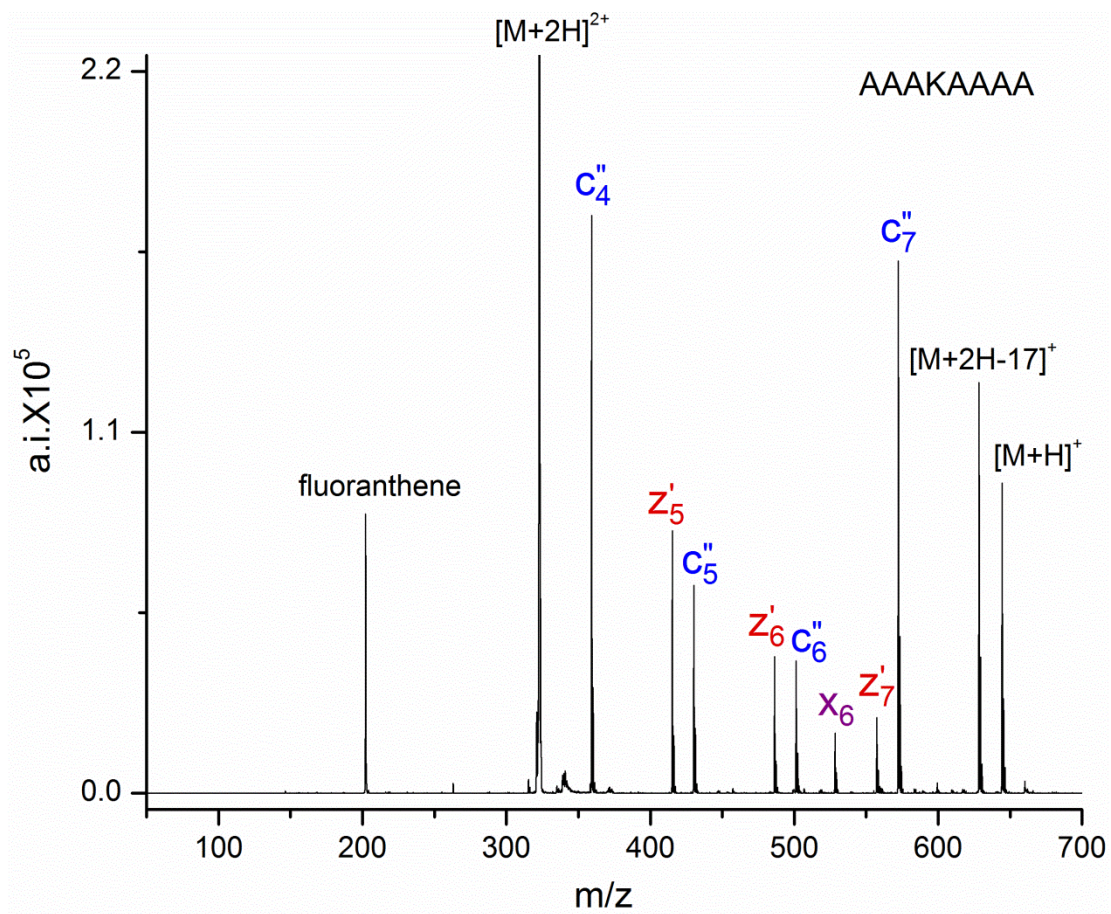


**Figure 3.4.** ETD mass spectrum of  $[M+2H]^{2+}$  from AAKKAAAA.

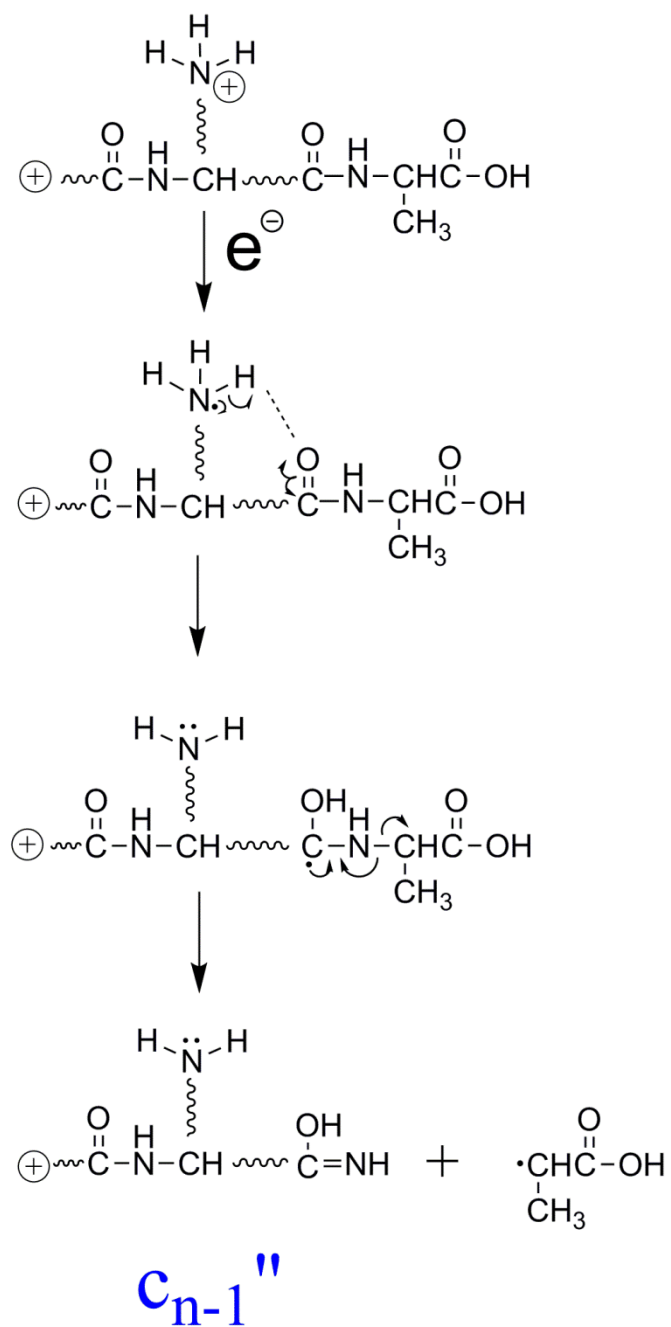


**Figure 3.5.** Scheme for  $c_{n-1}''$  ion formation from basic peptides.

### 3.4 Conclusions

In ETD, heptapeptides with one basic residue produce primarily  $c''$  and  $z'$  ions. Almost all the ETD products ions contain the basic residue, suggesting that the side chains of arginine, histidine, and lysine contain a charge site. In addition, side chain cleavage from arginine residues occurs and may be useful in detecting the presence of arginine residues in peptides. Histidine residues promote the formation of an electron transfer without dissociation product. In general, the presence of basic residues results in preferential cleavage at neighboring C-terminal or N-terminal residues. As was confirmed by ETD on an octapeptide, formation of  $c_{n-1}''$  is also enhanced slightly. When the basic residue is at the N-terminus, a complete series of  $c''$  ions is produced that may be very useful for sequencing.

## References

1. Tabb, D. L.; Huang, Y.; Wysocki, V. H.; Yates, J. R. Influence of Basic Residue Content on Fragment Ion Peak Intensities in Low-Energy Collision-induced Dissociation Spectra of Peptides. *Anal. Chem.* **2004**, *76*, 1243-1248.
2. Bensadek, D.; Monigatti, F.; Steen, J. A. J.; Steen, H. Why b, y's? Sodiation-induced Tryptic Peptide-Like Fragmentation of Non-Tryptic Peptides. *Int. J. Mass Spectrom.* **2007**, *268*, 181-189.
3. Sun, R.; Dong, M.; Song, C.; Chi, H.; Yang, B.; Xiu, L.; Tao, L.; Jing, Z.; Liu, C.; Wang, L.; Fu, Y.; He, S. Improved Peptide Identification for Proteomic Analysis Based on Comprehensive Characterization of Electron Transfer Dissociation Spectra. *J. Proteome Res.* **2010**, *9*, 6354-6367.
4. Kalli, A.; Håkansson, K. Electron Capture Dissociation of Highly Charged Proteolytic Peptides from Lys N, Lys C and Glu C Digestion. *Mol. BioSyst.* **2010**, *6*, 1668-1681.
5. Coon, J. J. Collisions or Electrons? Protein Sequence Analysis in the 21st Century. *Anal. Chem.* **2009**, *81*, 3208-3215.
6. Syka, J. E. P.; Coon, J. J.; Schroeder, M. J.; Shabanowitz, J.; Hunt, D. F. Peptide and Protein Sequence Analysis by Electron Transfer Dissociation Mass Spectrometry. *Proc. Natl. Acad. Sci. USA* **2004**, *101*, 9528-9533.
7. Kjeldsen, F.; Giessing, A. M. B.; Ingrell, C. R.; Jensen, O. N. Peptide Sequencing and Characterization of Post-Translational Modifications by Enhanced Ion-Charging and Liquid Chromatography Electron-Transfer Dissociation Tandem Mass Spectrometry. *Anal. Chem.* **2007**, *79*, 9243-9252.
8. Coon, J., J.; Syka, J. E. P.; Shabanowitz, J.; Hunt, D. F. Tandem Mass Spectrometry for Peptide and Protein Sequence Analysis. *BioTechniques* **2005**, *38*, 519-523.
9. Sasaki, K.; Osaki, T.; Minamino, N. Large-scale Identification of Endogenous Secretory Peptides Using Electron Transfer Dissociation Mass Spectrometry. *Mol. Cell. Proteomics* **2013**, *12*, 700-709.
10. Tang, X.; Thibault, P.; Boyd, R. K. Fragmentation Reactions of Multiply-Protonated Peptides and Implications for Sequencing by Tandem Mass Spectrometry with Low-Energy Collision-Induced Dissociation. *Anal. Chem.* **1993**, *65*, 2824-2834.
11. Vachet, R. W.; Asam, M. R.; Glish, G. L. Secondary Interactions Affecting the Dissociation Patterns of Arginine-Containing Peptide Ions. *J. Am. Chem. Soc.* **1996**, *118*, 6252-6256.
12. Wysocki, V. H.; Tsaprailis, G.; Smith, L. L.; Brei, L. A. Mobile and Localized Protons: A Framework for Understanding Peptide Dissociation. *J. Mass Spectrom.* **2000**, *35*, 1399-1406.

13. Tureček, F.; Chung, T. W.; Moss, C. L.; Wyer, J. A.; Ehlerding, A.; Holm, A. I. S.; Zettergren, H.; Nielsen, S. B.; Hvelplund, P.; Chamot-Rooke, J.; Bythell, B.; Paizs, B. The Histidine Effect. Electron Transfer and Capture Cause Different Dissociations and Rearrangements of Histidine Peptide Cation-Radicals. *J. Am. Chem. Soc.* **2010**, *132*, 10728-10740.
14. Tsybin, Y. O.; Haselmann, K. F.; Emmett, M. R.; Hendrickson, C. L.; Marshall, A. G. Charge Location Directs Electron Capture Dissociation of Peptide Dications. *J. Am. Soc. Mass Spectrom.* **2006**, *17*, 1704-1711.
15. Pu, D.; Clipston, N. L.; Cassady, C. J. A Comparison of Positive and Negative Ion Collision-induced Dissociation for Model Heptapeptides with One Basic Residue. *J. Mass Spectrom.* **2010**, *45*, 297-305.
16. Summerfield, S. G.; Gaskell, S. J. Fragmentation Efficiencies of Peptide Ions Following Low Energy Collisional Activation. *Int. J. Mass Spectrom. Ion Proc.* **1997**, *165*, 509-521.
17. Zhang, X.; Jai-Nhuknan, J.; Cassady, C. J. Collision-Induced Dissociation and Post-Source Decay of Model Dodecapeptide Ions Containing Lysine and Glycine. *Int. J. Mass Spectrom.* **1997**, *171*, 135-145.
18. Chen, X.; Tureček, F. The Arginine Anomaly: Arginine Radicals are Poor Hydrogen Atom Donors in Electron Transfer Induced Dissociations. *J. Am. Chem. Soc.* **2006**, *128*, 12520-12530.
19. Xia, Y.; Gunawardena, H. P.; Erickson, D. E.; McLuckey, S. A. Effects of Cation Charge-Site Identity and Position on Electron-Transfer Dissociation of Polypeptide Cations. *J. Am. Chem. Soc.* **2007**, *129*, 12232-12243.
20. Tsaprailis, G.; Nair, H.; Zhong, W.; Kuppannan, K.; Futrell, J. H.; Wysocki, V. H. A Mechanistic Investigation of the Enhanced Cleavage at Histidine in the Gas-Phase Dissociation of Protonated Peptides. *Anal. Chem.* **2004**, *76*, 2083-2094.
21. van der Rest, G.; Hui, R.; Frison, G.; Chamot-Rooke, J. Dissociation Channel Dependence on Peptide Size Observed in Electron Capture Dissociation of Tryptic Peptides. *J. Am. Soc. Mass Spectrom.* **2011**, *22*, 1631-1644.
22. Zhang, Z. Prediction of Electron-Transfer/Capture Dissociation Spectra of Peptides. *Anal. Chem.* **2010**, *82*, 1990-2005.
23. Mikes, L. M.; Ueberheide, B.; Chi, A.; Coon, J. J.; Syka, J. E. P.; Shabanowitz, J.; Hunt, D. F. The Utility of ETD Mass Spectrometry in Proteomic Analysis. *Biochim. Biophys. Acta.* **2006**, *1764*, 1811-1822.

24. Xia, Q.; Lee, M.; Rose, C.; Marsh, A.; Hubler, S.; Wenger, C.; Coon, J. Characterization and Diagnostic Value of Amino Acid Side Chain Neutral Losses Following Electron-Transfer Dissociation. *J. Am. Soc. Mass Spectrom.* **2011**, *22*, 255-264.
25. Savitski, M. M.; Nielsen, M. L.; Zubarev, R. A. Side-Chain Losses in Electron Capture Dissociation to Improve Peptide Identification. *Anal. Chem.* **2007**, *79*, 2296-2302.
26. Cooper, H. J.; Hudgkins, R. R.; Hakansson, K.; Marshall, A. G. Characterization of Amino Acid Side Chain Losses in Electron Capture Dissociation. *J. Am. Soc. Mass Spectrom.* **2002**, *13*, 241-249.
27. Haag, N.; Holm, A. I. S.; Johansson, H. A. B.; Zettergren, H.; Schmidt, H. T.; Nielsen, S. B.; Hvelplund, P.; Cederquist, H. Electron Capture Induced Dissociation of Doubly Protonated Pentapeptides: Dependence on Molecular Structure and Charge Separation. *J. Chem. Phys.* **2011**, *134*.
28. Cooper, H. J. Investigation of the Presence of b Ions in Electron Capture Dissociation Mass Spectra. *J. Am. Soc. Mass Spectrom.* **2005**, *16*, 1932-1940.
29. Liu, H.; Hakansson, K. Abundant b-Type Ions Produced in Electron Capture Dissociation of Peptides Without Basic Amino Acid Residues. *J. Am. Soc. Mass Spectrom.* **2007**, *18*, 2007-2013.
30. Zubarev, R. A.; Kruger, N. A.; Fridriksson, E. K.; Lewis, M. A.; Horn, D. M.; Carpenter, B. K.; McLafferty, F. W. Electron Capture Dissociation of Gaseous Multiply-Charged Proteins is Favored at Disulfide Bonds and Other Sites of High Hydrogen Atom Affinity. *J. Am. Chem. Soc.* **1999**, *121*, 2857-2862.
31. Axelsson, J.; Palmblad, M.; Hakansson, K.; Hakansson, P. Electron Capture Dissociation of Substance P Using a Commercially Available Fourier Transform Ion Cyclotron Resonance Mass Spectrometer. *Rapid Commun. Mass Spectrom.* **1999**, *13*, 474-477.
32. Zubarev, R. A.; Kelleher, N. L.; McLafferty, F. W. Electron Capture Dissociation of Multiply Charged Protein Cations. A Nonergodic Process. *J. Am. Chem. Soc.* **1998**, *120*, 3265-3266.
33. McLafferty, F. W.; Horn, D. M.; Breuker, K.; Ge, Y.; Lewis, M. A.; Cerda, B. A.; Zubarev, R. A.; Carpenter, B. K. Electron Capture Dissociation of Gaseous Multiply Charged Ions by Fourier Transform ion Cyclotron Resonance. *J. Am. Soc. Mass Spectrom.* **2001**, *12*, 245-249.
34. Lin, C.; Cournoyer, J. J.; O'Connor, P. B. Use of a Double Resonance Electron Capture Dissociation Experiment to Probe Fragment Intermediate Lifetimes. *J. Am. Soc. Mass Spectrom.* **2006**, *17*, 1605-1615.

35. Savitski, M. M.; Kjeldsen, F.; Nielsen, M. L.; Zubarev, R. A. Hydrogen Rearrangement to and from Radical z Fragments in Electron Capture Dissociation of Peptides. *J. Am. Soc. Mass Spectrom.* **2007**, *18*, 113-120.
36. Sobczyk, M.; Anusiewicz, I.; Berdys-Kochanska, J.; Sawicka, A.; Skurski, P.; Simons, J. Coulomb-Assisted Dissociative Electron Attachment: Application to a Model Peptide. *J. Phys. Chem. A* **2005**, *109*, 250-258.
37. Syrtstad, E. A.; Tureček, F. Toward a General Mechanism of Electron Capture Dissociation. *J. Am. Soc. Mass Spectrom.* **2005**, *16*, 208-224.
38. Chan, W. C.; White, P. D. *Fmoc Solid Phase Peptide Synthesis A Practical Approach*; Oxford University Press Inc., New York: 2000.
39. Swaney, D. L.; McAlister, G. C.; Wirtala, M.; Schwartz, J. C.; Syka, J. E. P.; Coon, J. J. Supplemental Activation Method for High-Efficiency Electron-Transfer Dissociation of Doubly Protonated Peptide Precursors. *Anal. Chem.* **2007**, *79*, 477-485.
40. Hamidane, H. B.; Chiappe, D.; Hartmer, R.; Vorobyev, A.; Moniatte, M.; Tsybin, Y. O. Electron Capture and Transfer Dissociation: Peptide Structure Analysis at Different Ion Internal Energy Levels. *J. Am. Soc. Mass Spectrom.* **2009**, *20*, 567-575.
41. Roepstorff, P.; Fohlman, J. Proposal for a Common Nomenclature for Sequence Ions in Mass Spectra of Peptides. *Biomed. Mass Spectrom.* **1984**, *11*, 601.
42. Bakken, V.; Helgaker, T.; Uggerud, E. Models of Fragmentations Induced by Electron Attachment to Protonated Peptides. *Eur. J. Mass Spectrom.* **2004**, *10*, 625-638.
43. Cooper, H. J.; Hudgins, R. R.; Håkansson, K.; Marshall, A. G. Secondary Fragmentation of Linear Peptides in Electron Capture Dissociation. *Int. J. Mass Spectrom.* **2003**, *228*, 723-728.
44. Zubarev, R.; Good, D.; Savitski, M. Radical a-Ions in Electron Capture Dissociation: On the Origin of Species. *J. Am. Soc. Mass Spectrom.* **2012**, *23*, 1015-1018.
45. P. J. Linstrom., W. G. Mallard. NIST standard reference database 69: *NIST Chemistry WebBook*. (accessed Aug 20, 2014).
46. Carr, S. R.; Cassady, C. J. Gas-Phase Basicities of Histidine and Lysine and their Selected Di- and Tripeptides. *J. Am. Soc. Mass Spectrom.* **1996**, *7*, 1203-1210.
47. Harrison, A. G. The Gas-Phase Basicities and Proton Affinities of Amino Acids and Peptides. *Mass Spectrom. Rev.* **1997**, *16*, 201-217.
48. Jones, A. W.; Cooper, H. J. Probing the Mechanisms of Electron Capture Dissociation Mass Spectrometry with Nitrated Peptides. *Phys. Chem. Chem. Phys.* **2010**, *12*, 13394-13399.

49. O'Connor, P. B.; Lin, C.; Cournoyer, J. J.; Pittman, J. L.; Belyayev, M.; Budnik, B. A. Long-Lived Electron Capture Dissociation Product Ions Experience Radical Migration Via Hydrogen Abstraction. *J. Am. Soc. Mass Spectrom.* **2006**, *17*, 576-585.
50. Leymarie, N.; Costello, C. E.; O'Connor, P. B. Electron Capture Dissociation Initiates a Free Radical Reaction Cascade. *J. Am. Chem. Soc.* **2003**, *125*, 8949-8958.
51. Fung, Y. M. E.; Chan, T. D. Experimental and Theoretical Investigations of the Loss of Amino Acid Side Chains in Electron Capture Dissociation of Model Peptides. *J. Am. Soc. Mass Spectrom.* **2005**, *16*, 1523-1535.
52. Tureček, F. NC $\alpha$  Bond Dissociation Energies and Kinetics in Amide and Peptide Radicals. Is the Dissociation a Non-ergodic Process? *J. Am. Chem. Soc.* **2003**, *125*, 5954-5963.
53. Chung, T. W.; Tureček, F. Amplified Histidine Effect in Electron-Transfer Dissociation of Histidine-Rich Peptides from Histatin 5. *Int. J. Mass Spectrom.* **2011**, *306*, 99-107.
54. Vollhardt, K.; Schore, N. E. In *Reactions of Alkanes: Bond-Dissociation Energies, Radical Halogenation, and Relative Reactivity*; Organic Chemistry; W. H. Freeman and Company: New York, 1998; pp 94-98.



## **CHAPTER 4: THE USE OF CHROMIUM(III) TO SUPERCHARGE PEPTIDES BY PROTONATION AT THE PEPTIDE BACKBONE**

### **4.1 Introduction**

The ability to protonate a molecule using electrospray ionization (ESI)<sup>1</sup> or matrix-assisted laser desorption ionization (MALDI)<sup>2</sup> is an important step in the structural analysis of peptides and other biomolecules by mass spectrometry. While MALDI produces almost exclusively singly charged ions from smaller biomolecules, ESI has the ability to produce multiply charged ions. In the sequencing of peptides and proteins by tandem mass spectrometry (MS/MS),<sup>3-5</sup> multiple charging can have several advantages. These include shifting the  $m/z$  of ions to a range of the spectrum where resolution is optimal<sup>6</sup> and increasing the ion intensity for mass spectrometers in which the signal detected is proportional to charge.<sup>7,8</sup> In addition, higher charge state ions from peptides and proteins generally require less energy to initiate dissociation and often provide more sequence-informative fragmentation than lower charge state ions.<sup>9-12</sup>

The ability to multiply charge a peptide is particularly important for the MS/MS techniques electron capture dissociation (ECD)<sup>13-15</sup> and electron transfer dissociation (ETD)<sup>16-18</sup>. In ECD and ETD, an electron is transferred to the precursor ion, resulting in a radical species that dissociates to yield structurally-informative product ions. ETD and ECD generally require that the precursor ion be multiply positively charged because addition of an electron to a singly charged ion forms a neutral species whose dissociation products are also neutrals and are not detected by mass spectrometry. An issue that has somewhat limited the utility of ECD and ETD in proteomics research is that acidic or neutral peptides may not doubly (or sometimes even

singly) protonate by ESI.<sup>19</sup> However, the analysis of natural and post-translational peptides containing acidic groups is important. For example, acidic peptides are common in biological processes related to neurology,<sup>20-22</sup> blood coagulation,<sup>23,24</sup> and HIV infection.<sup>25</sup> In addition, acidic peptides have been studied as potential vaccines for malaria<sup>26</sup> and HIV.<sup>27,28</sup>

Williams and coworkers<sup>29</sup> have developed a method for increasing the protonation of biomolecules by the addition of “supercharging” reagents to the solution being electrosprayed. The supercharging reagent is usually a small organic molecule and its presence causes the number of protons added to the analyte to increase, leading to more highly charged ions. Compounds found to promote supercharging include m-nitrobenzyl alcohol (m-NBA),<sup>29-32</sup> glycerol,<sup>32</sup> tetramethylene sulfone (sulfolane),<sup>33-35</sup> dimethyl sulfoxide (DMSO),<sup>36</sup> dimethylformamide (DMF),<sup>37</sup> and several benzyl alcohol and nitrobenzene derivatives.<sup>34</sup> These organic reagents enrich in concentration as the more volatile solvent evaporates during ESI. One mechanism proposed for supercharging is that enrichment affects the physical properties of the ESI droplet, which in turn results in changes to the conformation of the molecule under study.<sup>35,36,38,39</sup> A consequence of a more open (unfolded) conformation for a peptide or protein is that a greater number of basic sites are accessible to protons and the charge state distribution produced by ESI increases. An alternative mechanism, involving interaction of the supercharging reagent with the biomolecule, has been proposed by several groups.<sup>33,40,41</sup> Flick and Williams have also reported that lanthanum(III) chloride can supercharge proteins.<sup>41</sup> In addition, an electrothermal supercharging method has been developed that involves ESI from aqueous ammonium or sodium salt solutions, with the extent of protonation being dependent on solution conditions and on the ESI capillary temperature and spray potential.<sup>42-44</sup> A unique feature of electrothermal supercharging is that the number of protons added to the protein is

often greater than the number of highly basic sites; in contrast, organic supercharging reagents normally do not protonate beyond the number of highly basic sites on the protein or peptide.

The majority of supercharging studies have involved proteins. Only three studies<sup>11,12,45</sup> have included smaller peptides. Madsen and Brodbelt<sup>12</sup> used m-NBA to increase the charge on ions produced for a peptide with twelve residues; however, the number of protons added did not exceed the number of basic residues. Jensen and coworkers<sup>11</sup> incorporated 0.1% m-NBA into the solvent system during a liquid chromatography (LC) analysis of 33 peptides from a tryptic digest. They found that the average charge state for the peptide ions increased by approximately +0.25. Consequently, many peptides could be dissociated from the 3+ charge state rather than 2+, which caused an increase in ETD fragmentation efficiency and a better success rate in identifying the peptide sequences. (With the exception of a 16-residue peptide, these peptides did not protonate in excess of the number of highly basic sites in their sequences.) Tysbin and coworkers<sup>45</sup> demonstrated a dual-sprayer process for supercharging using several large proteins and also substance P, an 11-residue peptide that has three highly basic sites. The intensity of the 3+ charge state for substance P was tripled, but additional protonation along the backbone to form more highly charged ions did not occur.

During a recent study of the collision-induced dissociation (CID) of peptides cationized by the addition of metal salts to the electrosprayed solution, we noted that Cr(III) nitrate,  $\text{Cr}(\text{NO}_3)_3$ , causes the neutral peptide heptaalanine (A7) to doubly protonate.<sup>46</sup> In contrast, when Cr(III) is not present in the solution, A7 produces exclusively singly charge peptide,  $[\text{M}+\text{H}]^+$ . This formation of  $[\text{M}+2\text{H}]^{2+}$  was unexpected because A7 has only one highly basic site, the N-terminal amino group. In general, ESI protonates peptides at only the most basic sites, which are the N-terminal amino group and the side chains of arginine, lysine, and histidine residues.<sup>47</sup>

(Although this generalization does not always hold true, the exceptions are usually proteins and not small peptides.<sup>48,49</sup>) Because the side chain of alanine is a methyl group that will not protonate, the second proton must be located at an amide group of the peptide backbone.

In the present study, the use of Cr(III) as a supercharging reagent for small peptides is explored. Several other metal ions are also evaluated as supercharging reagents, although none proved to be as effective as Cr(III).

## **4.2 Experimental**

### **4.2.1 Peptides and Reagents**

The peptides A7, AAAAAGA, and EEEEGDD were purchased from Biomatik (Cambridge, Ontario, CA). Cytochrome c from bovine heart (12.3 kDa) was purchased from Sigma-Aldrich (St. Louis, MO, USA). All other peptides were synthesized in our laboratory with an Advanced ChemTech (Louisville, KY, USA) Model 90 automated peptide synthesizer using standard Fmoc procedures.<sup>50</sup> The peptides were used as synthesized, without further purification (which accounts for impurity peaks in the mass spectra shown). All peptide synthesis reagents were purchased from Advanced ChemTech or VWR (Radnor, PA, USA). Peptide methyl esters were produced by acid-catalyzed esterification with methanol, as discussed in Chapter 2.<sup>51</sup>

All metal salts were purchased from VWR or Thermo Fisher Scientific (Waltham, MA, USA). The organic supercharging reagents, DMSO and m-NBA, and the ESI solvents, HPLC grade acetonitrile and methanol, were also purchased from VWR. Deionized and distilled water was produced with a Barnstead E-pure system (Dubuque, IA, USA).

Peptides and proteins were dissolved to 1 mg/ml in a solvent of methanol:water at a 50:50 volume ratio. From these stock solutions, the solutions studied by ESI were generated at a concentration of 10  $\mu$ M in acetonitrile:water at a volume ratio of 50:50. Prior to ESI, metal salts or acids were added to these peptide solutions at the concentrations discussed below. The pH of the solutions being electrosprayed was measured with a Thermo Scientific Orion pH meter.

#### **4.2.2 Mass Spectrometry**

All studies were performed using a Bruker (Billerica, MA, USA) HCTultra PTM Discovery System high capacity quadrupole ion trap mass spectrometer. The ESI source has a grounded needle, and a high voltage of -3.5 kV was placed on the capillary entrance and endplate. The capillary exit voltage was 103 V. The drying gas was nitrogen with a temperature of 300°C and a flow rate of 5-10 L/min. The nebulizer gas was also nitrogen and the pressure was optimized between 5-10 psi to obtain the best ESI signal. Samples were infused at a flow rate of 2.5  $\mu$ L/min with a KD Scientific (Holliston, MA, USA) syringe pump. Single stage mass spectra were acquired in the positive ion mode. All the spectra shown here were obtained from signal averaging of 200 scans. The ETD experiment for EEEEGDD was also performed on this instrument using conditions reported elsewhere.<sup>52</sup>

For nanospray (nanoESI) experiments, sample was introduced using a syringe pump connected to fused silica transfer tubing (360  $\mu$ m x 50  $\mu$ m) and emitters (360  $\mu$ m x 75  $\mu$ m x 15  $\mu$ m). NanoESI emitters were purchased from New Objective (Woburn, MA, USA). A sample flow rate of 5-20  $\mu$ L/h was employed. There was no nebulizer gas. Nitrogen was the drying gas, used at a temperature of 120-150 °C and a flow rate of 3-10 L/min.

## 4.3 Results and Discussion

### 4.3.1 Effects of Selected Metal Ions on Supercharging of A7

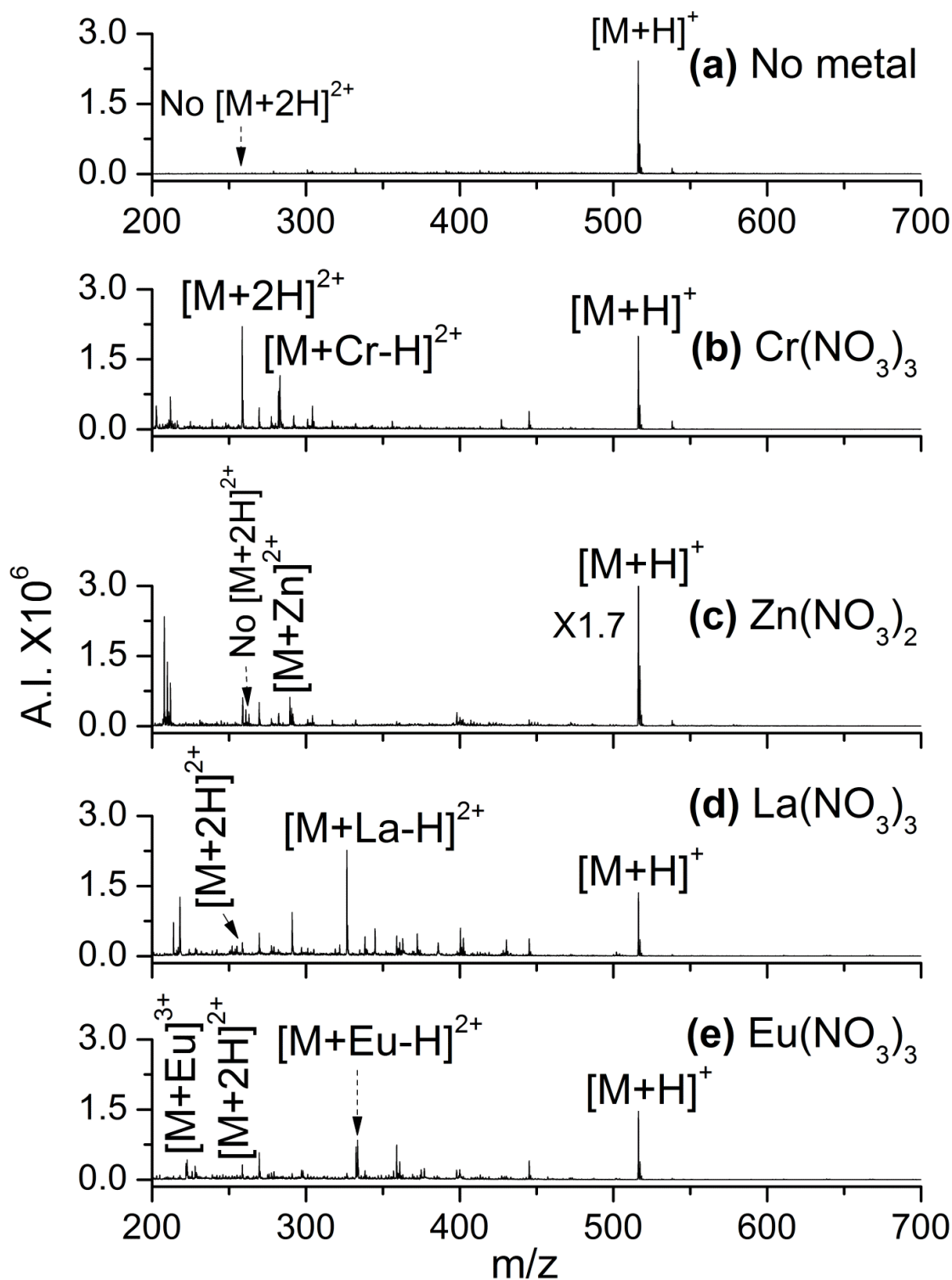
Heptaalanine, A7, was employed as the test peptide to study the ability of various metal ions to promote supercharging. Trivalent salts of aluminum (Al), chromium (Cr), iron (Fe), rhodium (Rh), lanthanum (La), and europium (Eu) were studied, as well as a tetravalent salt of cerium (Ce) and divalent salts of manganese (Mn), iron (Fe), copper (Cu), and zinc (Zn). Table 4.1 lists the metal salts studied and provides absolute signal intensity of  $[M+2H]^{2+}$  for several replicate trials using solutions with a peptide concentration of 10  $\mu$ M and a metal ion concentration of 100  $\mu$ M (metal:peptide molar ratio of 10:1). Table 4.1 also includes the measured pH for all solutions, information on the intensities of metal adduct ions found in the mass spectra, and reference values for pertinent physical properties of the metal ions.

Figure 4.1 shows typical mass spectra obtained for several mixtures of A7 with metal salts. For comparison, Figure 4.1(a) provides the ESI mass spectrum of a 10  $\mu$ M solution of A7 in a solvent system of 50:50 acetonitrile:water with no added metal ion. In the absence of metal ion,  $[M+2H]^{2+}$  is not produced. As seen in Figure 4.1(b), the presence of Cr(III) causes  $[M+2H]^{2+}$  to form in an intensity roughly equal to that of  $[M+H]^+$ . Addition of the other metal ions generally produces  $[M+2H]^{2+}$ , but in an intensity too low to be analytically useful; see, for example, the spectra of Figure 4.1(c)-(e). Mn(II), Zn(II), and Rh(III) are the only metal ions investigated that do not generate  $[M+2H]^{2+}$ . Although not included in the current study, Co(II), Ni(II), and Cu(I) did not significantly supercharge A7 in our previous study of CID of metal-A7 adducts.<sup>46</sup>

**Table 4.1.** Absolute signal intensity for  $[M+2H]^{2+}$  from heptaalanine (A7), pH of the solutions, and properties of the metal ions.

Metal Salt	Atomic Number of Metal	Ionic Charge	Coordination Number of Metal <sup>a</sup>	Metal Adducts in ESI MS Spectra <sup>b</sup>	$[M+2H]^{2+}$ Absolute Intensity ( $\times 10^5$ ), $\bar{x} \pm s$	pH of Solution, $\bar{x} \pm s$	$pK_1^c$	$E^0, V^d$	Residence Time, $\mu s^e$	Ionic Radius, $pm^f$	Hydrated Ionic Radius, $pm^g$
Al(NO <sub>3</sub> ) <sub>3</sub> •9H <sub>2</sub> O	13	3+	4,5,6	n	1.5±1.4	4.3±0.1	4.97	– <sup>h</sup>	6.3 x 10 <sup>6</sup>	67.5	450
CrCl <sub>3</sub> •6H <sub>2</sub> O	24	3+	6	m	7.9±0.6	5.3±0.3	4.0	-0.407	2.0 x 10 <sup>12</sup>	75.5	450
Cr(NO <sub>3</sub> ) <sub>3</sub> •9H <sub>2</sub> O	24	3+	6	m	17.3±3.9	5.2±0.1	4.0	-0.407	2.0 x 10 <sup>12</sup>	75.5	450
MnCl <sub>2</sub> •4H <sub>2</sub> O	25	2+	4,5,6	m	0	7.1±0.1	10.59	–	0.0316	97	300
FeCl <sub>3</sub> •6H <sub>2</sub> O	26	3+	4,5,6,8	n	3.7±2.2	3.7±0.6	3.05	+0.771	316	78.5	450
Fe(NO <sub>3</sub> ) <sub>3</sub> •9H <sub>2</sub> O	26	3+	4,5,6,8	n	5.1±4.5	3.5±0.2	3.05	+0.771	316	78.5	450
FeSO <sub>4</sub> •7H <sub>2</sub> O	26	2+	4,6,8	m	2.0 ±0.4	5.6±0.2	9.5	–	0.32	75	300
CuCl <sub>2</sub>	29	2+	4,5,6	m	1.5±1.1	5.6±0.2	8.0	+0.153	5.0 x 10 <sup>4</sup>	87	300
Zn(NO <sub>3</sub> ) <sub>2</sub> •6H <sub>2</sub> O	30	2+	4,5,6,8	w	0	6.6±0.1	8.96	–	0.032	88	300
RhCl <sub>3</sub>	45	3+	6	n	0	6.8±0.3	3.4	–	3.2 x 10 <sup>13</sup>	80.5	450
La(NO <sub>3</sub> ) <sub>3</sub> •6H <sub>2</sub> O	57	3+	6,7,8,9,10,12	s	1.8±1.4	5.9±0.6	8.5	–	0.050	117.2	450
(NH <sub>4</sub> ) <sub>2</sub> Ce(NO <sub>3</sub> ) <sub>6</sub>	58	4+	6,8,10,12	w	1.4±1.1	3.6±0.2	-1.1	+1.72	–	101	550
Eu(NO <sub>3</sub> ) <sub>3</sub> •6H <sub>2</sub> O	63	3+	6,7,8,9	w	1.6±1.4	5.9±0.4	7.8	-0.36	–	108.7	450

<sup>a</sup> Coordination numbers are from reference 53.<sup>b</sup> The metal adduct formed with Cr(III) and La(III) is  $[M+Met-H]^{2+}$ . The metal adduct with Mn(II), Fe(II), Cu(II) and Zn(II) is  $[M+Met]^{2+}$ . The metal adducts with Eu(III) are  $[M+Met]^{3+}$  and  $[M+Met-H]^{2+}$ . Adduct ion intensity is compared to the intensity of  $[M+H]^+$  with n = no adduct formed, w = weak intensity at <30%, m = medium intensity at 30-65%, and s = strong intensity at >65%.<sup>c</sup>  $pK_1$  values for dissociation of the first proton from the aquo-metal complex are at 298.15K and from references 54,55.<sup>d</sup> Standard reduction potentials,  $E^0$ , for the removal of one electron at 298.15K and 1atm are from reference 56.<sup>e</sup> Resident times for water exchange from the aquo-metal complex at 25 °C are from reference 54.<sup>f</sup> Ionic radii of the metals in a crystalline solid are from reference 57. The metal ions where low and high spin forms are known, the radii listed is for the spin that is most common for the aquo-complex.<sup>g</sup> Estimated hydrated ion radii are from reference 58.<sup>h</sup> – indicates that the value is not available in the literature, usually because the value cannot be measured.



**Figure 4.1.** ESI mass spectra of solutions containing a 10:1 molar ratio of metal:A7 for: (a) no metal, (b) Cr(III), (c) Zn(II), (d) La(III), and (e) Eu(III). For Figure 4.1(c), the low intensity peak below the arrow labelled “No  $[M+2H]^{2+}$ ” is not the ion of interest, but a singly charged impurity.



#### 4.3.2 Optimal Conditions for Supercharging A7 Using Cr(III)

Several molar ratios of Cr(III) to A7 were tested to determine the best conditions for supercharging. With a metal:peptide molar ratio of 5:1 or less a slight increase in  $[M+H]^+$  intensity is observed, although very little formation of  $[M+2H]^{2+}$  occurs. The maximum intensity of  $[M+2H]^{2+}$  is found at a 10:1 metal:peptide ratio. Greater concentrations of Cr(III) generally do not increase the  $[M+2H]^{2+}$  intensity further but instead lead to a gradual decline in intensities for both 2+ and 1+ species. Also, addition of Cr(III) to the solution causes peptide adduct ions containing sodium or potassium ions to greatly decrease in intensity, although Cr(III) adduct ions form instead. The most commonly observed Cr(III) adduct ion is  $[M + Cr - H]^{2+}$ .

Using Cr(III) and A7 in a 10:1 molar ratio, two organic solvent systems were tested, 50:50 acetonitrile:water and 50:50 methanol:water. With acetonitrile:water, the absolute intensity for both doubly and singly charged ions was approximately double that found for methanol:water. Therefore, acetonitrile:water was used for all other experiments.

The identity of the negative counter ion was considered because anions affect protonated ion generation by ESI in ways that relate to their structure and their acid/base properties.<sup>59,60</sup> As the intensity data in Table 4.1 show, the nitrate salts of Cr(III) and iron(III) produce an  $[M+2H]^{2+}$  signal for A7 that is almost twice as intense as the signal produced with the corresponding chloride salts. An attempt was made to study the acetate salt for Cr(III),  $Cr(OAc)_3 \cdot H_2O$ . Because of the volatility of the resulting neutrals, acetate salts are often employed in LC-MS experiments and acetate buffers are used to minimize salt-induced signal suppression in ESI.<sup>61,62</sup> However, the solubility of  $Cr(OAc)_3 \cdot H_2O$  in aqueous solutions is low<sup>63</sup> and we were unable to dissolve this salt to an adequate extent for the present study. Also, a low solubility salt is not desirable as an ESI solution additive because solid can clog the needle.

Ion production by nanoESI<sup>64</sup> was studied because this technique has a lower sample flow rate into the source and a greater tolerance for salt impurities than ESI. Low flow rates have been reported to increase ion intensity.<sup>65</sup> The flow rate in our ESI experiments was ~2.5  $\mu\text{L}/\text{min}$ , while the nanoESI flow rate was ~0.2  $\mu\text{L}/\text{min}$ . Addition of Cr(III) to the A7 solution increased the  $[\text{M}+2\text{H}]^{2+}$  intensity to the same extent for both ESI and nanoESI. No advantage was seen in using nanoESI. Therefore, all other experiments in this study employed ESI.

#### 4.3.3 Supercharging Other Peptides with Cr(III)

In addition to A7, the ability of Cr(III) to supercharge peptides was studied using a variety of neutral, basic, and acidic peptides. These experiments employed the nitrate salt,  $\text{Cr}(\text{NO}_3)_3 \cdot 9\text{H}_2\text{O}$ , with a 10:1 molar ratio of Cr(III) to peptide. In all cases for peptides of seven residues or more, the addition of Cr(III) was found to greatly enhance the production of  $[\text{M}+2\text{H}]^{2+}$ .

Peptides with five residues or less were not observed to form  $[\text{M}+2\text{H}]^{2+}$ . The small peptides studied were the tripeptides GAA and SSS and the pentapeptides GGGGG (G5) and AAAAA (A5). For example, the spectrum of A5 with Cr(III), that yields no  $[\text{M}+2\text{H}]^{2+}$  is shown in Figure 4.2(b). The short chain lengths of these peptides may inhibit their ability to accept two protons due to Coulomb repulsion of neighboring protons.

The ability of hexapeptides to undergo backbone protonation depends on the sequence of the peptides. The peptides GGGGGG (G6), AAAAAA (A6), and ASSAAA do not supercharge. Several other hexapeptides (as discussed below) produce  $[\text{M}+2\text{H}]^{2+}$ , although usually in lower intensities than are seen for similar hepta- and larger peptides.

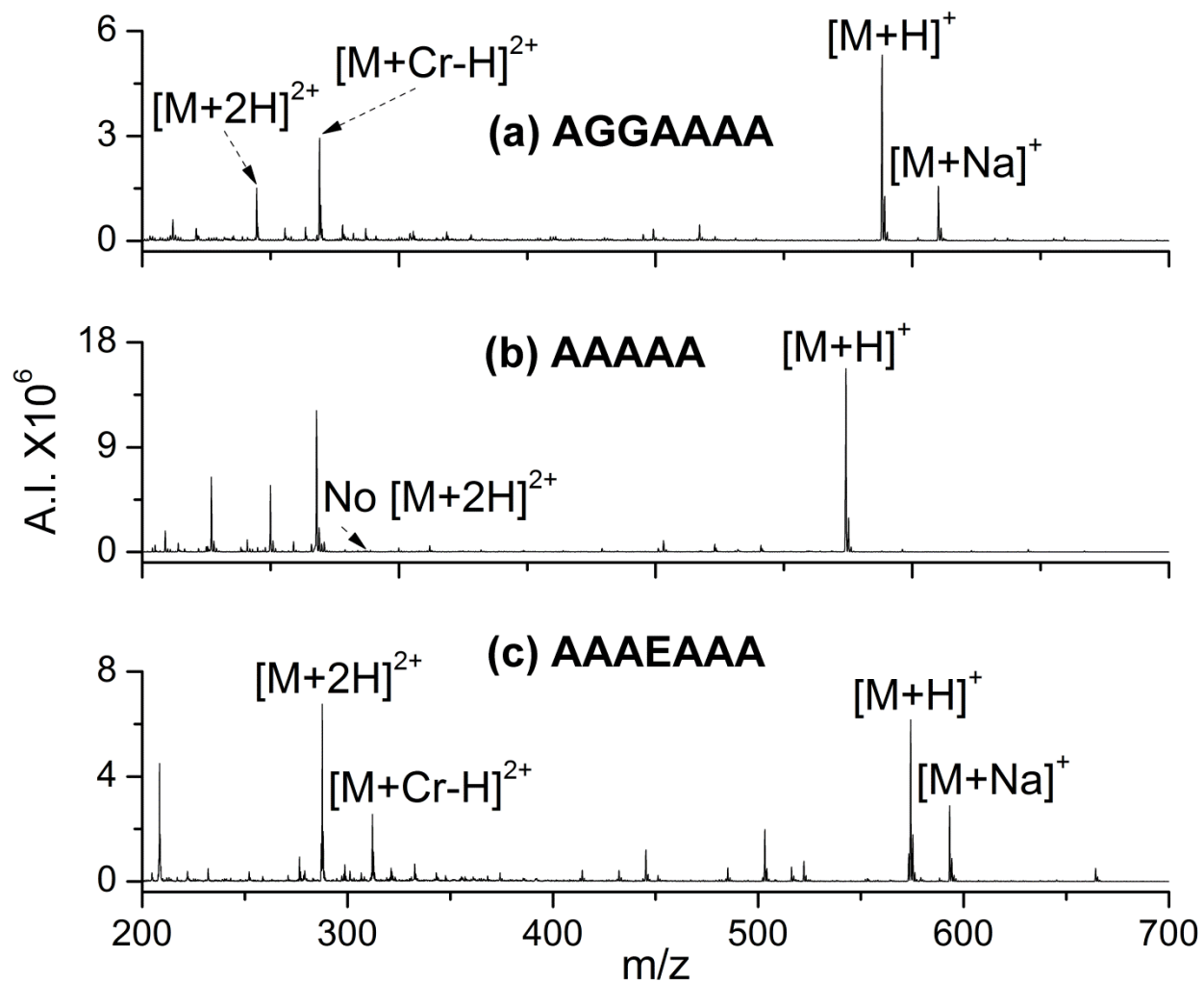


**Figure 4.2.** ESI mass spectra of the following peptides with Cr(III) added at a 10:1 molar ratio of metal ion to peptide: (a) AGGAAAA, (b) AAAAA (A5), and (c) AAEEAAA.

A variety of neutral peptides with exclusively alkyl side chains were studied. These included the 7-residue peptides AGAAAAA, AAAAAGA, AGGAAAA, AAIAAAA, AALAAAA, AAVAAAA, and GGAVAAA; the 8-residue peptide AGGAAAAA; the 9-residue peptide AGGAAAAAA; the 13-residue peptide A13; and the 14-residue peptide A14. All neutral peptides produced only  $[M+H]^+$  in the absence of Cr(III), and abundant  $[M+2H]^{2+}$  when Cr(III) was added to the solution. (As an example, the spectrum for AGGAAAA can be found in Figure 4.2(a).) The 6-residue peptide AVGIGA also generated  $[M+2H]^{2+}$  in the presence of Cr(III), but in low abundance. While addition of Cr(III) to the heptapeptides generally produced  $[M+2H]^{2+}$  in an abundance nearly equal to that of  $[M+H]^+$ , for the hexapeptide AVGIGA the intensity of the 2+ ion was only about 10% of the intensity of the 1+ ion upon Cr(III) addition. In addition, two hexapeptides with neutral side chains containing heteroatoms, TAAAAA and AAAAAN, undergo a limited amount of supercharging.

The analysis of peptides containing basic residues can also benefit from the addition of Cr(III). Figure 4.3 shows mass spectra for the heptapeptide AHAAAAA, where H is the basic histidine residue. As seen in Figure 4.3(a), a low intensity of  $[M+2H]^{2+}$  forms even without Cr(III), which is consistent with the fact that the sequence includes highly basic sites at the N-terminal amino group (residue 1) and at the side chain of histidine (residue 2). However, the absolute intensity of  $[M+2H]^{2+}$  increased from  $0.2 \times 10^6$  in the absence of Cr(III) to  $5.8 \times 10^6$  in the presence of Cr(III). This is a nearly 30-fold increase in  $[M+2H]^{2+}$  intensity due to the use of Cr(III) as a supercharging reagent. A similar affect was observed for the heptapeptide, GVAKAAAA, which has a basic lysine residue (K). For both peptides, not only did Cr(III) shift the predominant charge produced from 1+ to 2+, but the number of peptide molecules being protonated doubled or tripled. This is illustrated in Figure 4.3, where the combined 1+ and 2+

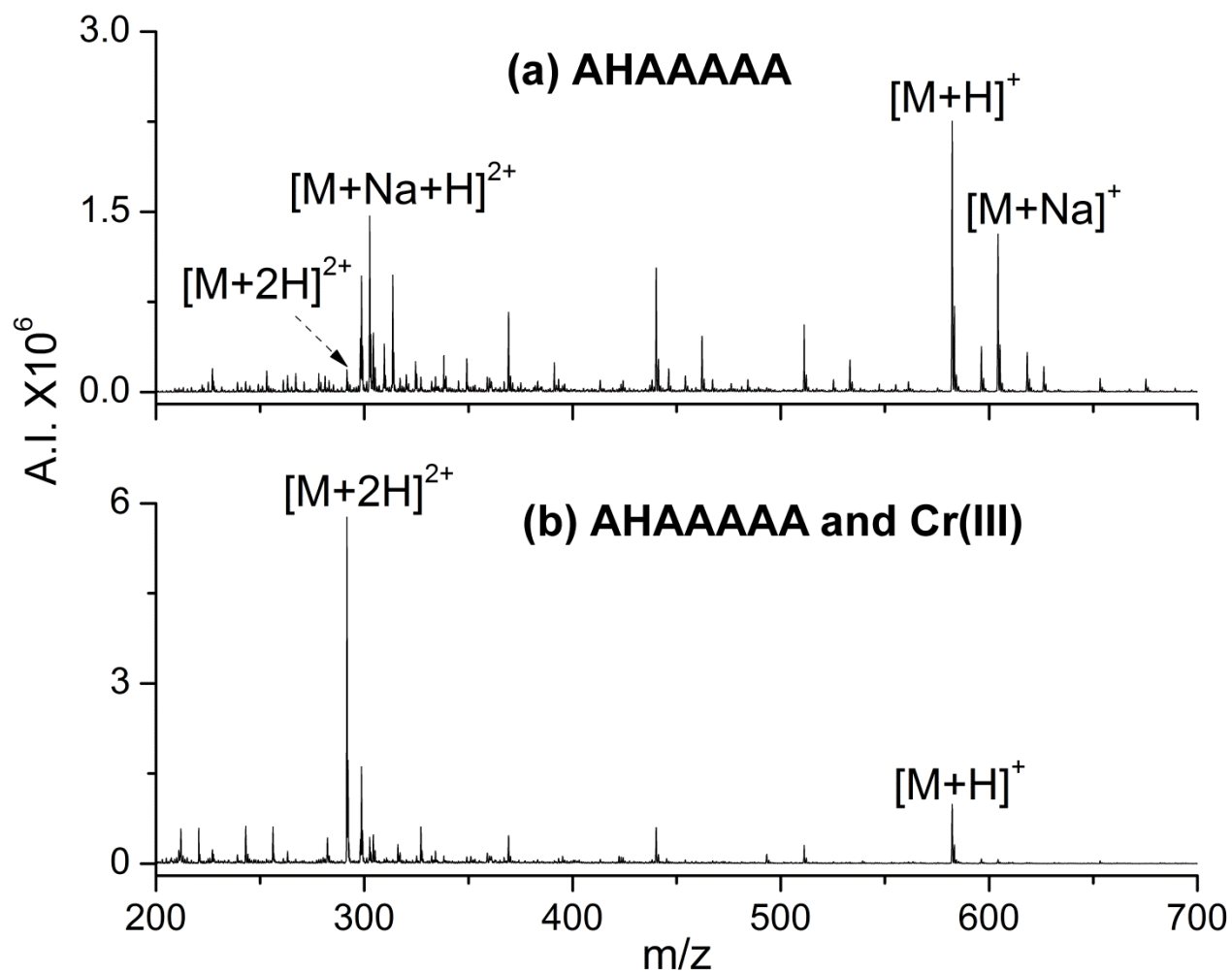


**Figure 4.3.** ESI mass spectra of AHAAAAA with (a) no Cr(III) and (b) Cr(III) at a 10:1 molar ratio of Cr:AHAAAAA.

absolute intensity in the absence of Cr(III) is  $2.4 \times 10^6$ , but is  $6.6 \times 10^6$  when Cr(III) is added. For neutral and acidic peptides, Cr(III) shifts the charge state (causing 2+ to form in place of 1+), but a dramatic increase in the overall intensity of protonated ions does not always occur.

Peptides containing acidic residues can be difficult to analyze by MS/MS in the positive ion mode because they may form protonated ions in low abundance. However, our studies show that acidic peptides can be readily supercharged in the presence of Cr(III). Again, these peptides produce little or no  $[M+2H]^{2+}$  in the absence of Cr(III), but form  $[M+2H]^{2+}$  upon addition of Cr(III). Our studies included 7-residue peptides of the types XAAAAAA, AAAXAAA, and AAAAAAX, where X = aspartic acid (D) and glutamic acid (E). (As an example, Figure 4.2(c) includes the ESI mass spectrum for AAAEAAA with addition of Cr(III).) In addition, with Cr(III) the following 6-residue peptides supercharged: DAAADA, EAAAEA, EAAAAE, and AAEEAA. For the hexapeptides, glutamic acid residues facilitate more supercharging than aspartic acid residues. In general, with glutamic acid, the intensity of  $[M+2H]^{2+}$  is 70-100 % of the intensity of  $[M+H]^+$ , while this value is only 10-30 % for the aspartic acid. The side chain of glutamic acid has one more methylene group than the side chain of aspartic acid. The longer glutamic acid side chain may better interact with Cr(III) and facilitate supercharging. Several highly acidic peptides were found to produce sufficient  $[M+2H]^{2+}$  for further study by MS/MS techniques upon addition of Cr(III). These peptides include heptaaspartic acid (D7), heptaglutamic acid (E7), and the biological peptide hirudin(54-65), which is involved in blood clotting and has the sequence GDFEEIPEEYLQ. In addition, the highly acidic peptide EEEEGDD readily supercharges, as is shown in Figure 4.4. The intensity of  $[M+2H]^{2+}$  increases by about 25-fold when Cr(III) is added to the solution and the number of peptide molecules

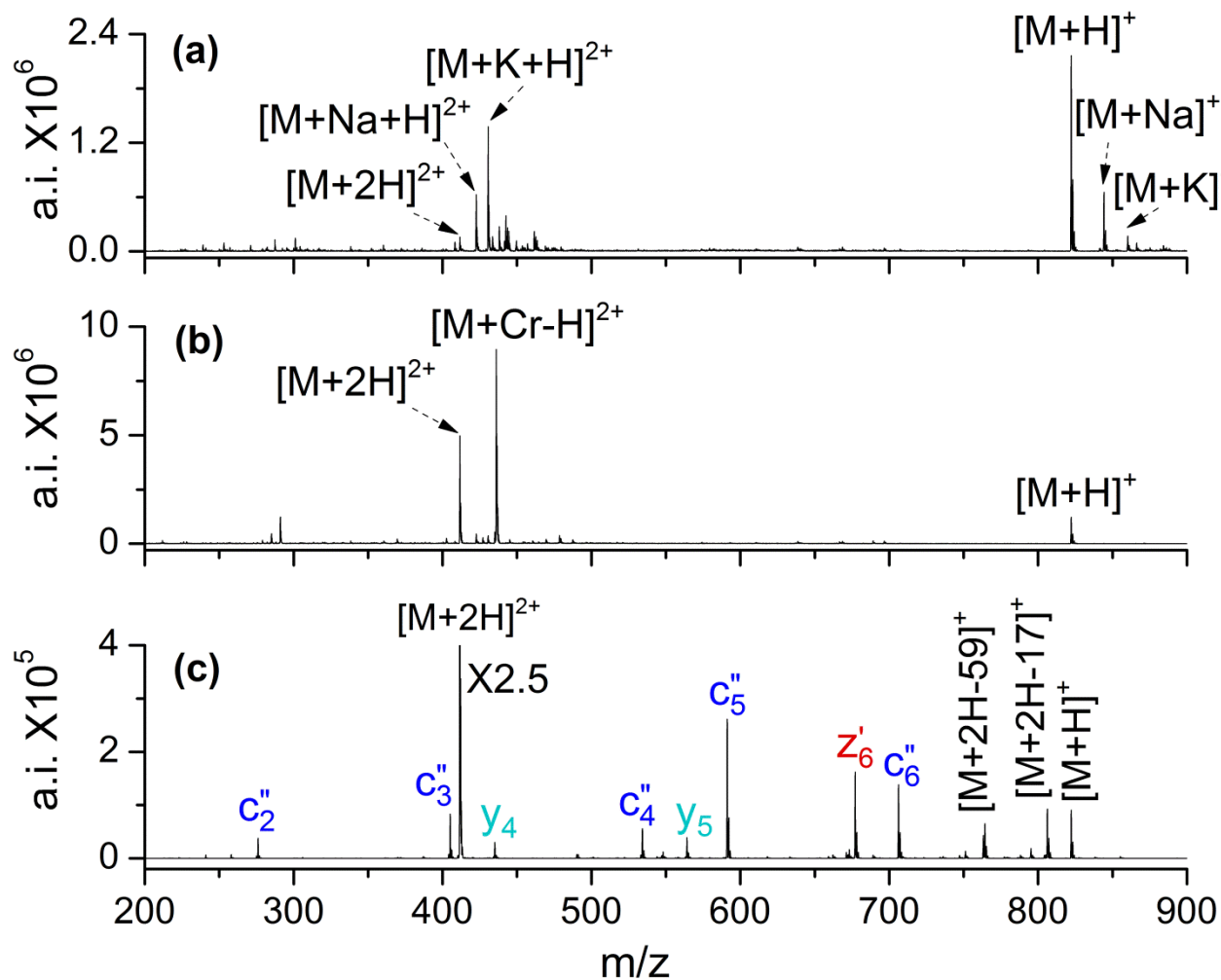


**Figure 4.4.** ESI mass spectra of EEEEGDD with (a) no Cr(III), (b) Cr(III) at a 10:1 molar ratio of Cr:EEEGDD, and (c) ETD on  $[M+2H]^{2+}$  produced by addition of Cr(III).

being protonated doubles [Figure 4.4(a) versus Figure 4.4(b)]. With added Cr(III),  $[M+2H]^{2+}$  is sufficiently intense to be studied by MS/MS techniques and, as an example, the ETD spectrum of this ion is shown in Figure 4.4(c). The signal-to-noise ratio (S/N) is excellent, and cleavage occurs at every residue, allowing the peptide to be readily sequenced from this spectrum. EEEEGDD is a fragment of low-molecular weight chromium-binding substance (LMWCr, also known as chromodulin), a biological peptide found in humans and animals that is involved in metabolism<sup>66-68</sup> and may have utility in diabetes treatment.<sup>69</sup> Our research group has recently sequenced a biological form of this peptide, pEEEEGDD.<sup>70</sup> This was a challenge because the high acidity of the peptide resulted in only deprotonation by ESI and MALDI. The negative ion mode CID and post-source decay (PSD) spectra contain an inconsistent mixture of backbone cleavage ions that often include intense water loss. We interpreted these spectra and sequenced the peptide conclusively only after synthesizing two candidate peptides and comparing their negative ion MS/MS spectra to those of the biological peptide. The project would have been much simpler if Cr(III) had been used to protonate the peptide, followed by either CID or ETD in the positive ion mode.

#### **4.3.4 Comparison of Cr(III) to Organic Supercharging Reagents**

The ability of Cr(III) to supercharge cytochrome c (bovine heart) was explored. Cytochrome c is a 102-residue protein with 24 highly basic residues (including the N-terminus). This protein was selected for study because it has been the subject of several reports using organic supercharging reagents.<sup>29,31,33,37,71</sup> Addition of Cr(III) was found to have no effect on the protonation of cytochrome c. For comparison, we added two organic supercharging reagents, m-



NBA<sup>29-32</sup> and DMSO,<sup>36</sup> to a cytochrome c solution and observed extensive supercharging consistent with literature reports.<sup>29,31,33</sup>

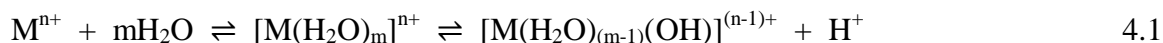
In the converse experiment, the organic supercharging reagents m-NBA and DMSO were separately added to solutions of our test peptide A7. The result was an extremely minor formation of  $[M+2H]^{2+}$ , which was not of sufficient intensity to be useful in MS or MS/MS experiments. This greatly contrasts the ability of Cr(III) to produce  $[M+2H]^{2+}$  in high abundance for A7.

These results suggest that organic supercharging reagents (e.g., m-NBA and DMSO) work best for protonation of larger molecules such as proteins, while Cr(III) excels at adding protons to smaller molecules such as peptides. Thus, organic supercharging agents and Cr(III) probably affect protonation by different mechanisms.

#### 4.3.5 Factors that May Contribute to the Ability of Cr(III) to Supercharge

The metal ions studied were selected to test the effects of specific properties on supercharging ability. These properties are discussed below, with pertinent reference values being given in Table 4.1.

One factor to consider in  $[M+2H]^{2+}$  formation is the acidity of the solution. In aqueous solutions, metal ions promote acidity by undergoing hydrolysis:



Cr(III) forms the hexaaquachromium(III) ion,  $[Cr(H_2O)_6]^{3+}$ , which has an hydrolysis dissociation constant ( $pK_1$ ) in the range of 3.8-4.2,<sup>54,55</sup> this is the acid dissociation constant ( $pK_a$ ) of the aquo-metal complex. This low  $pK_1$  value is consistent with our observation that the addition of Cr(III) to an A7 solution lowers the pH to  $5.3 \pm 0.3$ ; in contrast, the pH of the A7 solution without metal

ion is  $7.8 \pm 0.3$ . As the values in Table 4.1 indicate, aquo-metal complexes of divalent metal ions have higher  $pK_1$  values than complexes of trivalent metal ions. Thus, divalent metal ions produce less acidic solutions than trivalent metal ions, which is consistent with our experimental pH measurements. The divalent metal ions that were studied provide only a weak to non-existent enhancement of  $[M+2H]^{2+}$  intensity for A7, which may indicate that these ions do not provide an adequately acidic environment for supercharging. However, acidity is not the only factor affecting protonation. The most acidic metal ion in our study is Ce(IV), which has a  $pK_1$  of -1.1 for its aquo-complex<sup>55</sup> and a solution pH of  $3.6 \pm 0.2$  when mixed with A7; however, Ce(IV) produced only a low intensity of  $[M+2H]^{2+}$  for A7.

Acidifying the peptide solution in the absence of a metal ion also does not doubly protonate A7. Experiments were performed in which the A7 solution was acidified with 0.5-2.0 volume % of acetic acid, trifluoroacetic acid, hydrochloric acid, nitric acid, and an acidic buffer. A pH of 5.0 in the absence of the metal ions does not cause A7 to supercharge. Even when the pH was lowered to a highly acidic value of pH 2.0 using nitric acid, only a very low abundance of  $[M+2H]^{2+}$  forms. Also, addition of acetic acid to the solution containing A7 and Cr(III) does not result in a greater increase in protonation relative to the use of Cr(III) without added acid.

A noteworthy feature of Cr(III) is that it does not readily reduce. The standard reduction potential,  $E^0$ , for Cr(III) reduction to Cr(II) is -0.407 V.<sup>56</sup> In contrast, Fe(III) much more readily reduces to Fe(II), with  $E^0$  of +0.771 V.<sup>56</sup> This suggests that more chromium ions can survive the ESI process in a 3+ charge state than iron ions. As the data in Table 4.1 indicate, Fe(III) was found to doubly charge A7 in an intensity roughly one-third that of Cr(III). Of the metal ions studied, Fe(III) is second only to Cr(III) in the ability to supercharge A7. However, Fe(III) salts are not promising as supercharging reagents because the  $[M+2H]^{2+}$  intensity that they generate is

unstable. There is a pronounced ion intensity fluctuation and the  $[M+2H]^{2+}$  signal sometimes goes away entirely. This is illustrated by the mean  $\pm$  standard deviation ion intensity values of Table 4.1, which are  $3.7 \pm 2.2 ( \times 10^5 )$  for iron(III) chloride and  $5.1 \pm 4.5 ( \times 10^5 )$  for iron(III) nitrate. Electrochemical processes are known to occur during ESI<sup>72</sup> and it is possible that reduction of Fe(III) during ESI is causing instability of the  $[M+2H]^{2+}$  signal. Similarly, Ce(IV) readily reduces to Ce(III) with an  $E^0$  of +1.72<sup>56</sup> and reduction of Ce(IV) during ESI may limit the ability of this ion to supercharge peptides. Like Cr(III), the trivalent ions of Al, La, Eu, and Rh do not readily reduce. However, unlike Cr(III) and Fe(III), they do not promote supercharging for A7. Our conclusion is that the ability of a metal ion to resist reduction does not cause a metal ion to be a supercharging agent, but may allow the metal to remain in a form that is optimal for supercharging.

A distinguishing property of Cr(III) is the kinetic inertness of its complexes in aqueous solution.<sup>73-75</sup> The residence time of a water ligand in the first hydration shell around Cr(III) is  $2.0 \times 10^{12} \mu s$  (23 days).<sup>54</sup> In comparison, the residence time of a water ligand around Fe(III) is only  $316 \mu s$ .<sup>54</sup> Residence time for water ligands might correlate to the interactions of the metal ions with oxygens at the peptide backbone. To test this hypothesis, our study also included Rh(III), which like Cr(III), is known for its kinetic inertness to water exchange.<sup>76</sup> The residence time of a water ligand at Rh(III) is  $3.2 \times 10^{13} \mu s$ .<sup>54</sup> Al(III), which has a residence time of  $6.3 \times 10^6 \mu s$ ,<sup>54</sup> was also investigated. However, neither Rh(III) nor Al(III) were found to be good supercharging reagents. Thus, the residence time of water and other oxygen-containing functional groups around the metal ion does not significantly affect supercharging.

Metal ion size is another consideration in characterizing supercharging ability. There might be an optimal metal ion size to facilitate interactions of the ion with the peptide backbone

and promote protonation. In support of this theory, the two trivalent metal ions that cause the greatest supercharging, Cr(III) and Fe(III), have similar sizes. The ionic radius in solid crystals of Cr(III) is 75.5 pm, while the ionic radius of Fe(III) is 78.5 pm.<sup>54</sup> At 67.5 pm, the ionic radius of Al(III) is only slightly smaller than that of Cr(III) and Fe(III). All three metal ions also have the same estimated hydrated ionic radius in water, 450 pm.<sup>58</sup> In addition, at 80.5 pm, the ionic radius of Rh(III) is similar to that of Cr(III). However, Rh(III) and Al(III) are poor supercharging reagents. Therefore, while metal ion size may influence supercharging, it is not the major factor that causes Cr(III) and Fe(III) to supercharge.

In comparing the physical properties listed in Table 4.1 for the metal ions studied, the species most similar to Cr(III) is Rh(III). Yet, Cr(III) induces abundant supercharging, while Rh(III) induces none. This suggests that the primary reason that Cr(III) causes supercharging is not related to a physical property, but a chemical property. Chromium is a first row transition metal, while rhodium is a second row transition metal. Although their physical properties may be similar, the first and second transition series often have very different chemical properties. In general, first row metals are more reactive and form a greater number and diversity of metal-ligand complexes than second row metals.<sup>77</sup> Another factor supporting the premise that the ability of Cr(III) to supercharge relates to a chemical property is the fact Fe(III) also induces facile supercharging (although in an erratic manner). Like chromium, iron is a first row transition metal and their trivalent ions frequently have similar chemical properties; for example, both Cr(III) and Fe(III) are members of the “iron group” of classical qualitative inorganic analysis<sup>78</sup> and both are transported in the human body by the glycoprotein transferrin.<sup>79</sup>

Our experiments suggest that Cr(III) and organic supercharging agents enhance protonation by different mechanisms. Williams and coworkers have proposed that organic

supercharging agents act by causing the peptide to undergo conformational changes during droplet evaporation by ESI, which makes highly basic sites more accessible.<sup>30,35,36,38,39,80</sup> This is probably not the mechanism with Cr(III) because the peptides studied here are sufficiently small that backbone folding is unlikely to make basic sites entirely inaccessible. More important, these neutral and acidic peptides do not have a second highly basic site to protonate, but instead are undergoing protonation of a backbone amide group to form  $[M+2H]^{2+}$ . Changes in surface tension of the ESI droplets due to the addition of the organic reagents has also been proposed to play a role in protein supercharging,<sup>71</sup> although other studies suggest that surface tension may be of limited importance.<sup>81,82</sup> Surface tension is unlikely to be a factor in Cr(III) supercharging because the ability of a metal ion to affect aqueous surface tension primarily relates to ionic charge and not identity (e.g.,  $Ca^{2+}$  and  $Mg^{2+}$  salts have almost the same effect on surface tension).<sup>83</sup>

Supercharging with Cr(III) resembles electrothermal supercharging<sup>42-44</sup> in that both methods can add a greater number of protons than there are highly basic sites on the biomolecule. Electrothermal supercharging is believed to result from conformational changes and denaturation when a biomolecule is exposed to factors that include temperature, voltage, and ionic strength. However, the “over-protonating” of proteins by electrothermal supercharging probably does not involve the peptide backbone but instead results from protonation of less basic residues (i.e., proline, tryptophan, and glutamine).<sup>49</sup> The alkyl side chain peptides studied here, including A7, have no residues with side chains that will protonate.

#### 4.3.6 The Role of Cr(III)-Peptide Interactions in Supercharging

A proposed supercharging mechanism that is likely to be a factor for Cr(III) is interaction of the supercharging reagent with the biomolecule. Douglass and Venter suggested that the formation of adducts of cytochrome c and sulfolane are responsible for supercharging.<sup>33</sup> Based on data from thermal studies, Chingin et al. proposed that the supercharging mechanism involves direct interaction.<sup>40</sup> Flick and Williams suggested that La(III) adduction to the protein led to increased Coulomb repulsion and caused protein unfolding.<sup>41</sup> For supercharging with Cr(III), metal ion-peptide interaction goes along with the premise that a chemical factor is at work rather than a physical property.

Cr(III) coordinates in solution to ligands with oxygen<sup>75,84-88</sup> or nitrogen,<sup>89-93</sup> although this is not unique among transition metal ions. Cr(III) is a hard Lewis acid that prefers to bind to oxygen rather than nitrogen.<sup>94</sup> (The other hard metal ions in this study are Fe(III) and Al(III).) The binding of Cr(III) to oxygen ligands is usually strong and often involves coordinate covalent bonds.<sup>77</sup> Little is known of the ability of Cr(III) to bind to peptides, with the exception of work on the chromium-binding peptide found in animals, LMWCr. LMWCr is a small highly acidic peptide of 10-12 residues that tightly binds four Cr(III),<sup>95-97</sup> in fact, the EEEEGDD fragment of LMWCr (whose mass spectra are shown in Figure 4.4) binds four Cr(III) in solution.<sup>69</sup> The carboxylic acid groups on the side chains of the acidic residues and at the C-terminus are involved in Cr(III) binding. Also, both Cr(III) and Fe(III) are transported in animals by transferrin, and the two metal ions have very similar binding affinities to this glycoprotein.<sup>79</sup>

An hypothesis that carboxylic acid groups are involved in the Cr(III) supercharging mechanism is supported by the solution-phase data on Cr(III) binding to LMWCr and by our experimental observations that hexapeptides with acidic residues supercharge readily with the

identity of the acidic residue (glutamic acid versus aspartic acid) affecting protonation. To test this hypothesis, we removed the C-terminal carboxylic acid groups of A7, AAVAAAA, and AAIAAAA by converting these peptides to methyl esters. ESI on these peptide methyl esters showed no increased  $[M+2H]^{2+}$  signal when Cr(III) was added. In contrast, the acid forms of all three peptides supercharge in abundance upon addition of Cr(III) to produce  $[M+2H]^{2+}$  at near equal intensity to  $[M+H]^+$ .

Although no protonation enhancement occurs upon addition of Cr(III), even without Cr(III) the three methyl esters form  $[M+2H]^{2+}$  at ~30% the intensity of  $[M+H]^+$ . This result is interesting because the acid forms of these peptides produce almost no  $[M+2H]^{2+}$  without Cr(III). This is likely to be a conformational effect, with the methyl esters having more open structures due to less participation of the C-terminus in hydrogen bonding.<sup>51</sup> If so, this suggests that conformation has at least some effect on the protonation of even small peptides.

Interaction of Cr(III) with peptide C-terminal or side chain carboxylic acid groups appears to be an important step in the supercharging mechanism. Cr(III) forms almost exclusively hexacoordinate complexes of octahedral geometry.<sup>77</sup> Therefore, it is possible that several carbonyl oxygens along the peptide backbone coordinate at multiple sites of the Cr(III) octahedron in solution or during drying in ESI as coordinating water is stripped from the droplet. Using scale models in Figure 4.5, we found that at least four carbonyl oxygens on the A7 backbone can coordinate at octahedral sites of Cr(III) without severe distortion of the backbone. Such interaction might assist in transfer of a proton from aquo-Cr(III) complexes to the peptide backbone.

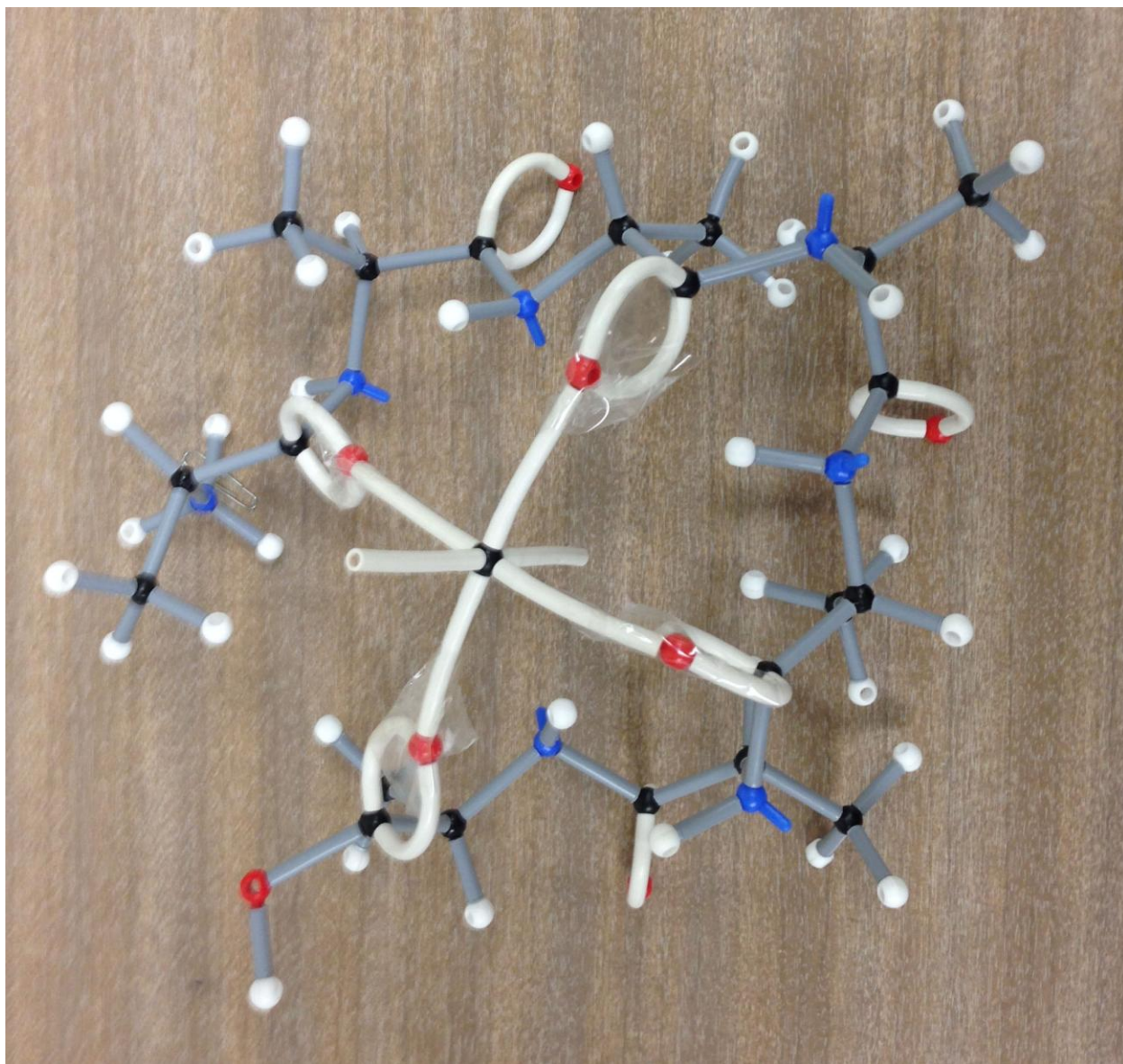


**Figure 4.5.** The ball-and-stick model of Cr(III) and A7.



## Conclusions

The addition of Cr(III) nitrate to solutions being electrosprayed is shown to dramatically increase  $[M+2H]^{2+}$  intensity for neutral and acidic peptides that normally produce only  $[M+H]^+$ . In addition, for slightly basic peptides that produce  $[M+2H]^{2+}$  in low abundance, addition of Cr(III) both shifts the charge state distribution to predominantly 2+ and causes the number of ions being protonated to double or triple. This greatly enhanced production of  $[M+2H]^{2+}$  has several advantages for peptide sequencing by MS/MS. First, production of abundant  $[M+2H]^{2+}$  allows ECD and ETD experiments to be performed on peptides that normally could not be studied because of the need for these electron-base techniques to have multiply charged precursor cations. (Such experiments are discussed in Chapters 5 and 6.) Second, for CID, which is the most common dissociation technique in peptide sequencing, the amount of structurally-informative fragmentation is generally greater for  $[M+2H]^{2+}$  than for  $[M+H]^+$ . This is why biological peptide sequencing by CID in proteomics research usually involves 2+ precursor ions.<sup>98,99</sup> Finally, the large increase in signal intensity for  $[M+2H]^{2+}$  precursor ion results in a corresponding increase in S/N of the MS/MS spectra. A limiting factor in the ability of bioinformatics techniques to correctly identify peptides is mass spectra with low S/N.<sup>100,101</sup> This makes selecting analyte peaks from noise difficult and results in false positive identifications for peptides. The ability of Cr(III) to increase both charge and ion intensity in the ESI mass spectra could prove to be very useful in peptide analysis and sequencing.

## References

1. Fenn, J. B.; Mann, M.; Meng, C. K.; Wong, S. F. Electrospray Ionization--Principles and Practice. *Mass Spectrom. Rev.* **1990**, *9*, 37-70.
2. Hillenkamp, F.; Karas, M.; Beavis, R. C.; Chait, B. T. Matrix-Assisted Laser Desorption/Ionization Mass Spectrometry of Biopolymers. *Anal. Chem.* **1991**, *63*, 1193A-1203A.
3. Nilsson, T.; Mann, M.; Aebersold, R.; Yates, J. R.; Bairoch, A.; Bergeron, J. J. M. Mass Spectrometry in High-throughput Proteomics: Ready for the Big Time. *Nat. Methods* **2010**, *7*, 681-685.
4. Vestal, M. L. The Future of Biological Mass Spectrometry. *J. Am. Soc. Mass Spectrom.* **2011**, *22*, 953-959.
5. Kollipara, S.; Agarwal, N.; Varshney, B.; Paliwal, J. Technological Advancements in Mass Spectrometry and Its Impact on Proteomics. *Anal. Lett.* **2011**, *44*, 1498-1520.
6. Marshall, A. G.; Hendrickson, C. L. Charge Reduction Lowers Mass Resolving Power for Isotopically Resolved Electrospray Ionization Fourier Transform Ion Cyclotron Resonance Mass Spectra. *Rapid Commun. Mass Spectrom.* **2001**, *15*, 232-235.
7. Marshall, A. G.; Hendrickson, C. L. High-Resolution Mass Spectrometers. *Ann. Rev. Anal. Chem.* **2008**, *1*, 579-599.
8. Perry, R. H.; Cooks, R. G.; Noll, R. J. Orbitrap Mass Spectrometry: Instrumentation, Ion Motion and Applications. *Mass Spectrom. Rev.* **2008**, *27*, 661-699.
9. Dongre, A. R.; Jones, J. L.; Somogyi, A.; Wysocki, V. H. Influence of Peptide Composition, Gas-Phase Basicity, and Chemical Modification on Fragmentation Efficiency: Evidence for the Mobile Proton Model. *J. Am. Chem. Soc.* **1996**, *118*, 8365-8374.
10. Wells, J. M.; Stephenson Jr., J. L.; McLuckey, S. A. Charge Dependence of Protonated Insulin Decompositions. *Intl. J.* **2000**, *203*, A1-A9.
11. Kjeldsen, F.; Giessing, A. M. B.; Ingrell, C. R.; Jensen, O. N. Peptide Sequencing and Characterization of Post-Translational Modifications by Enhanced Ion-Charging and Liquid Chromatography Electron-Transfer Dissociation Tandem Mass Spectrometry. *Anal. Chem.* **2007**, *79*, 9243-9252.
12. Madsen, J. A.; Brodbelt, J. S. Comparison of Infrared Multiphoton Dissociation and Collision-Induced Dissociation of Supercharged Peptides in Ion Traps. *J. Am. Soc. Mass Spectrom.* **2009**, *20*, 349-358.

13. Zubarev, R. A.; Kelleher, N. L.; McLafferty, F. W. Electron Capture Dissociation of Multiply Charged Protein Cations. A Nonergodic Process. *J. Am. Chem. Soc.* **1998**, *120*, 3265-3266.
14. McLafferty, F. W.; Horn, D. M.; Breuker, K.; Ge, Y.; Lewis, M. A.; Cerda, B. A.; Zubarev, R. A.; Carpenter, B. K. Electron Capture Dissociation of Gaseous Multiply Charged Ions by Fourier Transform ion Cyclotron Resonance. *J. Am. Soc. Mass Spectrom.* **2001**, *12*, 245-249.
15. Zubarev, R. A. Electron Capture Dissociation LC/MS/MS for Bottom-Up Proteomics. *Methods Mol. Biol.* **2009**, *492*, 413-416.
16. Syka, J. E. P.; Coon, J. J.; Schroeder, M. J.; Shabanowitz, J.; Hunt, D. F. Peptide and Protein Sequence Analysis by Electron Transfer Dissociation Mass Spectrometry. *Proc. Natl. Acad. Sci. USA* **2004**, *101*, 9528-9533.
17. Coon, J. J. Collisions or Electrons? Protein Sequence Analysis in the 21st Century. *Anal. Chem.* **2009**, *81*, 3208-3215.
18. Good, D. M.; Wirtala, M.; McAlister, G. C.; Coon, J. J. Performance Characteristics of Electron Transfer Dissociation Mass Spectrometry. *Mol. Cell Proteomics* **2007**, *6*, 1942-1951.
19. Huzarska, M.; Ugalde, I.; Kaplan, D. A.; Hartmer, R.; Easterling, M. L.; Polfer, N. C. Negative Electron Transfer Dissociation of Deprotonated Phosphopeptide Anions: Choice of Radical Cation Reagent and Competition between Electron and Proton Transfer. *Anal. Chem.* **2010**, *82*, 2873-2878.
20. Pierotti, A. R.; Prat, A.; Chesneau, V.; Gaudoux, F.; Leseney, A. M.; Foulon, T.; Cohen, P. N-Arginine Dibasic Convertase, a Metalloendopeptidase as a Prototype of a Class of Processing Enzymes. *Proc. Natl. Acad. Sci. USA* **1994**, *91*, 6078-6082.
21. Lemaire, S.; Yamashiro, D.; Rao, A. J.; Li, C. H. Synthesis and Biological Activity of Beta-Melanotropins and Analogs. *J. Med. Chem.* **1977**, *20*, 155-158.
22. Tatemoto, K. Neuropeptide Y: Complete Amino Acid Sequence of the Brain Peptide. *Proc. Natl. Acad. Sci. USA* **1982**, *79*, 5485-5489.
23. Ebert, R. F.; Bell, W. R. Assay of Human Fibrinopeptides by High-Performance Liquid Chromatography. *Anal. Biochem.* **1985**, *148*, 70-78.
24. Voet, D.; Voet, J. G. *Biochemistry*; John Wiley & Sons: New York, 1995.
25. Chan, D. C.; Kim, P. S. HIV Entry and Its Inhibition. *Cell* **1998**, *93*, 681-684.
26. Chougnet, C.; Troye-Blomberg, M.; Deloron, P.; Kabilan, L.; Lepers, J. P.; Savel, J.; Perlmann, P. Human Immune Response in Plasmodium Falciparum Malaria. Synthetic

Peptides Corresponding to Known Epitopes of The Pf155/RESA Antigen Induce Production of Parasite-Specific Antibodies in vitro. *J. Immunol.* **1991**, *147*, 2295-2301.

27. Nara, P. L.; Hwang, K. M.; Rausch, D. M.; Lifso, J. D.; Eiden, L. E. CD4 Antigen-Based Antireceptor Peptides Inhibit Infectivity of Human Immunodeficiency Virus In Vitro at Multiple Stages of the Viral Life Cycle. *Proc. Natl. Acad. Sci. USA* **1989**, *86*, 7139-7143.
28. Lifson, J. D.; Hwang, K. M.; Nara, P. L.; Fraser, B.; Padgett, M.; Dunlop, N. M.; Eiden, L. E. Synthetic CD4 Peptide Derivatives that Inhibit HIV Infection and Cytopathicity. *Science* **1988**, *241*, 712-716.
29. Iavarone, A. T.; Jurchen, J. C.; Williams, E. R. Supercharged Protein and Peptide Ions Formed by Electrospray Ionization. *Anal. Chem.* **2001**, *73*, 1455-1460.
30. Sterling, H. J.; Williams, E. R. Origin of Supercharging in Electrospray Ionization of Noncovalent Complexes from Aqueous Solution. *J. Am. Soc. Mass Spectrom.* **2009**, *20*, 1933-1943.
31. Iavarone, A. T.; Williams, E. R. Collisionally Activated Dissociation of Supercharged Proteins Formed by Electrospray Ionization. *Anal. Chem.* **2003**, *75*, 4525-4533.
32. Iavarone, A. T.; Williams, E. R. Supercharging in Electrospray Ionization: Effects on Signal and Charge. *Int. J. Mass Spectrom.* **2002**, *219*, 63-72.
33. Douglass, K. A.; Venter, A. R. Investigating the Role of Adducts in Protein Supercharging with Sulfolane. *J. Am. Soc. Mass Spectrom.* **2012**, *23*, 489-497.
34. Lomeli, S. H.; Peng, I. X.; Yin, S.; Ogorzalek Loo, R. R.; Loo, J. A. New Reagents for Increasing ESI Multiple Charging of Proteins and Protein Complexes. *J. Am. Soc. Mass Spectrom.* **2010**, *21*, 127-131.
35. Sterling, H. J.; Daly, M. P.; Feld, G. K.; Thoren, K. L.; Kintzer, A. F.; Krantz, B. A.; Williams, E. R. Effects of Supercharging Reagents on Noncovalent Complex Structure in Electrospray Ionization from Aqueous Solutions. *J. Am. Soc. Mass Spectrom.* **2010**, *21*, 1762-1774.
36. Sterling, H. J.; Prell, J. S.; Cassou, C. A.; Williams, E. R. Protein Conformation and Supercharging with DMSO from Aqueous Solution. *J. Am. Soc. Mass Spectrom.* **2011**, *22*, 1178-1186.
37. Valeja, S. G.; Tipton, J. D.; Emmett, M. R.; Marshall, A. G. New Reagents for Enhanced Liquid Chromatographic Separation and Charging of Intact Protein Ions for Electrospray Ionization Mass Spectrometry. *Anal. Chem.* **2010**, *82*, 7515-7519.

38. Sterling, H. J.; Cassou, C. A.; Trnka, M. J.; Burlingame, A. L.; Krantz, B. A.; Williams, E. R. The Role of Conformational Flexibility on Protein Supercharging in Native Electrospray Ionization. *Phys. Chem. Chem. Phys.* **2011**, *13*, 18288-18296.
39. Sterling, H. J.; Williams, E. R. Real-Time Hydrogen/Deuterium Exchange Kinetics via Supercharged Electrospray Ionization Tandem Mass Spectrometry. *Anal. Chem.* **2010**, *82*, 9050-9057.
40. Chingin, K.; Xu, N.; Chen, H. Soft Supercharging of Biomolecular Ions in Electrospray Ionization Mass Spectrometry. *J. Am. Soc. Mass Spectrom.* **2014**, *25*, 928-934.
41. Flick, T.; Williams, E. Supercharging with Trivalent Metal Ions in Native Mass Spectrometry. *J. Am. Soc. Mass Spectrom.* **2012**, *23*, 1885-1895.
42. Sterling, H. J.; Cassou, C. A.; Susa, A. C.; Williams, E. R. Electrothermal Supercharging of Proteins in Native Electrospray Ionization. *Anal. Chem.* **2012**, *84*, 3795-3801.
43. Cassou, C. A.; Sterling, H. J.; Susa, A. C.; Williams, E. R. Electrothermal Supercharging in Mass Spectrometry and Tandem Mass Spectrometry of Native Proteins. *Anal. Chem.* **2013**, *85*, 138-146.
44. Cassou, C. A.; Williams, E. R. Anions in Electrothermal Supercharging of Proteins with Electrospray Ionization Follow a Reverse Hofmeister Series. *Anal. Chem.* **2014**, *86*, 1640-1647.
45. Miladinovic, S. M.; Fornelli, L.; Lu, Y.; Piech, K. M.; Girault, H. H.; Tsybin, Y. O. In-Spray Supercharging of Peptides and Proteins in Electrospray Ionization Mass Spectrometry. *Anal. Chem.* **2012**, *84*, 4647-4651.
46. Watson, H. M.; Vincent, J. B.; Cassady, C. J. Effects of Transition Metal Ion Coordination on the Collision-induced Dissociation of Polyalanines. *J. Mass Spectrom.* **2011**, *46*, 1099-1107.
47. Covey, T. R.; Bonner, R. F.; Shushan, B. I.; Henion, J. The Determination of Protein, Oligonucleotide and Peptide Molecular Weights by Ion-spray Mass Spectrometry. *Rapid Commun. Mass Spectrom.* **1988**, *2*, 249-256.
48. Carr, S. R.; Cassady, C. J. Reactivity and Gas-Phase Acidity Determinations of Small Peptide Ions Consisting of 11 to 14 Amino Acid Residues. *J. Mass Spectrom.* **1997**, *32*, 959-967.
49. Schnier, P. D.; Gross, D. S.; Williams, E. R. On the Maximum Charge State and Proton Transfer Reactivity of Peptide and Protein Ions Formed by Electrospray Ionization. *J. Am. Soc. Mass Spectrom.* **1995**, *6*, 1086-1097.

50. Chan, W. C.; White, P. D. *Fmoc Solid Phase Peptide Synthesis A Practical Approach*; Oxford University Press Inc., New York: 2000.
51. Bokatzian-Johnson, S. S.; Stover, M. L.; Dixon, D. A.; Cassady, C. J. Gas-phase Deprotonation of the Peptide Backbone for Tripeptides and their Methyl Esters with Hydrogen and Methyl Side Chains. *J. Phys. Chem. B* **2012**, *116*, 14844-14858.
52. Feng, C.; Cassady, C. J. Effects of Arginine, Lysine, and Histidine Residues on Electron Transfer Dissociation Mass Spectrometry of Model Peptides with One Basic Residue. *Rapid Commun. Mass Spectrom.* submitted.
53. Huheey, J. E.; Keiter, E. A.; Keither, R. L. *Inorganic Chemistry*; Harper Collins: New York, 1993.
54. Burgess, J. *Metal Ions in Solution*; Ellis Horwood: Chichester, 1978.
55. Baes Jr., C. F.; Mesmer, R. E. *The Hydrolysis of Cations: A Critical Review of Hydrolytic Species and Their Stability Constants in Aqueous Solution*; Wiley-Interscience: New York, 1976.
56. Lide, D. R., Ed.; In *CRC Handbook of Chemistry and Physics*; CRC Press: Cleveland, OH, 1992-1993.
57. Shannon, R. D. Revised Effective Ionic Radii and Systematic Studies of Interatomic Distances in Halides and Chalcogenides. *Acta Crystallogr. Sect. A* **1976**, *A32*, 751-767.
58. Harris, D. C. *Quantitative Chemical Analysis*; W. H. Freeman and Company: New York, 2010.
59. Mirza, U. A.; Chait, B. T. Effects of Anions on the Positive Ion Electrospray Ionization Mass Spectra of Peptides and Proteins. *Anal. Chem.* **1994**, *66*, 2898-2904.
60. Dai, J.; Mendonsa, S. D.; Bowser, M. T.; Lucy, C. A.; Carr, P. W. Effect of Anionic Additive Type on Ion Pair Formation Constants of Basic Pharmaceuticals. *J. Chromatogr. A* **2005**, *1069*, 225-234.
61. Iavarone, A. T.; Udekwu, O. A.; Williams, E. R. Buffer Loading for Counteracting Metal Salt-Induced Signal Suppression in Electrospray Ionization. *Anal. Chem.* **2004**, *76*, 3944-3950.
62. Sterling, H. J.; Batchelor, J. D.; Wemmer, D. E.; Williams, E. R. Effects of Buffer Loading for Electrospray Ionization Mass Spectrometry of a Noncovalent Protein Complex that Requires High Concentrations of Essential Salts. *J. Am. Soc. Mass Spectrom.* **2010**, *21*, 1045-1049.

63. Perry, D. L.; Phillips, S. L., Eds.; In *Handbook of Inorganic Compounds*; CRC Press: Boca Raton, FL, 1995.
64. Wilm, M.; Shevchenko, A.; Houthaeve, T.; Breit, S.; Schweigerer, L.; Fotsis, T.; Mann, M. Femtomole Sequencing of Proteins from Polyacrylamide Gels by Nano-Electrospray Mass Spectrometry. *Nature* **1996**, *379*, 466-469.
65. Reschke, B.; Timperman, A. A Study of Electrospray Ionization Emitters with Differing Geometries with Respect to Flow Rate and Electrospray Voltage. *J. Am. Soc. Mass Spectrom.* **2011**, *22*, 2115-2124.
66. Speetjens, J. K.; Parand, A.; Crowder, M. W.; Vincent, J. B.; Woski, S. A. Low-molecular Weight Chromium-binding Substance and Biomimetic  $[\text{Cr}_3\text{O}(\text{O}_2\text{CH}_2\text{CH}_3)_6(\text{H}_2\text{O})_3]^+$  Do Not Cleave DNA Under Physiologically-relevant Conditions. *Polyhedron* **1999**, *181821*, 2617-2624.
67. Vincent, J. B. Elucidating a Biological Role for Chromium at a Molecular Level. *Acc. Chem. Res.* **2000**, *33*, 503-510.
68. Davis, C. M.; Vincent, J. B. Isolation and Characterization of a Biologically Active Chromium Oligopeptide from Bovine Liver. *Arch. Biochem. Biophys.* **1997**, *339*, 335-343.
69. Panzhinskiy, E.; Ren, J.; Vincent, J. B.; Sreejayan, N. A Novel Endogenous Chromium Binding Peptide Augments Glucose Uptake and Insulin Signaling in Myotubes. *Diabetes* **2012**, *61* (Suppl. 1), A412.
70. Chen, Y.; Watson, H. M.; Gao, J.; Sinha, S. H.; Cassady, C. J.; Vincent, J. B. Characterization of the Organic Component of Low-Molecular-Weight Chromium-Binding Substance and Its Binding of Chromium. *J. Nutr.* **2011**, *141*, 1225-1232.
71. Iavarone, A. T.; Williams, E. R. Mechanism of Charging and Supercharging Molecules in Electrospray Ionization. *J. Am. Chem. Soc.* **2003**, *125*, 2319-2327.
72. Van Berkel, G. J.; Kertesz, V. Using the Electrochemistry of the Electrospray Ion Source. *Anal. Chem.* **2007**, *79*, 5510-5520.
73. Taube, H. Rates and Mechanisms of Substitution in Inorganic Complexes in Solution. *Chem. Rev.* **1952**, *50*, 69-126.
74. Drljaca, A.; Spiccia, L. Early Stages of the Hydrolysis of Chromium(III) in Aqueous Solution. XII. Kinetics of Cleavage of the Trimer and Tetramer in Acidic Solution. *Polyhedron* **1996**, *15*, 4373-4385.
75. Aksoy, M. S.; Oezer, U. Potentiometric and Spectroscopic Studies with Chromium (III) Complexes of Hydroxysalicylic Acid Derivatives in Aqueous Solution. *Turk. J. Chem.* **2003**, *27*, 667-673.

76. Drljaca, A.; Spiccia, L.; Krouse, H. R.; Swaddle, T. W. Kinetics of Water Exchange on the Hydrolytic Doubly Hydroxo-Bridged Rhodium(III) Dimer. *Inorg. Chem.* **1996**, *35*, 985-990.
77. Cotton, F. A.; Wilkinson, G. *Advanced Inorganic Chemistry*; John Wiley and Sons: New York, 1988.
78. Vogel, A. I. *A Textbook of Macro and Semimicro Qualitative Inorganic Analysis*; Longman: London, 1954.
79. Hopkins Jr., L. L.; Schwarz, K. Chromium (III) Binding to Serum Proteins, Specifically Siderophilin. *Biochimica et Biophysica Acta (BBA) - General Subjects* **1964**, *90*, 484-491.
80. Sterling, H. J.; Kintzer, A. F.; Feld, G. K.; Cassou, C. A.; Krantz, B. A.; Williams, E. R. Supercharging Protein Complexes from Aqueous Solution Disrupts their Native Conformations. *J. Am. Soc. Mass Spectrom.* **2012**, *23*, 191-200.
81. Samalikova, M.; Matecko, I.; Mueller, N.; Grandori, R. Interpreting Conformational Effects in Protein Nano-ESI-MS Spectra. *Anal. Bioanal. Chem.* **2004**, *378*, 1112-1123.
82. Lomeli, S. H.; Yin, S.; Ogorzalek Loo, R. R.; Loo, J. A. Increasing Charge While Preserving Noncovalent Protein Complexes for ESI-MS. *J. Am. Soc. Mass Spectrom.* **2009**, *20*, 593-596.
83. Dutcher, C. S.; Wexler, A. S.; Clegg, S. L. Surface Tensions of Inorganic Multicomponent Aqueous Electrolyte Solutions and Melts. *J Phys Chem A* **2010**, *114*, 12216-12230.
84. Banks, C. V.; Singh, R. S. Composition and Stability of Some Metal-5-Sulfosalicylate Complexes. *J. Inorg. Nucl. Chem.* **1960**, *15*, 125-132.
85. Yasarawan, N.; Thipyapong, K.; Sirichai, S.; Ruangpornvisuti, V. Synthesis of Chromium(III) Complex with 1-hydroxy-2-pyridinone-6-carboxylic Acid as Insulin-Mimetic Agent and its Spectroscopic and Computational Studies. *J. Mol. Struct.* **2013**, *1031*, 144-151.
86. Rebenstorf, B.; Larsson, R. IR Studies of Coordinatively Unsaturated Surface Compounds on Silica gel. IV. Carbonyl Complexes of Chromium(II) and Chromium(III). *Z. Anorg. Allg. Chem.* **1981**, *478*, 119-138.
87. Lukehart, C. M.; Torrence, G. P. Reactions of Coordinated Molecules. 19. Metalla-Beta-Diketonate Complexes of Copper(II), Iron(III), Chromium(III), Zinc(II), and Magnesium(II). *Inorg. Chem.* **1979**, *18*, 3150-3155.
88. Simoncini, A. The effect of Dialdehydes on Chromium Salts. *Cuoio, Pelli, Mater. Concianti* **1964**, *40*, 9-31;84-95.
89. Rakesh, K. P.; Shiva Prasad, K.; Shridhara Prasad, K. Synthesis and Characterization of Chromium (III) Complexes of 4(3H)-Quinazolinone Derived Schiff Base: Antimicrobial and DNA Interaction Studies. *Int. J. Res. Chem. Environ.* **2012**, *2*, 221-225.



90. Radford, R. J.; Lim, M. D.; Santana Da Silva, R.; Ford, P. C. Photochemical Cleavage of Nitrate Ion Coordinated to a Cr(III) Porphyrin. *J. Coord. Chem.* **2010**, *63*, 2743-2749.
91. Belock, C. W.; Cetin, A.; Barone, N. V.; Ziegler, C. J. Transition Metal Coordination Chemistry of N,N-Bis(2-{pyrid-2-yl}ethyl)hydroxylamine. *Inorg. Chem.* **2008**, *47*, 7114-7120.
92. Sattari, D.; Alipour, E.; Shirani, S.; Amighian, J. Metal Complexes of N-Salicylideneamino Acids. *J. Inorg. Biochem.* **1992**, *45*, 115-122.
93. Broderick, W. E.; Legg, J. I. Synthesis of the First Stable Nitrogen Coordinated Nicotinic acid Chromium(III) Complexes: cis- and trans-H[Cr(mal)<sub>2</sub>(nic-N)<sub>2</sub>]. *Inorg. Chem.* **1985**, *24*, 3724-3725.
94. Pearson, R. G. Hard and Soft Acids and Bases—the Evolution of a Chemical Concept. *Coord. Chem. Rev.* **1990**, *100*, 403-425.
95. Davis, C. M.; Vincent, J. B. Chromium Oligopeptide Activates Insulin Receptor Tyrosine Kinase Activity. *Biochemistry* **1997**, *36*, 4382-4385.
96. Hatfield, M. J.; Gillespie, S.; Chen, Y.; Li, Z.; Cassady, C. J.; Vincent, J. B. Low-Molecular-Weight Chromium-Binding Substance from Chicken Liver and American Alligator Liver. *Comp. Biochem. Physiol. Part B: Biochem. Mol. Biol.* **2006**, *144B*, 423-431.
97. Sun, Y.; Ramirez, J.; Woski, S. A.; Vincent, J. B. The Binding of Trivalent Chromium to Low-Molecular-Weight Chromium-Binding Substance (LMWCr) and the Transfer of Chromium from Transferrin and Cr(pic)<sub>3</sub> to LMWCr. *J. Biol. Inorg. Chem.* **2000**, *5*, 129-136.
98. Savitski, M. M.; Faelth, M.; Fung, Y. M. E.; Adams, C. M.; Zubarev, R. A. Bifurcating Fragmentation Behavior of Gas-Phase Tryptic Peptide Dications in Collisional Activation. *J. Am. Soc. Mass Spectrom.* **2008**, *19*, 1755-1763.
99. Faelth, M.; Savitski, M. M.; Nielsen, M. L.; Kjeldsen, F.; Andren, P. E.; Zubarev, R. A. SwedCAD, a Database of Annotated High-Mass Accuracy MS/MS Spectra of Tryptic Peptides. *J. Proteome Res.* **2007**, *6*, 4063-4067.
100. Aebersold, R.; Mann, M. Mass Spectrometry-Based Proteomics. *Nature.* **2003**, *422*, 198-207.
101. Michalski, A.; Cox, J.; Mann, M. More than 100,000 Detectable Peptide Species Elute in Single Shotgun Proteomics Runs but the Majority is Inaccessible to Data-Dependent LC-MS/MS. *J. Proteome Res.* **2011**, *10*, 1785-1793.

## CHAPTER 5: ELECTRON TRANSFER DISSOCIATION OF NEUTRAL PEPTIDES WITH ALKYL SIDE CHAINS

### 5.1 Introduction

Electron transfer dissociation (ETD)<sup>1</sup> and electron capture dissociation (ECD)<sup>2</sup> are two important tandem mass spectrometry techniques (MS/MS) in peptide and protein sequencing.<sup>3-11</sup> In post-translational modifications (PTMs), the modified side chains remain intact during ETD and ECD, which makes the two techniques especially useful in protein sequencing. ETD and ECD are reported as new methods for increasing sequence coverage in the Human Proteome Project.<sup>12</sup> The two techniques are complementary to collision-induced dissociation (CID). ETD and ECD produce c- and z-ions by random backbone N-C<sub>α</sub> bond cleavages, while CID cleaves at C-N bonds to make b- and y-ions.<sup>11,13</sup> Although the methods by which a multiply protonated peptide obtains an electron are different in ETD and ECD, the fragments produced and mechanisms involved are similar.<sup>14</sup>

Two major mechanisms have been proposed to explain fragmentation in ETD and ECD. In the Cornell mechanism,<sup>2</sup> proposed by McLafferty and co-workers, an electron localized at a positively charged functional group (e.g., ammonium or guanidinium) captures a hydrogen atom (H•) to form an odd-electron ion and initiate N-C<sub>α</sub> bond dissociation.<sup>15</sup> Backbone dissociation produces c- and z-fragment ions. The non-ergodic N-C<sub>α</sub> bond dissociation process<sup>2</sup> is affected by intramolecular solvation of protons from the side chains of basic residues. However, this mechanism does not explain N-C<sub>α</sub> bond dissociations that are remote from the basic residues.

The other mechanism proposed by the Simons<sup>16</sup> and Tureček<sup>13</sup> groups independently is known as the Utah-Washington (UW) mechanism. The electron in ECD or ETD is captured in a Coulomb stabilized amide  $\pi^*$  orbital that turns the amide bond into a superbase. The amide superbase can either accept a proton from a close proton donor group, which triggers backbone cleavage, or undergo N-C $_{\alpha}$  bond dissociation to form an enole-imidate anion, which then abstracts a proton to form c- and z-product ions.<sup>17</sup> The most important difference between the two mechanisms is that the UW mechanism does not need the side chains of basic residues to be involved in proton-coupled electron transfer.

In order to perform ETD or ECD experiments, a peptide should be at least doubly positive charged under electrospray ionization (ESI) conditions. Peptides without basic residues, such as neutral peptides, often do not readily multiply charge<sup>18</sup> and therefore cannot be studied by ETD or ECD. However, it has been reported that in one case the neutral peptides DYMGWMDF-NH<sub>2</sub>, pEVNFSPGWGT-NH<sub>2</sub> and pEQWFWWM-NH<sub>2</sub> were studied by ECD.<sup>19</sup> Håkansson and coworkers<sup>19</sup> found that abundant b-ions were produced by ECD on these amide peptides that do not contain residues with basic side chains. There are a few reports<sup>20-26</sup> regarding b-ions produced from basic peptides in ECD. Cooper and coworkers found that lysine-containing peptides easily produce b-ions in ECD.<sup>21,26</sup> Oh and coworkers observed b-ions in ECD of peptides containing a lysine homologue (a species with an n-propylamine side chain as opposed to the n-butylamine side chain of lysine).<sup>23</sup> Two different groups, Haselmann<sup>22</sup> and Uggerud<sup>20</sup> and their coworkers, observed b-ions in ECD of amide peptides. Chamot-Rooke and coworkers<sup>25</sup> found b-ions in ECD of basic peptides containing five residues and proposed that the peptide size changes the redistribution of energy after electron capture and affects fragmentation pathways. Although b-ions have been observed in ECD, ETD studies have not shown the

formation of b-ions from  $[M+nH]^{n+}$ ; however, this may be because most fundamental studies of electron-induced dissociation techniques have involved ECD rather than ETD.

Two independent groups, Julian<sup>27</sup> and Hess<sup>28</sup> and their coworkers, reported b-ions in the ECD spectra of hydrogen-deficient peptide radical cations. However, special methods<sup>29-36</sup> were needed to produce hydrogen-deficient radical cations in the gas phase, such as CID of metal-peptide complexes. In addition, the precursor ion and fragmentation mechanisms of hydrogen-deficient peptides are different from those of the multiply protonated peptides in ECD. For hydrogen-deficient peptides, the radical ion undergoing dissociation is  $[M+nH]^{(n+1)+\bullet}$  and the dissociation is a competition between charge driven and radical driven processes.<sup>28,37,38</sup> In traditional ETD, the ion under dissociation is  $[M+nH]^{(n-1)+\bullet}$  and dissociation is only a radical driven process.

Sequencing and analysis of peptides without basic residues is important because numerous peptides with predominately neutral or acidic side chains exist in nature.<sup>39-42</sup> For example, in proteomics research, chymotrypsin protease is widely used to digest proteins into smaller peptides that contain tyrosine, tryptophan, or phenylalanine residues at the C-terminus.<sup>43</sup> The resulting peptides sometimes lack basic residues and may not be readily sequenced by positive ion mode electron-induced dissociation techniques.<sup>18</sup>

As discussed in Chapter 4, addition of Cr(III) nitrate to the solutions of peptides with neutral side chains can greatly increase the formation of doubly protonated ions,  $[M+2H]^{2+}$ , by ESI. This allows these peptides to be studied by ETD. This chapter discusses ETD experiments that were performed on  $[M+2H]^{2+}$  from neutral peptides composed of alanine, glycine, valine, leucine, and isoleucine residues. Because alanine, glycine, valine, leucine, and isoleucine are

amino acids with alkyl side chains, this allows investigation of ETD on neutral peptides with simple structures that do not contain additional heteroatoms.

## 5.2 Experimental

### 5.2.1 Peptides

Neutral peptides with an alkyl side chain synthesized were AAAAAAAAAAAAAA (A13), AAAAAAAAAAAAAA (A14), AAIAAAA, AALAAAA, AAVAAAA, AGGAAAA, and GGAVAAA, where A is alanine, G is glycine, I is isoleucine, L is leucine, and V is valine. The structures of these amino acids are given in Section 2.6. These peptides were synthesized with an Advanced Chem Tech (Louisville, KY, USA) model 90 automated peptide synthesizer by standard Fmoc synthetic procedures.<sup>44</sup> In addition, the peptides AAAAAAA, AAAAAAGA, AGGAAAAA, AGGAAAAA were purchased from Biomatik Co (Cambridge, Ontario, CA). Chromium (III) nitrate,  $\text{Cr}(\text{NO}_3)_3 \cdot 9\text{H}_2\text{O}$ , and HPLC grade acetonitrile and methanol were purchased from VWR (Radnor, PA, USA). Deionized and distilled water was produced with a Barnstead E-pure system (Dubuque, IA, USA).

The neutral peptides were first dissolved in a solvent of methanol:water at 50:50 volume:volume ratio or water using a concentration of 1 mg peptide per mL of solvent. From this stock solution, solutions for analysis by ESI were dissolved to 10  $\mu\text{M}$  in acetonitrile:water at a volume ratio of 50:50. A solution containing a molar ratio of Cr(III) to peptide at 10:1 was used to generate doubly protonated ions.

### 5.2.2 Mass Spectrometry

All experiments were performed using a Bruker (Billerica, MA, USA) HCTultra PTM Discovery System high capacity quadrupole ion trap mass spectrometer, as discussed in Chapter 2. Additional experimental details are also provided in Chapter 3.

### 5.3 Results

ETD experiments were performed on the doubly protonated peptides,  $[M+2H]^{2+}$ , with seven to fourteen residues. A comparison of ETD spectra for neutral and basic peptides is shown in Figure 5.1. Neutral peptide A7, in Figure 5.1(a), produces  $b_n$ ,  $n = 3-6$ ,  $[b_n+H-17]^+$ ,  $n = 4-6$ ,  $y_2$  and  $c_n''$ ,  $n = 3-5$ . The basic peptide AAARAAA in Figure 5.1(b) produces  $c_n''$ ,  $n = 4-6$ ,  $z_n'$ ,  $n = 4-6$ , and side chain losses ( $59\text{Da} \equiv \text{CH}_5\text{N}_3$ ,  $43\text{Da} \equiv \text{CH}_3\text{N}_2\bullet$ ,  $17\text{Da} \equiv \text{NH}_3$ ). These two peptides were dissociated under the same ETD conditions. ETD of the peptide A7 is dominated by b- and c-ions, which is very different from the spectrum of AAARAAA that contains mainly c- and z-ions.

Other neutral peptides containing seven or eight residues also primarily produce the b- and c-ion series and a few y- and z-ions by ETD. A summary of the ETD product ions for the peptides studied is given in Table 5.1. Examples of the spectra for various alkyl side chain residues are shown in Figure 5.2, which displays the products of the peptides AAIAAAA, AALAAAA, and AAVAAAA after undergoing the ETD reaction.

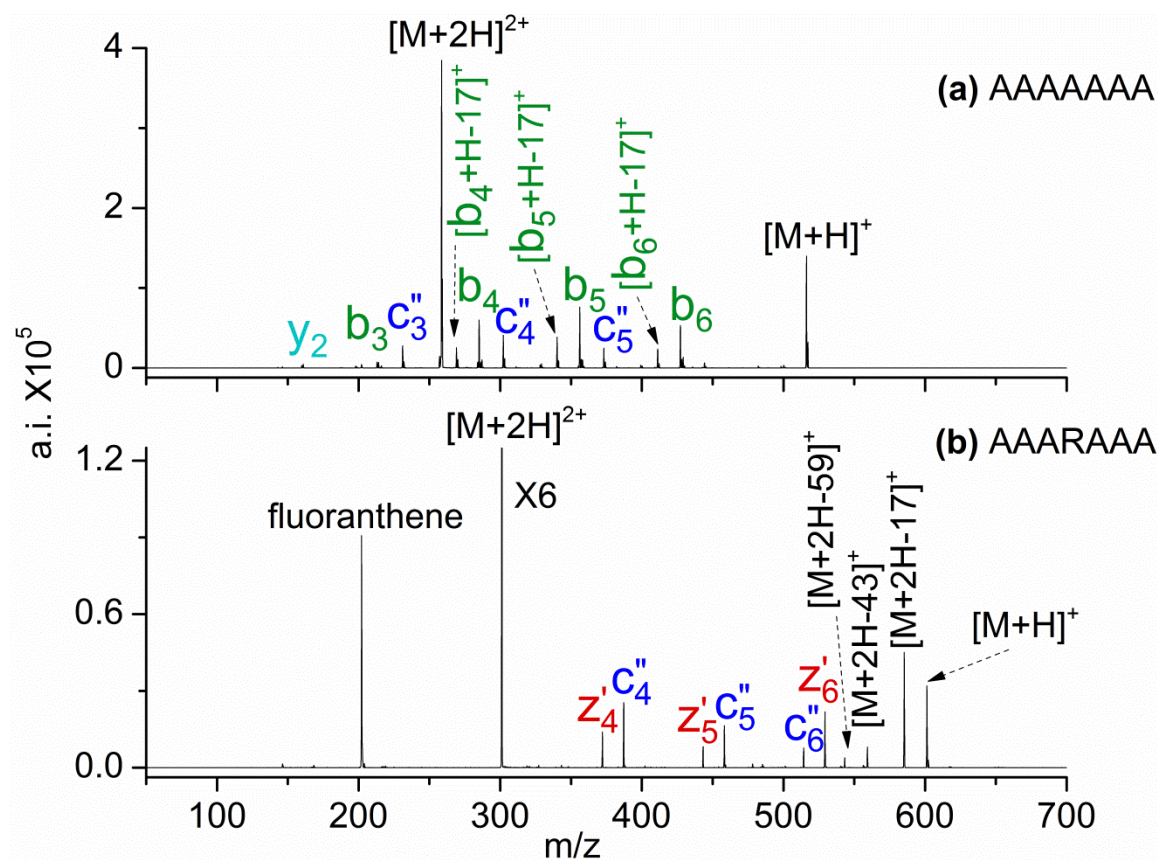


**Figure 5.1.** The ETD spectra of  $[M+2H]^{2+}$  from (a) AAAAAAA (A7) and (b) AAARAAA.

**Table 1.** Product ions produced by ETD on  $[M+2H]^{2+}$  of peptides with alkyl side chains.<sup>a</sup>

Peptides	n =	$b_n$	$[b_n+H-17]$	$c_n''$	$y_n$	$z_n'$
AAARAAA				4-6		4-6
A7		3-6	4-6	3-5	2	
AAIAAAA		3-6	4-6	3-6	3	
AALAAAA		3-6	4-6	3-6	3	
AAVAAAA		3-6	3-6	2-6	3	4
AAAAAGA		3-6	4-6	3-6	3	
AGGAAAA		4-6	5-6	3-6	2	4
AGGAAAAA		4-7	5-7	3-7		5
GGAVAAA		4-6	4-6	3-6	2-3	4-5
AGGAAAAAA		6-8	6-8	4-8	5	5
A13		7, 12		7-12		
A14		12-13		8-13		10

<sup>a</sup> Numerical values in the table indicate the range of n values (position of cleavage sites) observed in the ETD spectra.



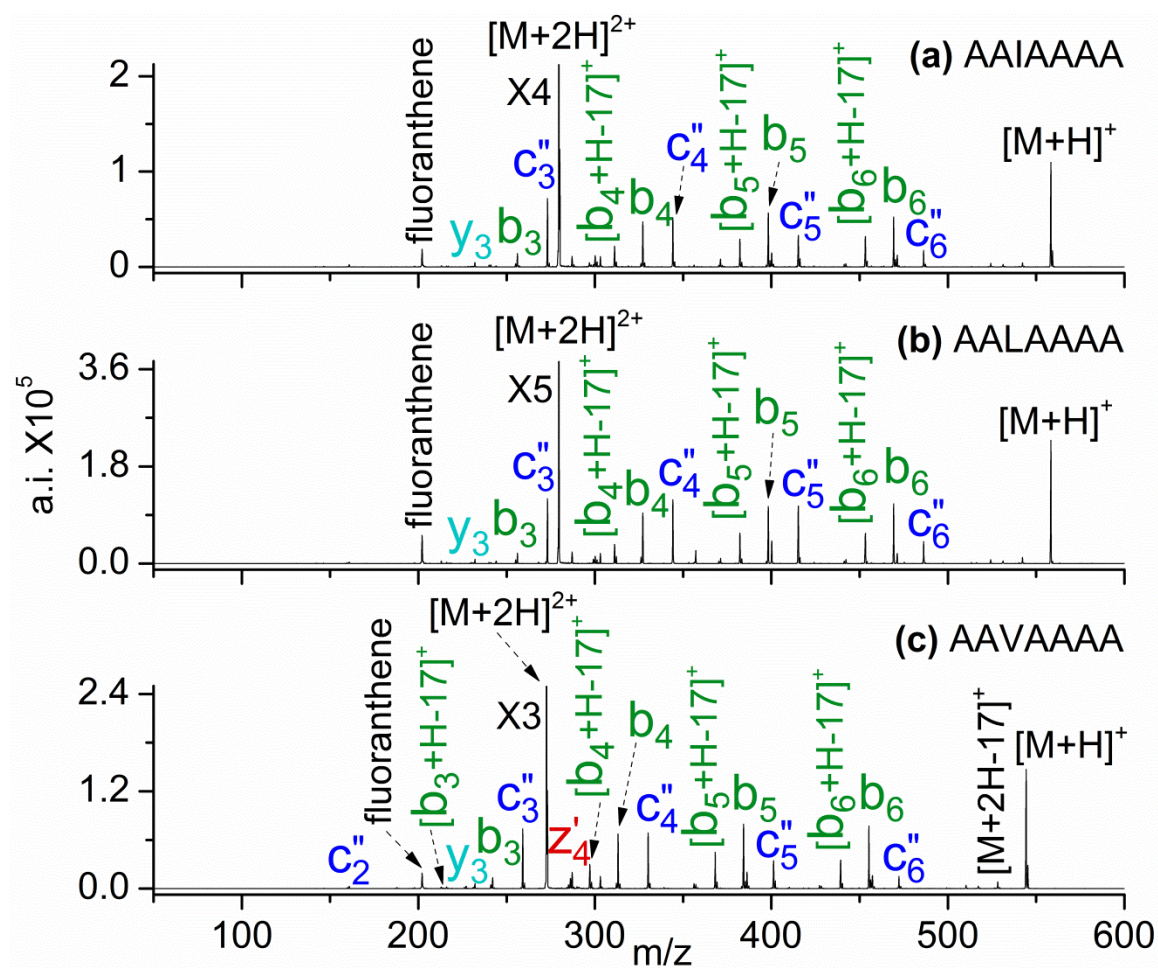


**Figure 5.2.** The ETD spectra of  $[M+2H]^{2+}$  from (a) AAIAAAA, (b) AALAAAA, and (c) AAVAAAA.

When the chain length increases, the ETD fragmentation pattern of the neutral peptides begins to change. In Figure 5.3(a) of the nine residue peptide AGGAAAAAA,  $b_n$ ,  $n = 6-8$ ,  $[b_n+H-17]^+$ ,  $n = 6-8$ ,  $y_5$ ,  $z_5'$ ,  $c_n''$ ,  $n = 4-8$ , and  $[M+2H-17]^+$  were produced. The dominant peaks are only from the c-ion series and not the b-ion series. In Figure 5.3(b), A14 produces  $b_n$ ,  $n = 12-13$ ,  $z_{10}'$  and  $c_n''$ ,  $n = 8-13$ . The same trend can also be observed in Figure 5.4 for GGAVAAA and Figure 5.5 for A13. When the peptide size increases, the product ions of neutral peptides gradually change from members of the b- and c-ion series to primarily the c-ion series.

## 5.4 Discussion

### 5.4.1 Effect of the Identity of the Neutral Residue with Alkyl Side Chain on ETD

The identity of the neutral residues has no effect on ETD. Alanine (A), isoleucine (I), leucine (L), and valine (V) are the four residues with alkyl side chains. ETD of the peptides AAAAAAA, AAIAAAA, AALAAAA, AAVAAAA in Figure 5.1(a) and Figure 5.2 have similar product ions. As discussed in Chapter 3, for basic peptides, arginine, lysine, and histidine residues have different effects on ETD, which is due to the structures and basicities of their side chains.<sup>2,17,45</sup> The alkyl side chains of the neutral residues cannot protonate and have minimal effect on dissociation as compared to the peptide backbone, which can protonate.

### 5.4.2 Mechanism of b-Ion Formation in ETD of Neutral Peptides

In ETD or ECD studies, the major product ions have been c- and z-ions, which are produced by cleavage of backbone N-C $_{\alpha}$  bonds.<sup>1,2</sup> There are few reports about b-ions produced in ETD or ECD.<sup>19-28</sup> In the ETD experiments discussed here, for neutral heptapeptides or the octapeptide AGGAAAAA, the b- and c-ion series are the dominant product ions. In CID, b- and

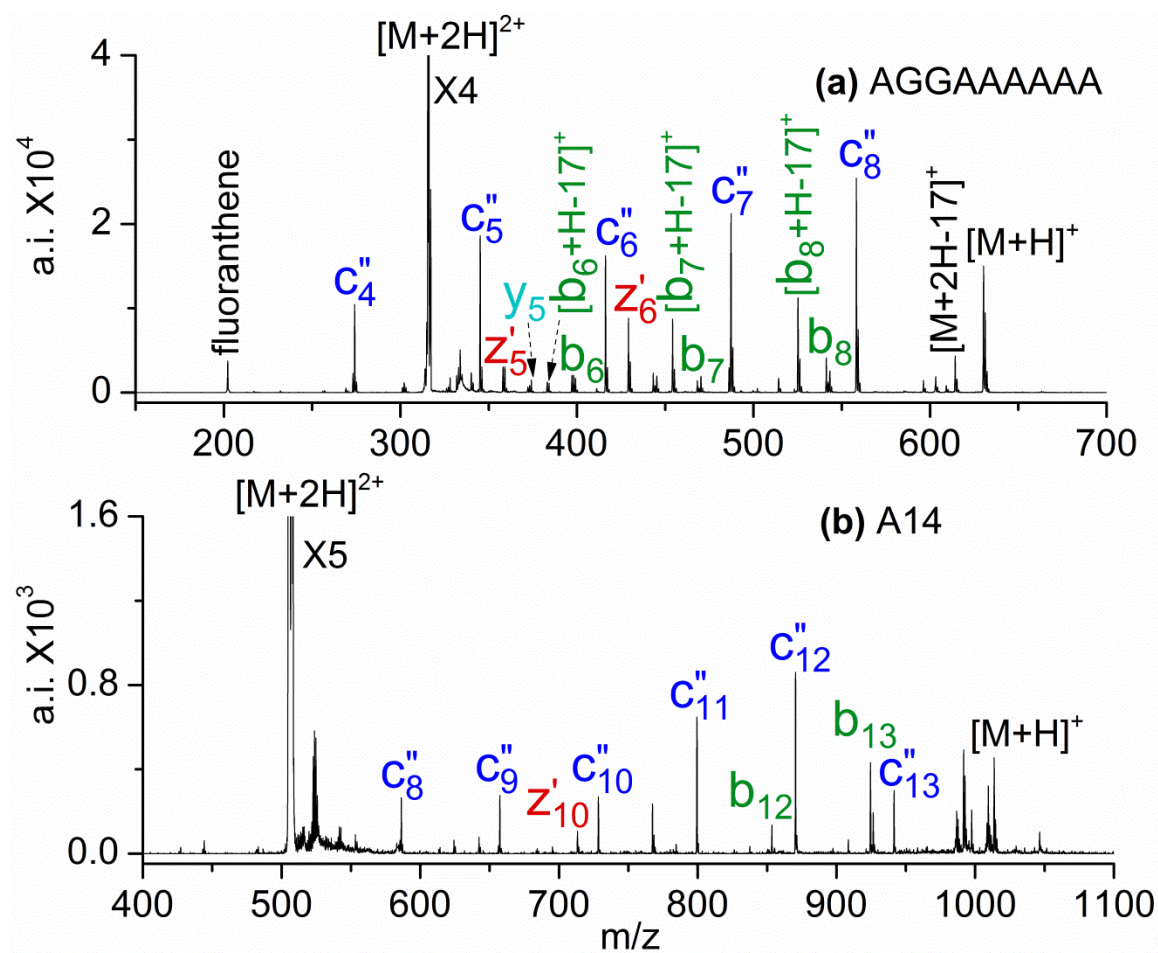


**Figure 5.3.** The ETD spectra of  $[M+2H]^{2+}$  from (a) AGGAAAAAA, and (b) A14.



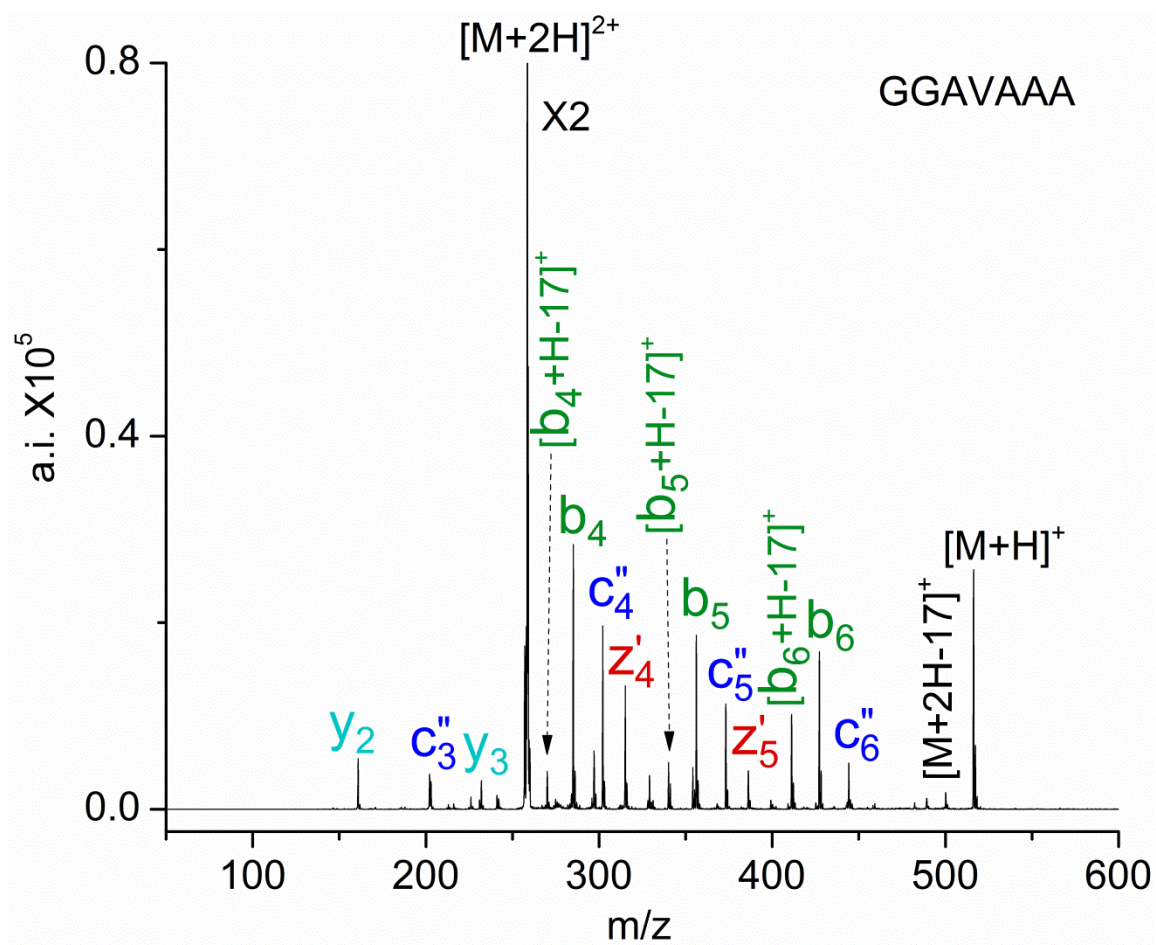


**Figure 5.4.** The ETD spectrum of  $[M+2H]^{2+}$  from GGAVAAA.

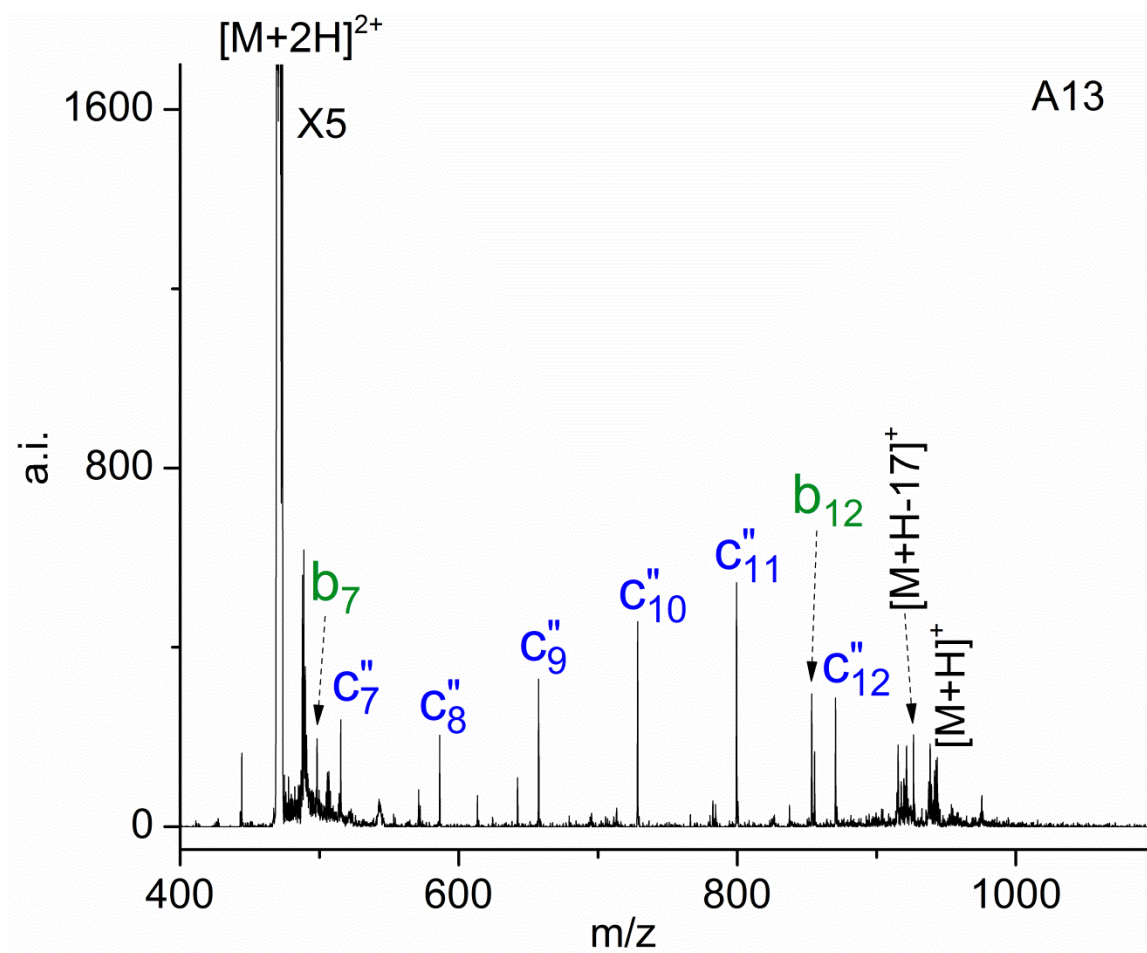


**Figure 5.5.** The ETD spectrum of  $[M+2H]^{2+}$  from A13.

y-ions are the major product ions, and are produced by cleavage of amide C-N bonds along the backbone.<sup>46,47</sup>

In order to know if the b-ions produced in ETD are also present in CID, singly protonated ions,  $[M+H]^+$ , were subjected to CID. Figure 5.6 shows CID on  $[M+H]^+$  from the peptide A7. The mass spectrum contains  $b_n$ ,  $n = 3-6$ , that were also produced in ETD. To confirm if these b-ions produced in ETD and CID have the same structure, MS/MS/MS experiments were performed. Figure 5.7(a) and (b) displays the CID of  $b_6$  from the peptide A7. The  $b_6$  precursor ion in Figure 5.7(a) was generated from  $[M+H]^+$  by CID; therefore, this is a MS/MS/MS experiment involving CID/CID. The  $b_6$  precursor ion in Figure 5.7(b) was produced by  $[M+2H]^{2+}$  in ETD; the spectrum is from an ETD/CID experiment. The two MS/MS/MS spectra are virtually identical. Additional MS/MS experiments show that the other b-ions produced from A7 in Figures 5.8 and 5.9 also have the same structures. Other peptides such as AAAAAGA, AGGAAAA and AGGAAAAA, whose spectra are shown in Figures 5.10 through 5.20, give the same results as A7. Thus, b-ions generated by ETD have the same structures as b-ions from CID.

Cooper<sup>21</sup> has performed experiments to confirm that the b-ions found in ECD are not from a CID process but instead result directly from ECD of the precursor ion. The b-ions are also not from loss of ammonia,  $NH_3$ , from c-ions. Cooper<sup>21</sup> used resonant single-frequency dipolar excitation to continuously eject c-ions produced by ECD, and the resulting spectrum did not have c-ions, but still contained b-ions.<sup>21</sup> In addition, if b-ions observed in ETD and CID of neutral peptides have the same mechanism of formation, the basic peptide AAARAAA should also have b-ions upon ETD fragmentation. Figure 5.1(b) shows no b-ion production. Therefore, b-ions formed in ETD of neutral peptides, unlike the b-ions originating from CID, are not formed by collisions of the precursor ion with an inert gas. In addition, our spectra (e.g., Figure 5.1(b)),



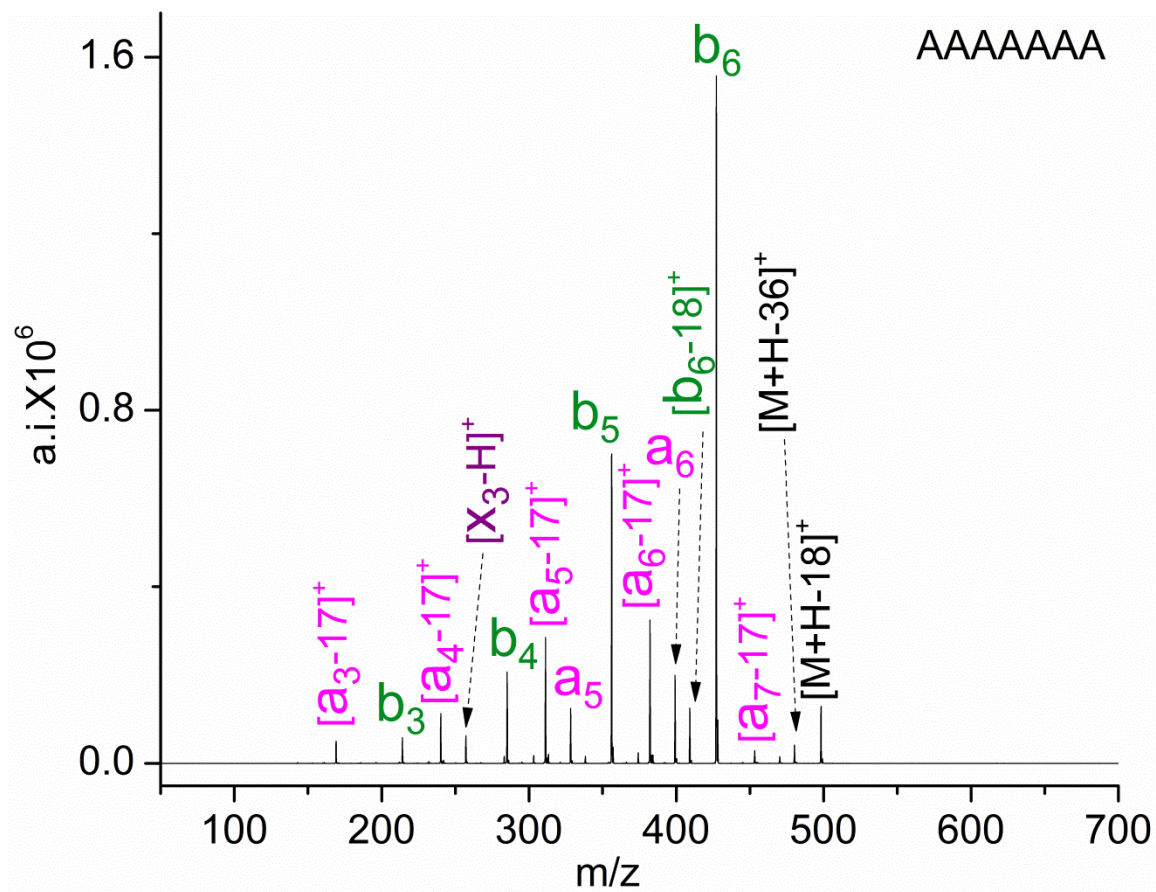


**Figure 5.6.** The CID spectrum of  $[M+H]^+$  from A7.

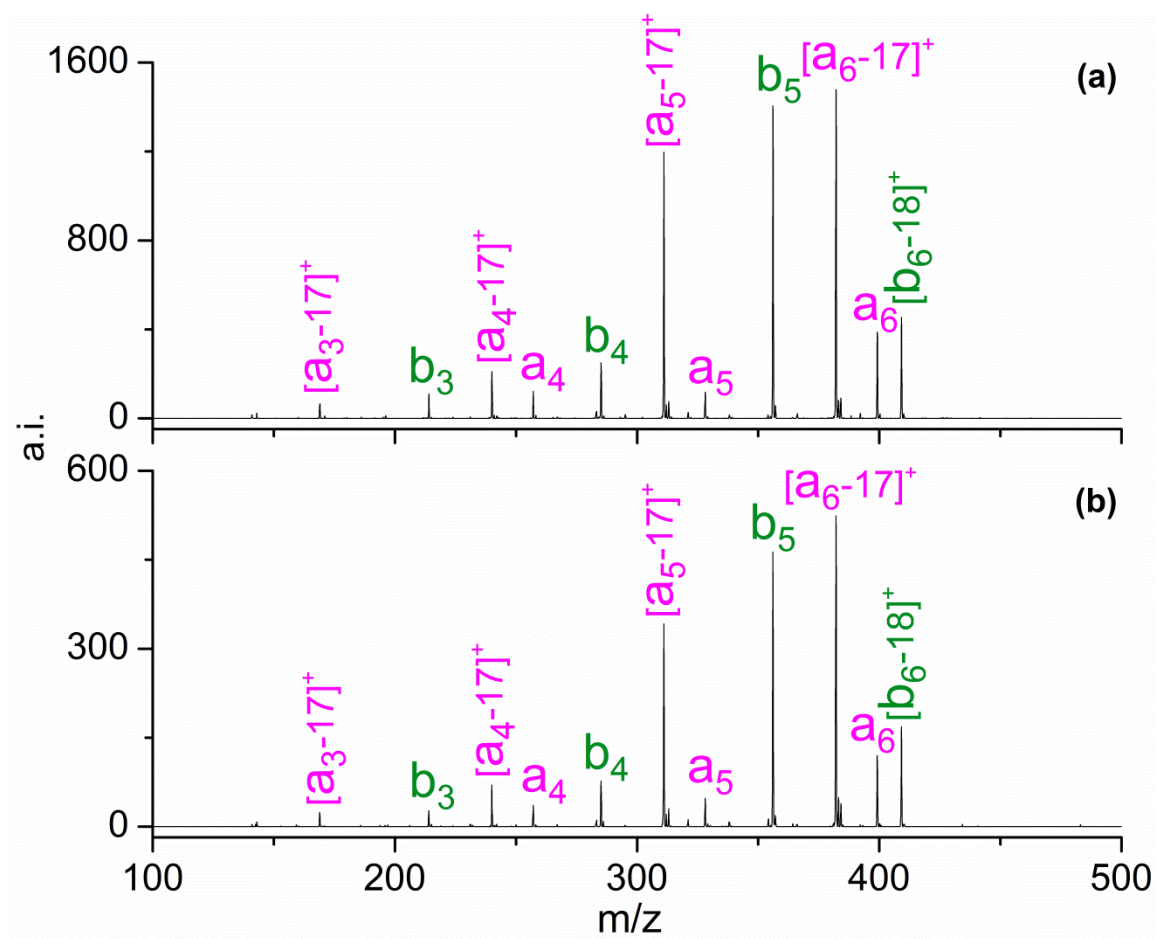


**Figure 5.7.** The CID spectra (MS/MS/MS) of  $b_6$  produced by (a) ETD on  $[M+2H]^{2+}$  on A7 and by (b) CID on  $[M+H]^+$  on A7.



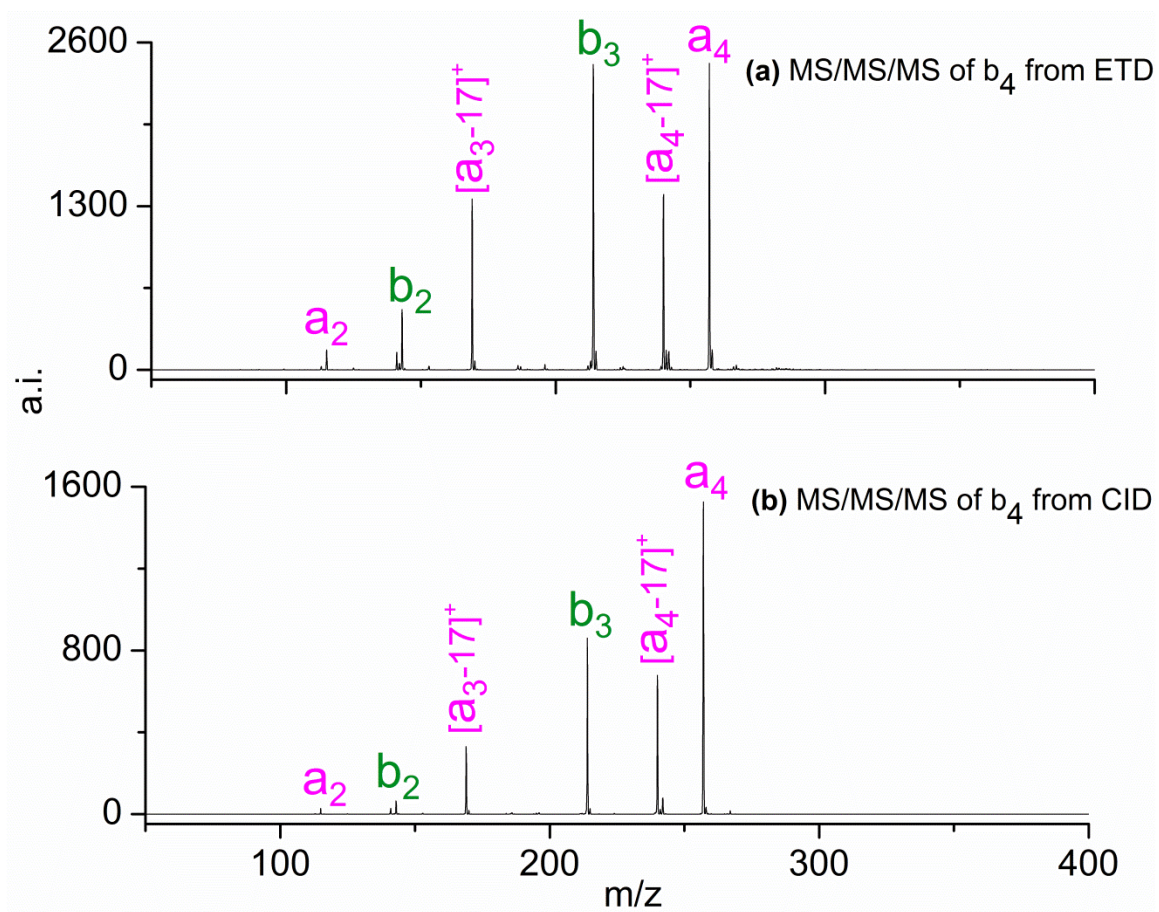


**Figure 5.8.** The CID spectra (MS/MS/MS) of  $b_4$  produced by (a) ETD on  $[M+2H]^{2+}$  on A7 and by (b) CID on  $[M+H]^+$  on A7.

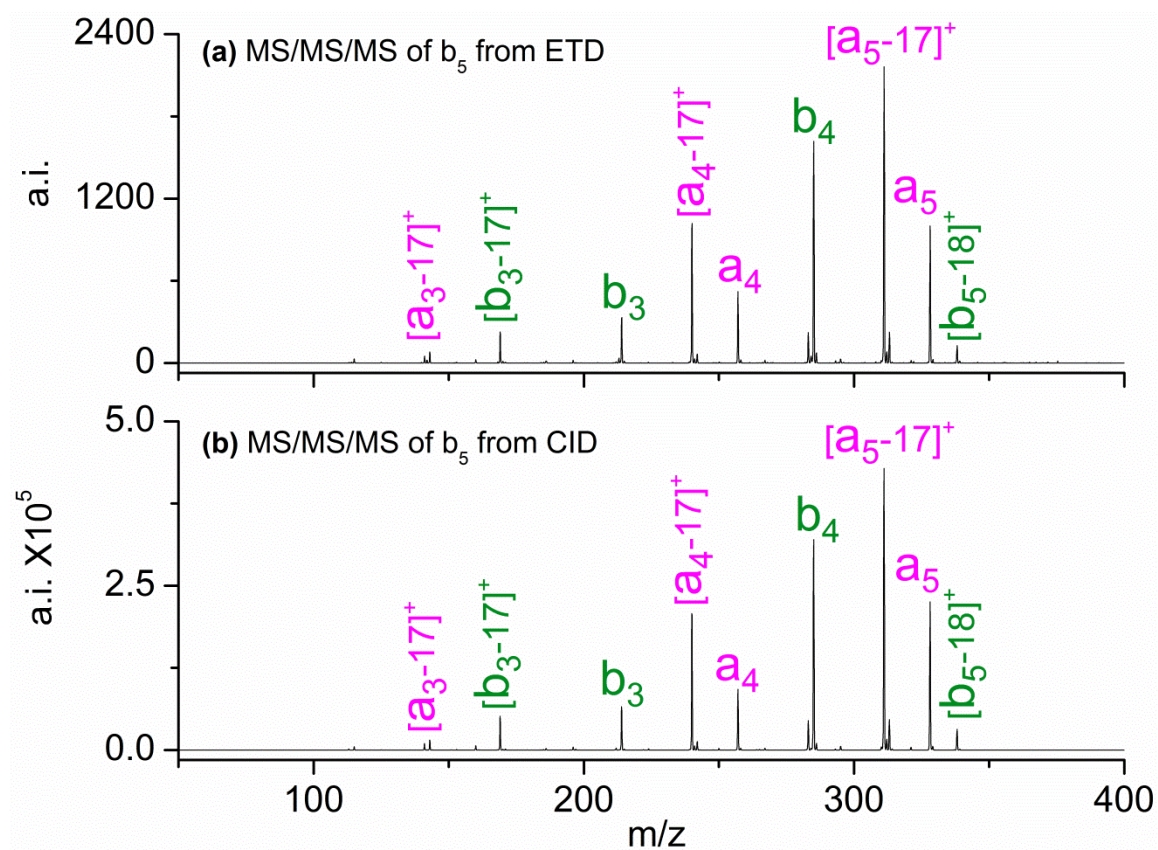


**Figure 5.9.** The CID spectra (MS/MS/MS) of  $b_5$  produced by (a) ETD on  $[M+2H]^{2+}$  on A7 and by (b) CID on  $[M+H]^+$  on A7.

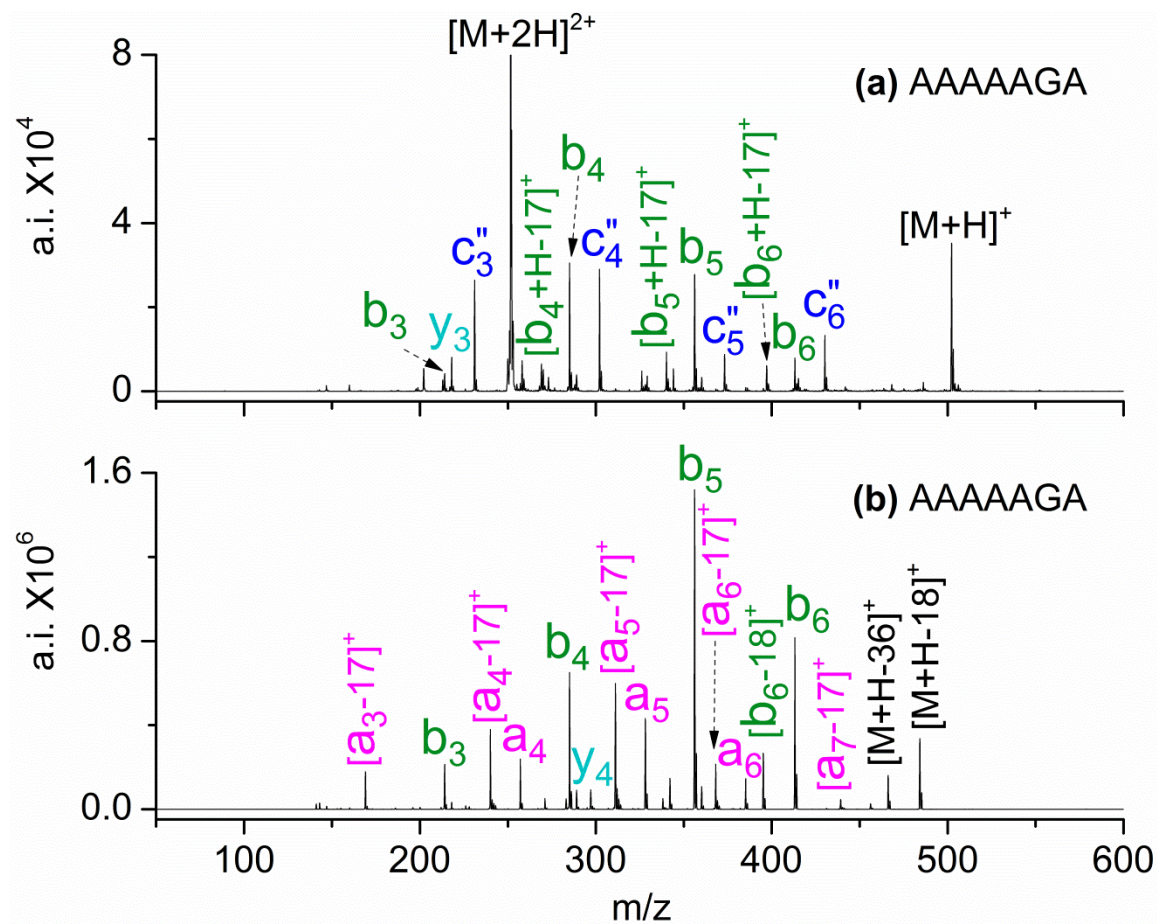


**Figure 5.10.** (a) ETD spectrum of  $[M+2H]^{2+}$  from AAAAAAGA and (b) CID spectrum of  $[M+H]^+$  from AAAAAAGA.



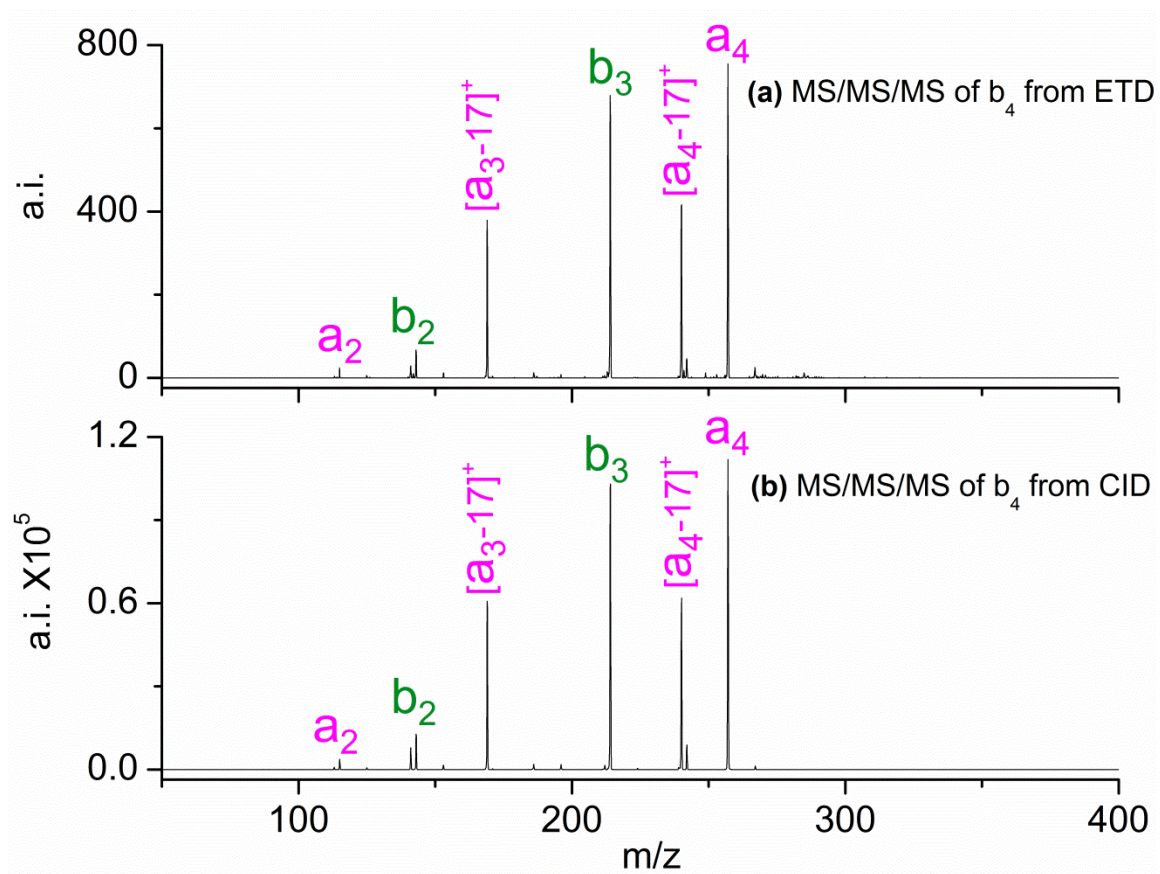


**Figure 5.11.** The CID spectra (MS/MS/MS) of  $b_4$  produced by (a) ETD on  $[M+2H]^{2+}$  on AAAAAGA and by (b) CID on  $[M+H]^+$  on AAAAAGA.

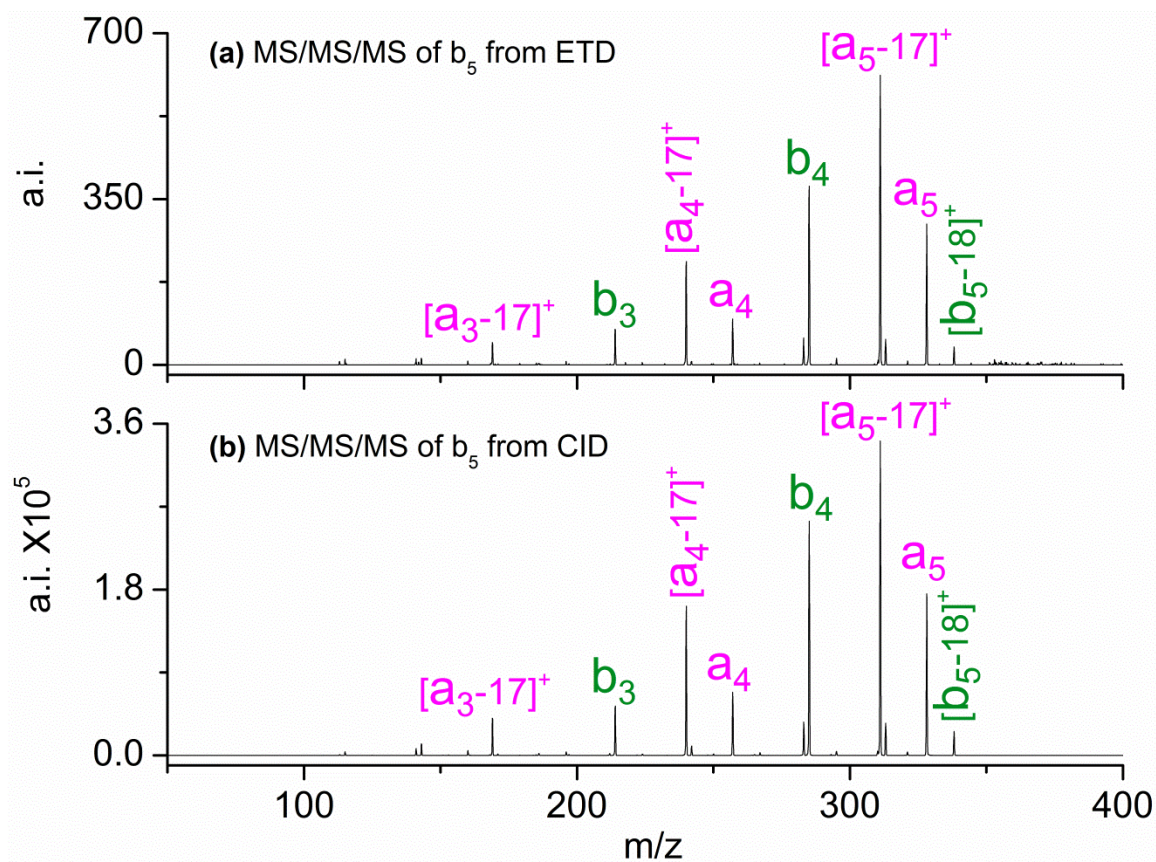


**Figure 5.12.** The CID spectra (MS/MS/MS) of  $b_5$  produced by (a) ETD on  $[M+2H]^{2+}$  on AAAAAGA and by (b) CID on  $[M+H]^+$  on AAAAAGA.

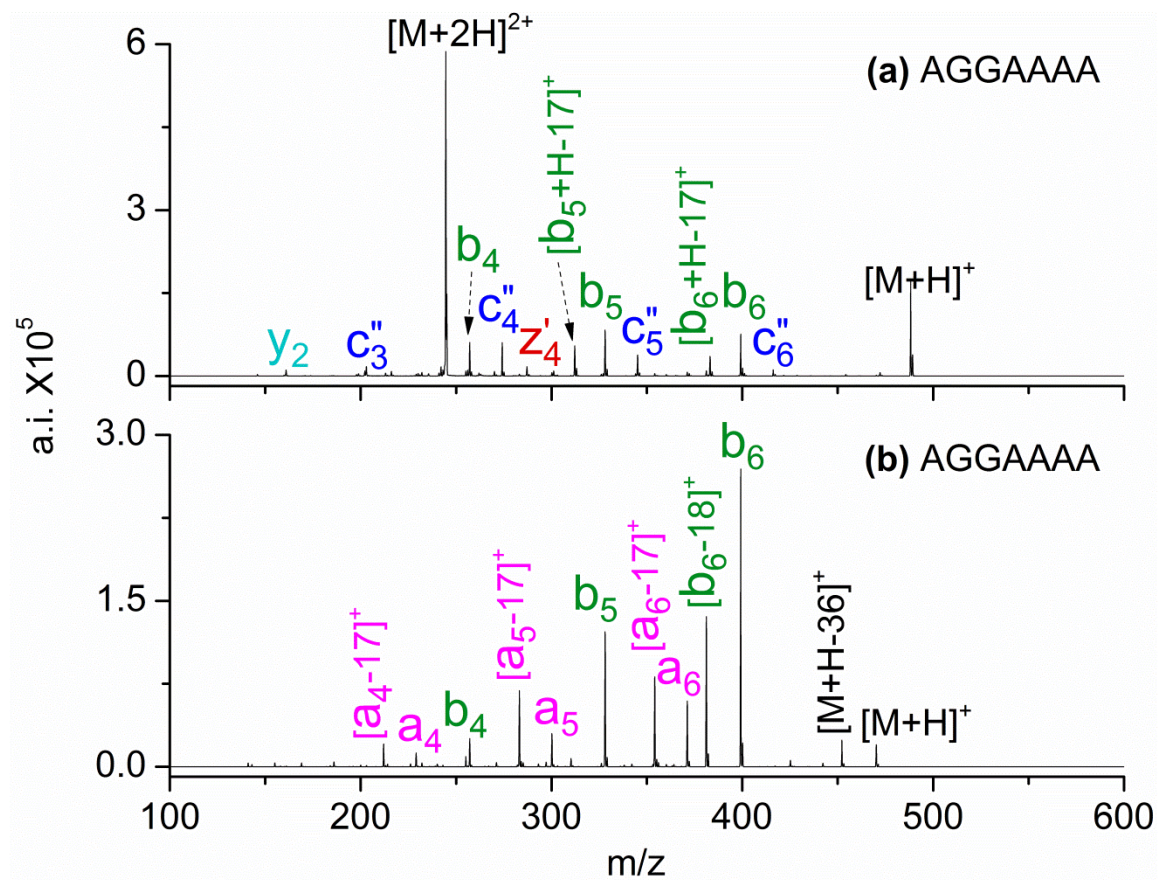


**Figure 5.13.** (a) ETD spectrum of  $[M+2H]^{2+}$  from AGGAAAA and (b) CID spectrum of  $[M+H]^+$  from AGGAAAA.



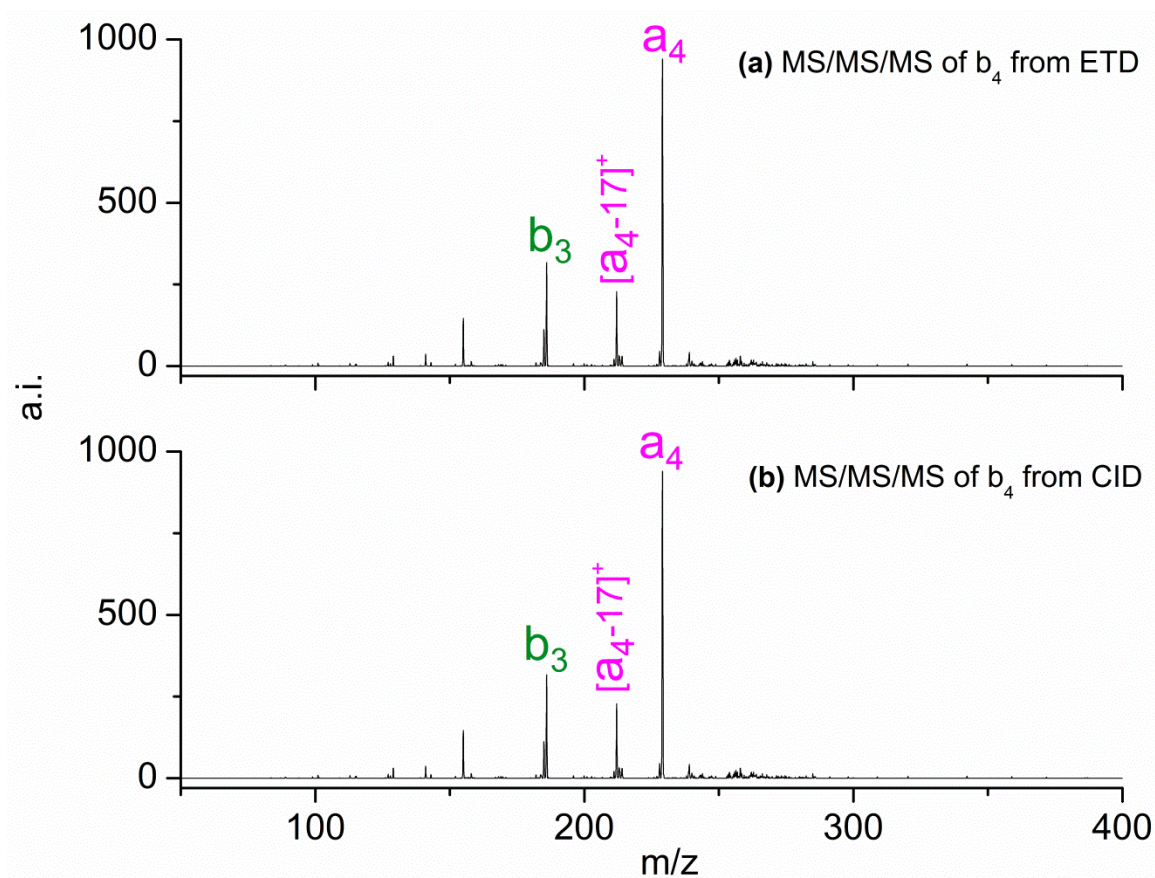


**Figure 5.14.** The CID spectra (MS/MS/MS) of  $b_4$  produced by (a) ETD on  $[M+2H]^{2+}$  on AGGAAAA and by (b) CID on  $[M+H]^+$  on AGGAAAA.

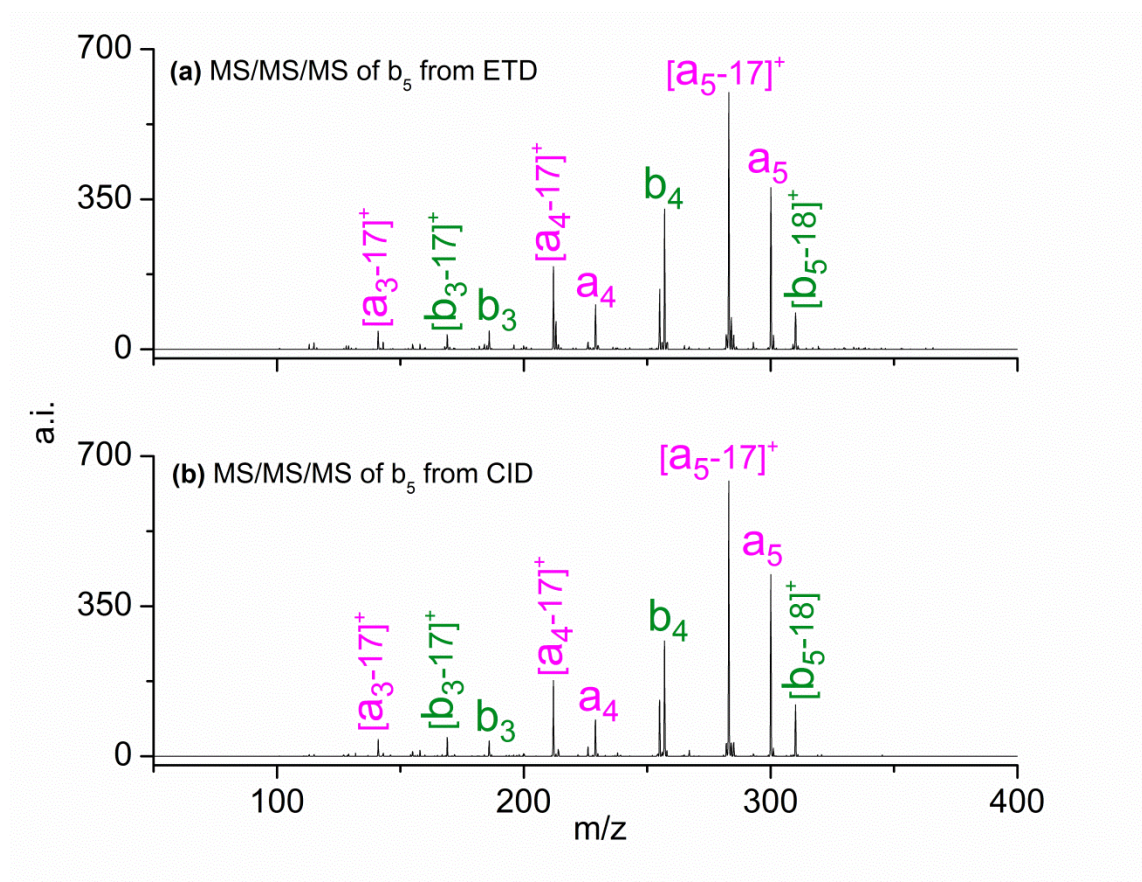


**Figure 5.15.** The CID spectra (MS/MS/MS) of  $b_5$  produced by (a) ETD on  $[M+2H]^{2+}$  on AGGAAAA and by (b) CID on  $[M+H]^+$  on AGGAAAA.



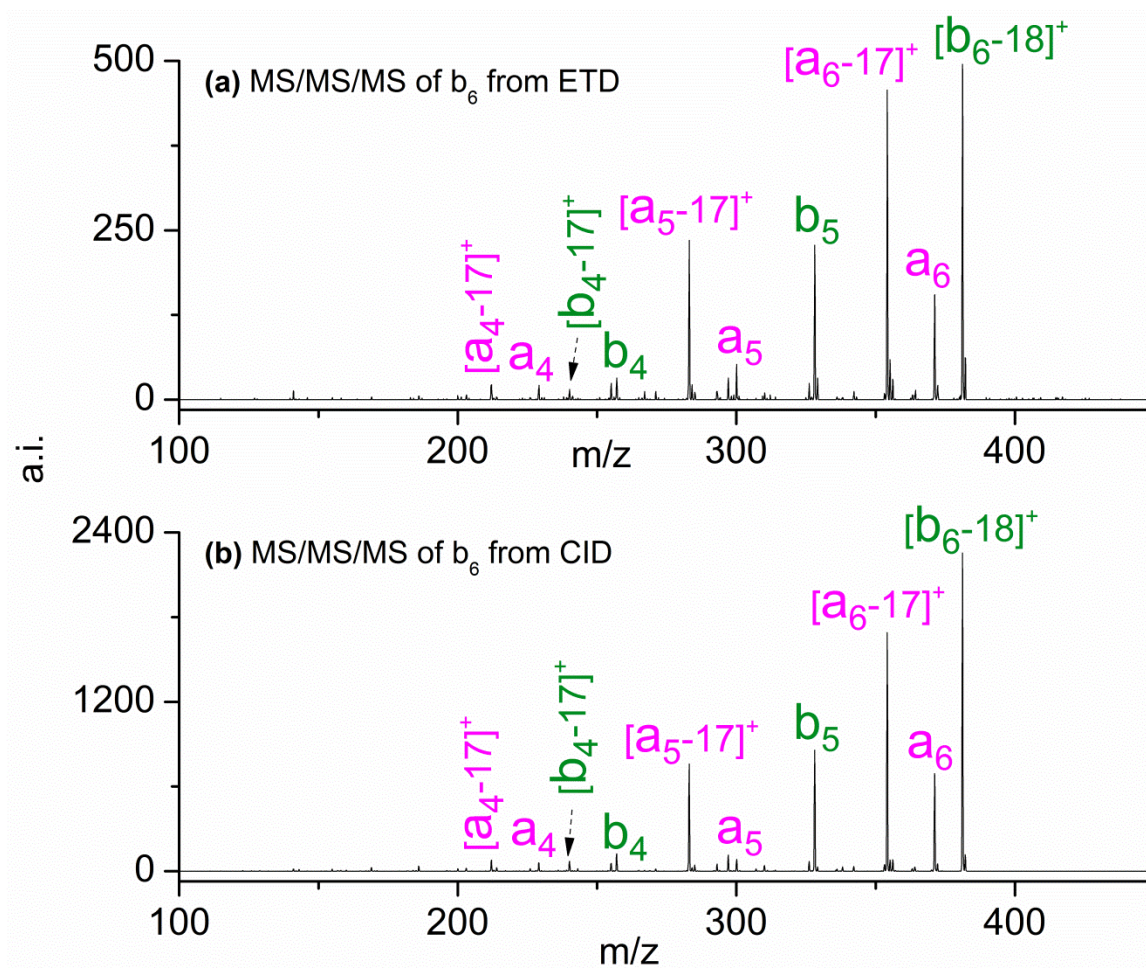


**Figure 5.16.** CID spectra (MS/MS/MS) of  $b_6$  produced by (a) ETD on  $[M+2H]^{2+}$  on AGGAAAA and by (b) CID on  $[M+H]^+$  on AGGAAAA.

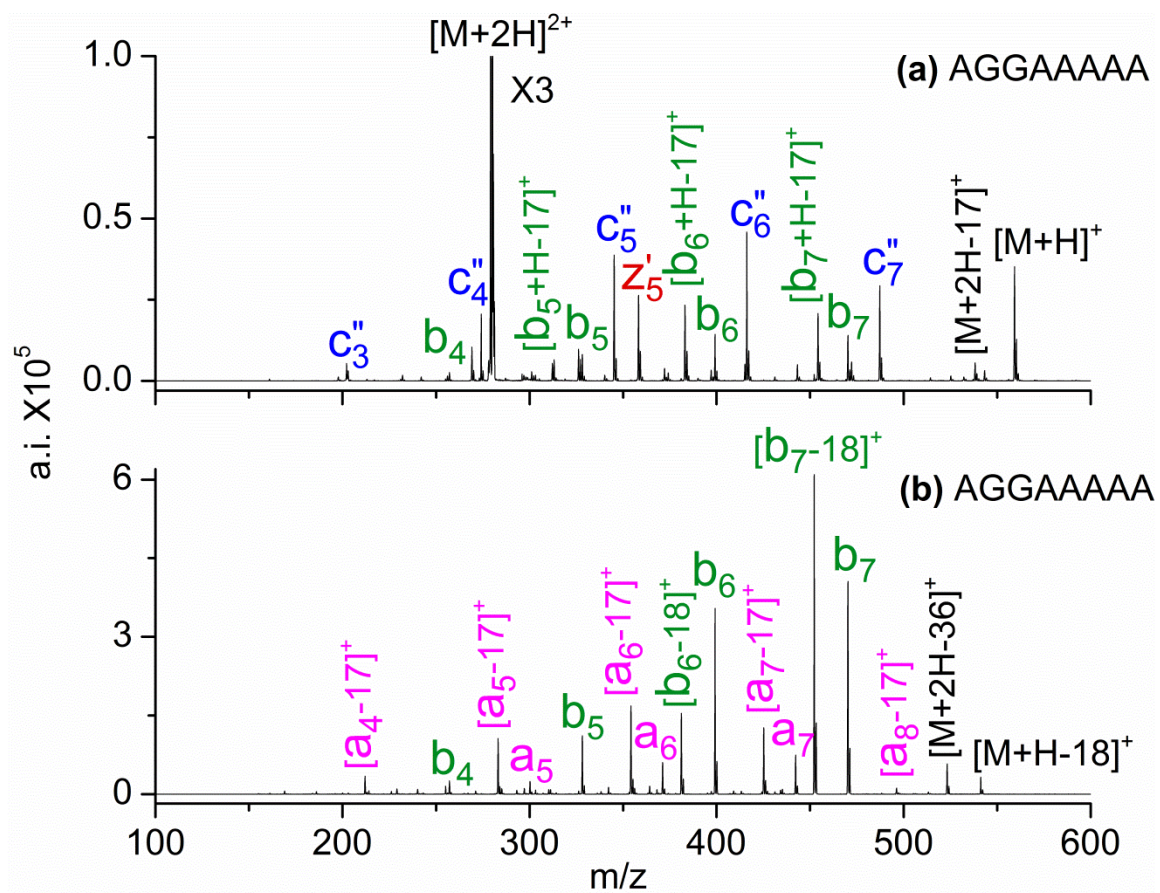


**Figure 5.17.** (a) ETD spectrum of  $[M+2H]^{2+}$  from AGGAAAAA and (b) CID spectrum of  $[M+H]^+$  from AGGAAAAA.

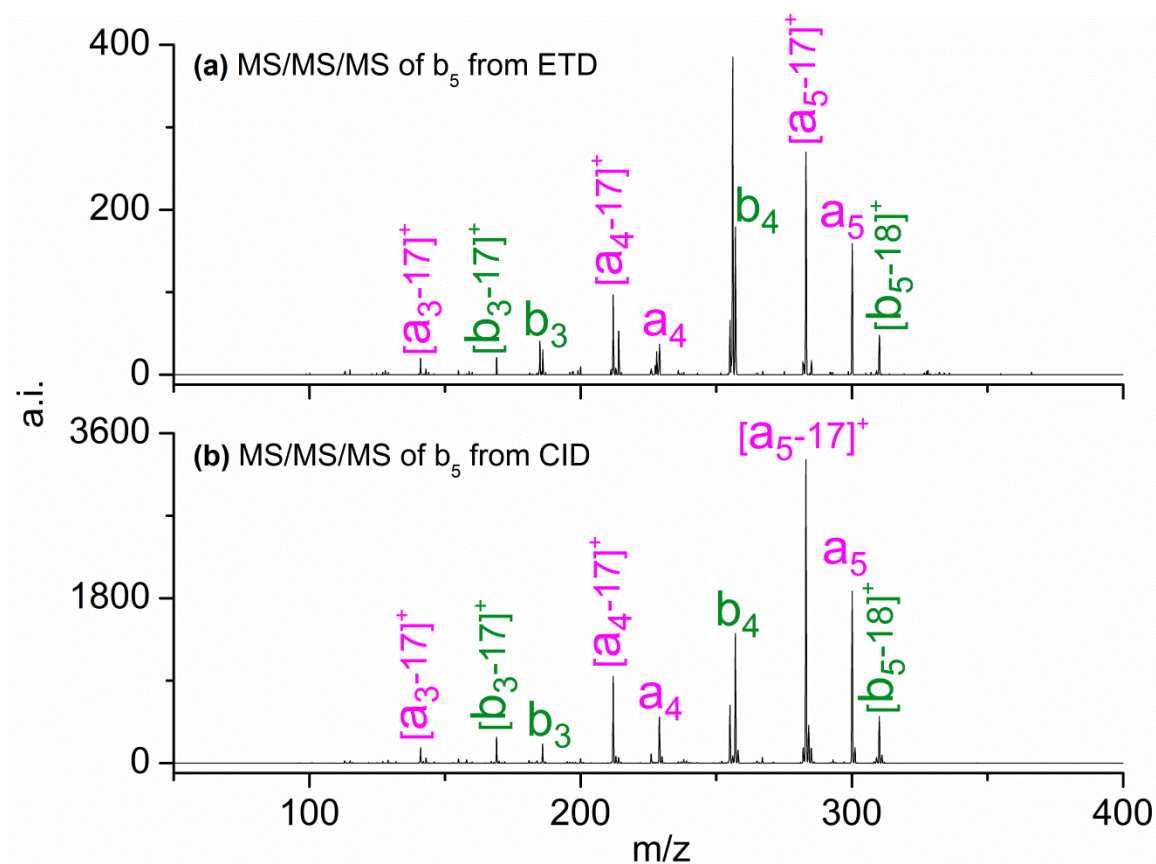


**Figure 5.18.** The CID spectra (MS/MS/MS) of  $b_5$  produced by (a) ETD on  $[M+2H]^{2+}$  on AGGAAAAA and by (b) CID on  $[M+H]^+$  on AGGAAAAA.



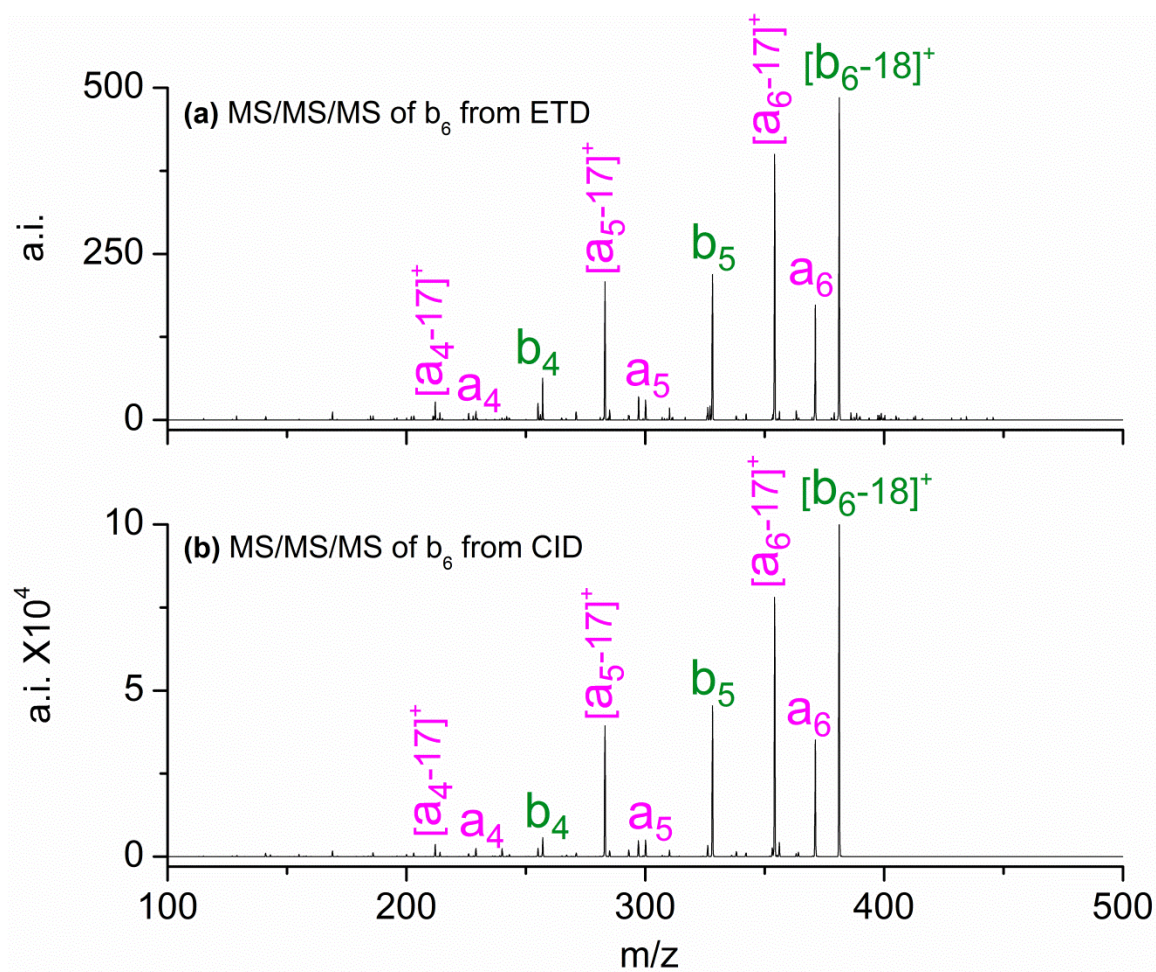


**Figure 5.19.** The CID spectra (MS/MS/MS) of  $b_6$  produced by (a) ETD on  $[M+2H]^{2+}$  on AGGAAAAA and by (b) CID on  $[M+H]^+$  on AGGAAAAA.

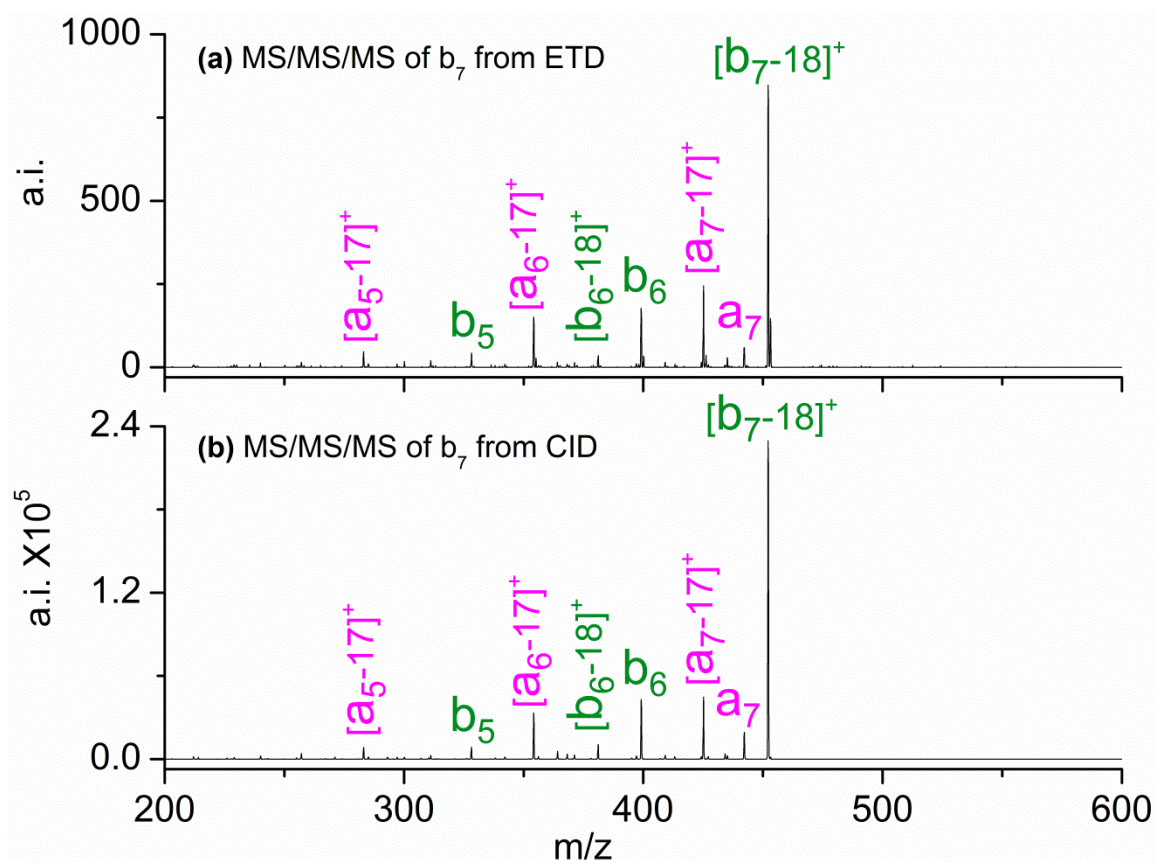


**Figure 5.20.** The CID spectra (MS/MS/MS) of  $b_7$  produced by (a) ETD on  $[M+2H]^{2+}$  on AGGAAAAA and by (b) CID on  $[M+H]^+$  on AGGAAAAA.

do not contain b-ions that might result from secondary fragmentation of c-ions.

Uggerud and coworkers<sup>20</sup> performed calculations showing that peptides protonated at a backbone amide nitrogen produce b- and y-ions while protonation at a backbone carbonyl oxygen produces c- and z-ions. In neutral peptides, the N-terminus is a basic site and has a high possibility of protonation. The second proton can be located at an amide carbonyl oxygen or an amide nitrogen along the backbone. There is still a conflict in the literature as to whether peptides are primarily O-protonated or N-protonated at the backbone.<sup>47-50</sup> Amide carbonyl oxygens are more basic than amide nitrogens,<sup>50</sup> while protonation at the nitrogen has been calculated to decrease the C(O)-N bond order, which facilitates cleavage.<sup>49</sup> Our experimental results on neutral peptides with alkyl side chains support the acquisition of the second proton at amide nitrogen on the backbone, as discussed below. In basic peptides, such as AAARAAA in Figure 5.1(b), the arginine side chain and N-terminus are two basic sites capable of acquiring protons. Therefore, for AAARAAA, protonation along the peptide backbone, which leads to b-ion production, is unlikely. The gas-phase basicity (GB) of lysine (227.3 kcal/mol) is lower than the GB of arginine (240.58 kcal/mol),<sup>51-53</sup> therefore, arginine is more basic and more likely to protonate at the side chain than lysine. The possibility of protonation at the backbone of a lysine-containing peptide is larger than for an arginine-containing peptide. According to Uggerud's calculations,<sup>20</sup> protonation at the backbone amide nitrogen produces b- and y-ions. This could explain why some b-ions exist in ETD and ECD of lysine-containing peptides. In neutral peptides with alkyl side chains, the second proton should be either O-protonated or N-protonated at a backbone amide group, as there are no other potential protonation sites. Our results show that b-ions are found in the ETD spectra of neutral heptapeptides. Therefore, the

second proton has a very high possibility of being located at the backbone amide nitrogen rather than at the carbonyl oxygen, which produces c- and z-ions.

Cooper<sup>21</sup> has proposed a mechanism where, after an electron is captured by the  $[M+nH]^{n+}$  to produce  $[M+nH]^{(n-1)+\bullet}$ , a hydrogen radical ( $H\bullet$ ) loss follows to produce vibrationally excited  $[M+(n-1)H]^{(n-1)+}$ . These non-radical ions undergo mobile proton pathways to produce b- and y-ions like the ions formed by CID. In ETD of the doubly protonated peptides studied here,  $[M+H]^+$  that forms as an ETD product dissociates like in CID. Cooper's mechanism could explain how the b-ions produced in ETD and CID have the same structure, as shown in Figure 5.7 According to our experimental results, b-ions are found in the ETD spectra of neutral peptides but not in the spectra of basic peptides; this implies neutral peptides undergo  $H\bullet$  loss more readily than basic peptides. In addition, the ability of a peptide to undergo  $H\bullet$  loss relates to its basicity.<sup>22</sup>

#### 5.4.3 Effect of Peptide Chain Length on b-Ion Formation

In order to determine if peptide size (chain length) affects b-ion formation, ETD experiments were performed on peptides with different numbers of residues. Due to Coulomb repulsion, it is generally not possible to put two protons on the backbone of neutral peptides with less than seven residues (see Chapter 4). The seven, nine, thirteen, and fourteen residue peptides A7, AGGAAAAAA, A13, A14 were chosen to compare the size effect in ETD.

When peptide size increases, more c-ions and fewer b-ions are produced. Compared to A7 in Figure 5.1(a), b-ion formation is greatly reduced and c-ions dominate as the neutral peptide size increases as observed for nine-residue AGGAAAAAA (Figure 5.3(a)) and A14 (Figure 5.3(b)). A decrease in peptide chain length does not prevent the formation of c-ions but

changes the ratio of fragmentation pathways. When peptide size increases, the internal solvation of the charge bearing group and the increase of internal hydrogen bonds may lead to a decrease in H• loss.<sup>25,54</sup> The lower abundance of  $[M+H]^+$  produces fewer b-ions. McLuckey and coworkers<sup>54</sup> found that the degree of H• loss from  $[M+nH]^{(n-1)+\bullet}$  in ECD is higher than in ETD. Although all the b-ions observed by other researchers involved ECD experiments, the effect of b-ion formation in ETD may arise from the same mechanism. Both the ETD and ECD process can involve H• loss; however, there is a discrepancy about the amount of loss comparatively in the two techniques.<sup>54</sup> This difference involves either the angular momentum of the electron transfer/capture no dissociation process or the internal energy difference arising from how the electron states are populated.<sup>54</sup> Even though this discrepancy exists, H• loss leading to b-ion production is expected to follow the same mechanism in both ETD and ECD.<sup>54</sup> When peptide size increases, H• loss is decreased, a less vibrationally excited  $[M+H]^+$  is produced, and the ion under dissociation is mainly  $[M+2H]^+$ .<sup>25</sup> Based on the work of this chapter it is clear that the size of the peptide can change the fragmentation mechanism from vibrational excitation to a radical-initiated dissociation.

## 5.5 Conclusions

The ability to produce  $[M+2H]^{2+}$  from non-basic peptides by addition of Cr(III) to the electrosprayed solution has allowed ETD experiments to be performed on a series of neutral peptides. Compared to ETD on basic peptides, neutral peptides primarily produce b- and c''-ions instead of c''- and z'-ions. The identity of the alkyl residue has minimal effect on ETD, which is due to their similar side chain structure functionalities and basicities. Two mechanisms from the literature are used here to explain the formation of b-ions.<sup>20,21</sup> The first explanation is that a



hydrogen attaches to a backbone amide nitrogen to produce the b-ions.<sup>20</sup> The possibility of backbone protonation is high for neutral peptides, which do not have side chains that protonate. The extent (sequence coverage) and intensity of b-ions formed in ETD of neutral peptides is also much larger than for the b-ions reported in ETD of basic peptides.<sup>20-26</sup> The second explanation is that there is a H• loss after  $[M+2H]^{++}$  formation to produce a vibrationally excited  $[M+H]^+$ . This singly protonated ion undergoes mobile proton pathways to produce b-ions similar to CID.<sup>21</sup> In addition, peptide size can change the fragmentation pathway. Energetically, the larger the peptide, the lower the internal energy per degrees of freedom, so loss of H• is much less likely. Also, the increased internal solvation of larger peptides (i.e., increases intramolecular hydrogen bonding) may limit H• loss, which could explain the decrease in b-ion formation.<sup>25</sup> Based on the work of this chapter it is clear that the dissociation channel changes from vibrational excitation to a radical-initiated process.

## References

1. Syka, J. E. P.; Coon, J. J.; Schroeder, M. J.; Shabanowitz, J.; Hunt, D. F. Peptide and Protein Sequence Analysis by Electron Transfer Dissociation Mass Spectrometry. *Proc. Natl. Acad. Sci. USA* **2004**, *101*, 9528-9533.
2. Zubarev, R. A.; Kelleher, N. L.; McLafferty, F. W. Electron Capture Dissociation of Multiply Charged Protein Cations. A Nonergodic Process. *J. Am. Chem. Soc.* **1998**, *120*, 3265-3266.
3. Coon, J. J. Collisions or Electrons? Protein Sequence Analysis in the 21st Century. *Anal. Chem.* **2009**, *81*, 3208-3215.
4. Good, D. M.; Wirtala, M.; McAlister, G. C.; Coon, J. J. Performance Characteristics of Electron Transfer Dissociation Mass Spectrometry. *Mol. Cell. Proteomics* **2007**, *6*, 1942-1951.
5. Kjeldsen, F.; Giessing, A. M. B.; Ingrell, C. R.; Jensen, O. N. Peptide Sequencing and Characterization of Post-Translational Modifications by Enhanced Ion-Charging and Liquid Chromatography Electron-Transfer Dissociation Tandem Mass Spectrometry. *Anal. Chem.* **2007**, *79*, 9243-9252.
6. Mikesch, L. M.; Ueberheide, B.; Chi, A.; Coon, J. J.; Syka, J. E. P.; Shabanowitz, J.; Hunt, D. F. The Utility of ETD Mass Spectrometry in Proteomic Analysis. *Biochim. Biophys. Acta.* **2006**, *1764*, 1811-1822.
7. Sasaki, K.; Osaki, T.; Minamino, N. Large-scale Identification of Endogenous Secretory Peptides Using Electron Transfer Dissociation Mass Spectrometry. *Mol. Cell. Proteomics* **2013**, *12*, 700-709.
8. Haag, N.; Holm, A. I. S.; Johansson, H. A. B.; Zettergren, H.; Schmidt, H. T.; Nielsen, S. B.; Hvelplund, P.; Cederquist, H. Electron Capture Induced Dissociation of Doubly Protonated Pentapeptides: Dependence on Molecular Structure and Charge Separation. *J. Chem. Phys.* **2011**, *134*.
9. Vestal, M. L. The Future of Biological Mass Spectrometry. *J. Am. Soc. Mass Spectrom.* **2011**, *22*, 953-959.
10. Kalli, A.; Håkansson, K. Electron Capture Dissociation of Highly Charged Proteolytic Peptides from Lys N, Lys C and Glu C Digestion. *Mol. BioSyst.* **2010**, *6*, 1668-1681.
11. Zhang, Z. Prediction of Electron-Transfer/Capture Dissociation Spectra of Peptides. *Anal. Chem.* **2010**, *82*, 1990-2005.
12. Kim, M.; Pinto, S. M.; Getnet, D.; Nirujogi, R. S.; Manda, S. S.; Chaerkady, R.; Madugundu, A. K.; Kelkar, D. S.; Isserlin, R.; Jain, S.; Thomas, J. K.; Muthusamy, B.; Leal-Rojas, P.; Kumar, P.; Sahasrabudhe, N. A.; Balakrishnan, L.; Advani, J.; George, B.; Renuse, S.; Selvan, L. D. N.; Patil, A. H.; Nanjappa, V.; Radhakrishnan, A.; Prasad, S.; Subbannayya, T.;

- Raju, R.; Kumar, M.; Sreenivasamurthy, S. K.; Marimuthu, A.; Sathe, G. J.; Chavan, S.; Datta, K. K.; Subbannayya, Y.; Sahu, A.; Yelamanchi, S. D.; Jayaram, S.; Rajagopalan, P.; Sharma, J.; Murthy, K. R.; Syed, N.; Goel, R.; Khan, A. A.; Ahmad, S.; Dey, G.; Mudgal, K.; Chatterjee, A.; Huang, T.; Zhong, J.; Wu, X.; Shaw, P. G.; Freed, D.; Zahari, M. S.; Mukherjee, K. K.; Shankar, S.; Mahadevan, A.; Lam, H.; Mitchell, C. J.; Shankar, S. K.; Satishchandra, P.; Schroeder, J. T.; Sirdeshmukh, R.; Maitra, A.; Leach, S. D.; Drake, C. G.; Halushka, M. K.; Prasad, T. S. K.; Hruban, R. H.; Kerr, C. L.; Bader, G. D.; Iacobuzio-Donahue, C.; Gowda, H.; Pandey, A. A Draft Map of the Human Proteome. *Nature* **2014**, *509*, 575-581.
13. Syrstad, E. A.; Tureček, F. Toward a General Mechanism of Electron Capture Dissociation. *J. Am. Soc. Mass Spectrom.* **2005**, *16*, 208-224.
  14. Coon, J. J.; Syka, J. E. P.; Shabanowitz, J.; Hunt, D. F. Tandem Mass Spectrometry for Peptide and Protein Sequence Analysis. *BioTechniques* **2005**, *38*, 519-523.
  15. McLafferty, F. W.; Horn, D. M.; Breuker, K.; Ge, Y.; Lewis, M. A.; Cerda, B. A.; Zubarev, R. A.; Carpenter, B. K. Electron Capture Dissociation of Gaseous Multiply Charged Ions by Fourier Transform ion Cyclotron Resonance. *J. Am. Soc. Mass Spectrom.* **2001**, *12*, 245-249.
  16. Sobczyk, M.; Anusiewicz, I.; Berdys-Kochanska, J.; Sawicka, A.; Skurski, P.; Simons, J. Coulomb-Assisted Dissociative Electron Attachment: Application to a Model Peptide. *J. Phys. Chem. A* **2005**, *109*, 250-258.
  17. Chen, X.; Tureček, F. The Arginine Anomaly: Arginine Radicals are Poor Hydrogen Atom Donors in Electron Transfer Induced Dissociations. *J. Am. Chem. Soc.* **2006**, *128*, 12520-12530.
  18. Huzarska, M.; Ugalde, I.; Kaplan, D. A.; Hartmer, R.; Easterling, M. L.; Polfer, N. C. Negative Electron Transfer Dissociation of Deprotonated Phosphopeptide Anions: Choice of Radical Cation Reagent and Competition between Electron and Proton Transfer. *Anal. Chem.* **2010**, *82*, 2873-2878.
  19. Liu, H.; Håkansson, K. Abundant b-Type Ions Produced in Electron Capture Dissociation of Peptides Without Basic Amino Acid Residues. *J. Am. Soc. Mass Spectrom.* **2007**, *18*, 2007-2013.
  20. Bakken, V.; Helgaker, T.; Uggerud, E. Models of Fragmentations Induced by Electron Attachment to Protonated Peptides. *Eur. J. Mass Spectrom.* **2004**, *10*, 625-638.
  21. Cooper, H. J. Investigation of the Presence of b Ions in Electron Capture Dissociation Mass Spectra. *J. Am. Soc. Mass Spectrom.* **2005**, *16*, 1932-1940.
  22. Haselmann, K. F.; Schmidt, M. Do b-Ions Occur from Vibrational Excitation upon H-Desorption in Electron Capture Dissociation? *Rapid Commun. Mass Spectrom.* **2007**, *21*, 1003-1008.

23. Lee, S.; Chung, G.; Kim, J.; Oh, H. B. Electron Capture Dissociation Mass Spectrometry of Peptide Cations Containing a Lysine Homologue: a Mobile Proton Model for Explaining the Observation of b-type Product Ions. *Rapid Commun. Mass Spectrom.* **2006**, *20*, 3167-3175.
24. Tsybin, Y. O.; Haselmann, K. F.; Emmett, M. R.; Hendrickson, C. L.; Marshall, A. G. Charge Location Directs Electron Capture Dissociation of Peptide Dications. *J. Am. Soc. Mass Spectrom.* **2006**, *17*, 1704-1711.
25. van der Rest, G.; Hui, R.; Frison, G.; Chamot-Rooke, J. Dissociation Channel Dependence on Peptide Size Observed in Electron Capture Dissociation of Tryptic Peptides. *J. Am. Soc. Mass Spectrom.* **2011**, *22*, 1631-1644.
26. Cooper, H. J.; Hudgins, R. R.; Håkansson, K.; Marshall, A. G. Secondary Fragmentation of Linear Peptides in Electron Capture Dissociation. *Int. J. Mass Spectrom.* **2003**, *228*, 723-728.
27. Moore, B. N.; Ly, T.; Julian, R. R. Radical Conversion and Migration in Electron Capture Dissociation. *J. Am. Chem. Soc.* **2011**, *133*, 6997-7006.
28. Kalli, A.; Hess, S. Electron Capture Dissociation of Hydrogen-Deficient Peptide Radical Cations. *J. Am. Soc. Mass Spectrom.* **2012**, *23*, 1729-1740.
29. Bagheri-Majdi, E.; Ke, Y.; Orlova, G.; Chu, I. K.; Hopkinson, A. C.; Siu, K. W. M. Copper-Mediated Peptide Radical Ions in the Gas Phase. *J. Phys. Chem. B* **2004**, *108*, 11170-11181.
30. Barlow, C. K.; Wee, S.; McFadyen, W. D.; O'Hair, R. A. J. Designing Copper(II) Ternary Complexes to Generate Radical Cations of Peptides in the Gas Phase: Role of the Auxiliary Ligand. *Dalton Trans.* **2004**, 3199-3204.
31. Barlow, C. K.; McFadyen, W. D.; O'Hair, R. A. J. Formation of Cationic Peptide Radicals by Gas-Phase Redox Reactions with Trivalent Chromium, Manganese, Iron, and Cobalt Complexes. *J. Am. Chem. Soc.* **2005**, *127*, 6109-6115.
32. Chu, I. K.; Rodriguez, C. F.; Lau, T.; Hopkinson, A. C.; Siu, K. W. M. Molecular Radical Cations of Oligopeptides. *J. Phys. Chem. B* **2000**, *104*, 3393-3397.
33. Hao, G.; Gross, S. S. Electrospray Tandem Mass Spectrometry Analysis of S- and N-Nitrosopeptides: Facile Loss of NO and Radical-Induced Fragmentation. *J. Am. Soc. Mass Spectrom.* **2006**, *17*, 1725-1730.
34. Masterson, D. S.; Yin, H.; Chacon, A.; Hachey, D. L.; Norris, J. L.; Porter, N. A. Lysine Peroxycarbamates: Free Radical-Promoted Peptide Cleavage. *J. Am. Chem. Soc.* **2004**, *126*, 720-721.
35. Ly, T.; Julian, R. R. Residue-Specific Radical-Directed Dissociation of Whole Proteins in the Gas Phase. *J. Am. Chem. Soc.* **2008**, *130*, 351-358.

36. Budnik, B. A.; Zubarev, R. A.  $MH^{2+}$  Ion Production from Protonated Polypeptides by Electron Impact: Observation and Determination of Ionization Energies and a Cross-Section. *Chem. Phys. Lett.* **2000**, *316*, 19-23.
37. Laskin, J.; Yang, Z.; Ng, C. M. D.; Chu, I. K. Fragmentation of  $\alpha$ -Radical Cations of Arginine-Containing Peptides. *J. Am. Soc. Mass Spectrom.* **2010**, *21*, 511-521.
38. Wee, S.; O'Hair, R. A. J.; McFadyen, W. D. The Role of the Position of the Basic Residue in the Generation and Fragmentation of Peptide Radical Cations. *Int. J. Mass Spectrom.* **2006**, *249/250*, 171-183.
39. Pierotti, A. R.; Prat, A.; Chesneau, V.; Gaudoux, F.; Leseney, A. M.; Foulon, T.; Cohen, P. N-Arginine Dibasic Convertase, a Metalloendopeptidase as a Prototype of a Class of Processing Enzymes. *Proc. Natl. Acad. Sci. USA* **1994**, *91*, 6078-6082.
40. Ebert, R. F.; Bell, W. R. Assay of Human Fibrinopeptides by High-Performance Liquid Chromatography. *Anal. Biochem.* **1985**, *148*, 70-78.
41. Nara, P. L.; Hwang, K. M.; Rausch, D. M.; Lifso, J. D.; Eiden, L. E. CD4 Antigen-based Antireceptor Peptides Inhibit Infectivity of Human Immunodeficiency Virus In Vitro at Multiple Stages of the Viral Life Cycle. *Proc. Natl. Acad. Sci. USA* **1989**, *86*, 7139-7143.
42. Lifson, J. D.; Hwang, K. M.; Nara, P. L.; Fraser, B.; Padgett, M.; Dunlop, N. M.; Eiden, L. E. Synthetic CD4 Peptide Derivatives that Inhibit HIV Infection and Cytotoxicity. *Science* **1988**, *241*, 712-716.
43. Nelson, D. L.; Cox, M. M. *Lehninger. Principles of Biochemistry*, W. H. Freeman: New York, 2004.
44. Chan, W. C.; White, P. D. *Fmoc Solid Phase Peptide Synthesis A Practical Approach*, Oxford University Press Inc., New York: 2000.
45. Tureček, F.; Chung, T. W.; Moss, C. L.; Wyer, J. A.; Ehlerding, A.; Holm, A. I. S.; Zettergren, H.; Nielsen, S. B.; Hvelplund, P.; Chamot-Rooke, J.; Bythell, B.; Paizs, B. The Histidine Effect. Electron Transfer and Capture Cause Different Dissociations and Rearrangements of Histidine Peptide Cation-Radicals. *J. Am. Chem. Soc.* **2010**, *132*, 10728-10740.
46. Papayannopoulos, I. A. The Interpretation of Collision-induced Dissociation Tandem Mass Spectra of Peptides. *Mass Spectrom. Rev.* **1995**, *14*, 49-73.
47. Wysocki, V. H.; Tsaprailis, G.; Smith, L. L.; Brei, L. A. Mobile and Localized Protons: A Framework for Understanding Peptide Dissociation. *J. Mass Spectrom.* **2000**, *35*, 1399-1406.

48. Schlosser, A.; Lehmann, W. D. Five-Membered Ring Formation in Unimolecular Reactions of Peptides: a Key Structural Element Controlling Low-Energy Collision-Induced Dissociation of Peptides. *J. Mass Spectrom.* **2000**, *35*, 1382-1390.
49. Somogyi, A.; Wysocki, V. H.; Mayer, I. The Effect of Protonation Site on Bond Strength in Simple Peptides: Application of Ab Initio and Modified Neglect of Differential Overlap Bond Orders and Modified Neglect of Differential Overlap Energy Partitioning. *J. Am. Soc. Mass Spectrom.* **1994**, *5*, 704-717.
50. Zhang, K.; Zimmerman, D. M.; Chung-Phillips, A.; Cassady, C. J. Experimental and Ab Initio Studies of the Gas-Phase Basicities of Polyglycines. *J. Am. Chem. Soc.* **1993**, *115*, 10812-10822.
51. P. J. Linstrom., W. G. Mallard. NIST Standard Reference Database 69: *NIST Chemistry WebBook*. (accessed Aug 20, 2014).
52. Carr, S. R.; Cassady, C. J. Gas-Phase Basicities of Histidine and Lysine and their Selected Di- and Tripeptides. *J. Am. Soc. Mass Spectrom.* **1996**, *7*, 1203-1210.
53. Harrison, A. G. The Gas-Phase Basicities and Proton Affinities of Amino Acids and Peptides. *Mass Spectrom. Rev.* **1997**, *16*, 201-217.
54. Mentinova, M.; Crizer, D.; Baba, T.; McGee, W.; Glish, G.; McLuckey, S. Cation Recombination Energy/Coulomb Repulsion Effects in ETD/ECD as Revealed by Variation of Charge per Residue at Fixed Total Charge. *J. Am. Soc. Mass Spectrom.* **2013**, *24*, 1676-1689.

## CHAPTER 6: ELECTRON TRANSFER DISSOCIATION OF ACIDIC PEPTIDES WITHOUT BASIC AMINO ACID RESIDUES

### 6.1 Introduction

Acidic peptides and proteins are very important in biological systems. In neurological systems, peptides and proteins often contain a large number of acidic amino acid residues.<sup>1-3</sup> For example, the protein N-arginine dibasic convertase has a 71-residue acidic segment.<sup>1</sup> Many peptides related to blood coagulation are acidic.<sup>4,5</sup> In proteomics, *staphylococcus aureus* V8 protease is widely used to digest proteins into smaller peptides that contain aspartic acid or glutamic acid residues at the C-terminus. Asp-N-protease also digests proteins to produce peptides with aspartic acid or glutamic acid at the N-terminus.<sup>6</sup> These resulting digested peptides are often sequenced by mass spectrometry.<sup>7-10</sup>

Peptides containing acidic residues such as aspartic acid (Asp, D) and glutamic acid (Glu, E) easily donate protons and are difficult to multiply protonate in the positive ion mode by electrospray ionization mass spectrometry (ESI-MS). For example, the stomach peptide gastrin I (1-14)<sup>11</sup> and the blood coagulation peptide hirudin(54-65)<sup>12</sup> are highly acidic and are more easily deprotonated than protonated. Therefore, these peptides are difficult (sometimes impossible) to analyze by positive ion mode ESI. In addition, post-translational modifications, such as sulfation or phosphorylation, make peptides very acidic, which leads to a preference for deprotonation.<sup>13-18</sup> A noticeable example is low-molecular-weight chromium-binding substance (LMWCr),<sup>19</sup> an important biological peptide that cannot be sequenced by positive ion mode ESI or matrix-assisted laser desorption ionization (MALDI).<sup>20</sup> A LMWCr clip, which is not protonated in the

gas phase, is a heptapeptide with five acidic residues and a pyroglutamic acid residue at the N-terminus.<sup>20</sup>

Tandem mass spectrometry techniques are very important for the analysis of acidic peptides and proteins. Electron transfer dissociation (ETD)<sup>21</sup> and electron capture dissociation (ECD)<sup>22</sup> produce c- and z-ions<sup>23</sup> and are complementary techniques to collision-induced dissociation (CID), which produces b- and y-ions. Deamidation, a very important post-translational modification, is associated with aging and diseases such as Alzheimer's.<sup>24</sup> Under physiological conditions, deamidation of asparagine (N) in proteins forms a mixture of aspartic acid (D) and isoaspartic acid (isoD).<sup>25</sup> Aspartic acid and isoaspartic acid residues have a +0.984 Da difference in mass. O'Connor and coworkers<sup>26</sup> reported that mass spectrometry is the best method to distinguish aspartic acid and isoaspartic acid. However, these isomers are difficult to differentiate by CID.<sup>27</sup> ETD or ECD can distinguish aspartic acid and isoaspartic acid.<sup>26,28-31</sup> A diagnostic ion pair of [c+57] and [z'-57] produced by homolytic cleavage of isoaspartyl residue at the N-C<sub>α</sub> bond is used to distinguish the two amino acids.<sup>26,28-31</sup> These acidic peptides used by O'Connor and coworkers<sup>26</sup> contain at least one basic amino residue.

In ETD or ECD, the precursor ions should be at least doubly protonated. Highly acidic peptides often do not readily multiply protonate and cannot be studied by ETD or ECD. To obtain a doubly protonated ion, most of the peptides or proteins subjected to ETD or ECD contain at least one basic amino acid residue such as lysine (K), histidine (H), or arginine (R). In ETD or ECD of these acidic peptides, c- and z-ions are the major product ions.<sup>30,32</sup> The very acidic phosphorylated amino acid residues do not hinder or impact ECD's ability to produce c- and z-ions.<sup>33</sup> In ECD, aspartic acid has a side chain loss of •CHO<sub>2</sub> (44.9971 Da) and glutamic acid has a loss of •C<sub>2</sub>H<sub>3</sub>O<sub>2</sub> (59.0128 Da).<sup>34-36</sup>



In post-source decay (PSD) and CID, peptides containing aspartic acid or glutamic acid show selective cleavage adjacent to the acidic amino acid residues.<sup>37-39</sup> Suhai and coworkers<sup>40</sup> suggested that the carboxylic acid group, -COOH, of the aspartic acid side chain is involved in enhancing the amide bond cleavage in CID.

In the work of Chapter 4 on supercharging, addition of Cr(III) salts to the solution being electrosprayed was found to increase the charge of non-basic peptide ions. Using this procedure, acidic peptides without basic amino acid residues (BAARs) can be doubly protonated and studied by ETD or ECD. There are very few literature reports of ETD or ECD on acidic peptides without BAARs. One exception is that Håkansson and coworkers were able to perform ECD of peptide amides without BAARs.<sup>41</sup> Because of the biological importance of acidic peptides, ETD or ECD is used in peptide sequencing. In the work of this chapter, Cr(III) nitrate has been used to enhance the protonation of acidic peptides by ESI and to investigate ETD fragmentation of acidic peptides without BAARs.

## **6.2 Experimental**

### **6.2.1 Peptides**

The acidic peptides AAEEAAA, EAAAEA, EAAAAE, AAEEAA, AAAAAAD, AAAADD, DDDDDDD (D7), EEEEEEE (E7), and EEEEGDD, where A is alanine, D is aspartic acid, and E is glutamic acid, were synthesized with an Advanced Chem Tech (Louisville, KY, USA) model 90 automated peptide synthesizer. The peptides were synthesized by standard Fmoc synthetic procedures, as discussed in Chapter 2.<sup>42</sup> Peptides AAAAAAE, EAAAAA, AAADAAA, DAAAAA, DAAADA were purchased from Biomatik Co (Cambridge, Ontario, CA). Cr(NO<sub>3</sub>)<sub>3</sub>·9H<sub>2</sub>O and HPLC grade acetonitrile and methanol were purchased from VWR

(Radnor, PA, USA). Deionized water was produced with a Barnstead/thermolyne E-pure system (Dubuque, IA, USA).

To dissolve the acidic peptides, they were first added to a solvent of methanol:water at 50:50 volume:volume ratio or to water at a concentration of 1 mg peptide per mL of solvent. From this stock solution, solutions for analysis by ESI were dissolved to 10  $\mu$ M in acetonitrile:water at a volume ratio of 50:50. A molar ratio of Cr(III) to peptide at 10:1 was used to enhance protonation.

### 6.2.2 Mass Spectrometry

The peptides were analyzed on a Bruker (Billerica, MA, USA) HCTultra PTM Discovery System high capacity quadrupole ion trap mass spectrometer, as discussed in Chapter 2. Additional experimental details are also provided in Chapter 3.

## 6.3 Results and Discussion

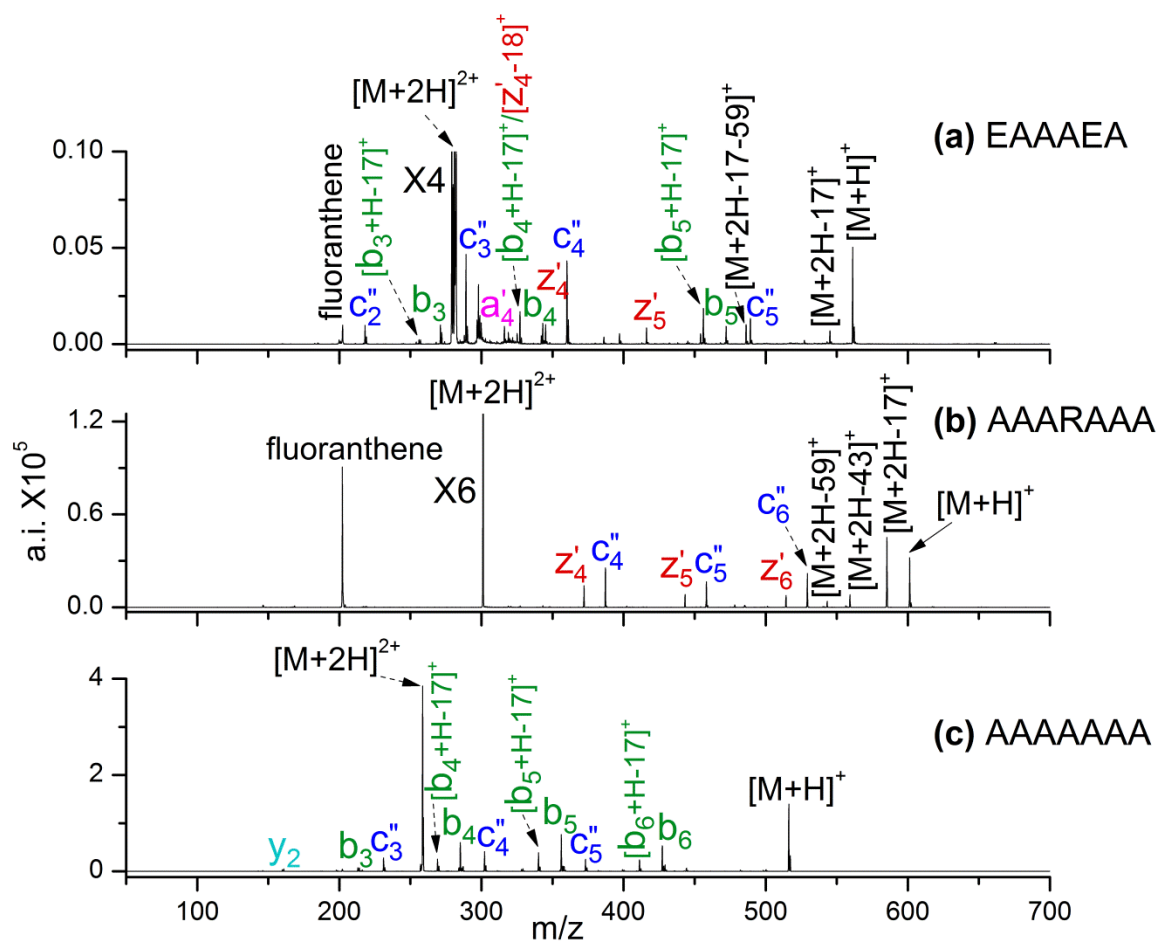
### 6.3.1 Effects of Glutamic Acid Residues on ETD

Figure 6.1 shows the ETD spectra of  $[M+2H]^{2+}$  from EAAAEA, AAARAAA, and AAAAAAA. These acidic peptides produce mainly members of the b-, c-, and z-ion series, which is a combination of the fragment ions series that are found in the spectra of basic and neutral peptides. In Figure 6.1(a), the acidic peptide EAAAEA gives  $c_n''$ ,  $n = 2-5$ ,  $z_n'$ ,  $n = 4-5$ ,  $b_n$ ,  $n = 3-5$ ,  $[b_n+H-17]^+$ ,  $n = 3-5$ ,  $a_4'$ ,  $[M+2H-17-59]^+$  and  $[M+2H-17]^+$ . Figure 6.1(b) is a spectrum of the basic peptide AAARAAA, which produces  $c_n''$ ,  $n = 4-6$ ,  $z_n'$ ,  $n = 4-6$ , and side chain fragment ions. For  $[M+2H-17-59]^+$ , loss of 59 Da is  $\bullet\text{CH}_2\text{COOH}$  from the glutamic acid side chain and loss of 17 Da is  $\text{NH}_3$  elimination.<sup>43</sup> The neutral peptide AAAAAAA (A7) in Figure

6.1(c) gives  $b_n$ ,  $n = 3-6$ ,  $[b_n+H-17]^+$ ,  $n = 4-6$ ,  $c_n''$ ,  $n = 3-5$  and  $y_2$  ions. Basic peptides mainly produce  $c_n''$  and  $z_n'$ , while neutral peptides yield primarily  $b_n$ ,  $[b_n+H-17]^+$ , and  $c_n''$ . The product ions of EAAAEA in Figure 6.1(a) show a combination of c- and z-ions similar to the basic peptide spectrum of Figure 6.1(b) and b-ions like the neutral peptide spectrum of Figure 6.1(c). Peptide EAAAAE (Figure 6.2) and AAEEAA (Figure 6.3) also have the similar ETD product ions. ETD product ions from all acidic peptide studied are listed in Table 6.1. Unlike CID,<sup>37-39</sup> no preferential cleavages were observed near glutamic acid residues. Compared to ETD of basic peptides discussed in Chapter 3, the product ions from acidic peptides do not always contain an acidic residue.

The b-ions from ETD of acidic peptides may produced by the same mechanism as from neutral peptides. One explanation for this mechanism is that a hydrogen attaches to the amide nitrogen backbone to produce the b-ions.<sup>44</sup> The second explanation is that there is a  $H\bullet$  loss after  $[M+2H]^{2+}$  to produce vibrationally excited  $[M+H]^+$ . The singly protonated ion then undergoes mobile proton pathways to produce b-ions in a manner similar to CID.<sup>45</sup>

In order to determine the effect of the position of the glutamic acid residue on fragmentation in ETD, glutamic acid was placed in different positions in three heptapeptides. Figure 6.4 shows the ETD spectra of  $[M+2H]^{2+}$  from EAAAAAA, AAAEAAA, and AAAAAAE. These peptides produce mainly b-, c- and z-ion series with a few a-ions, y-ions and side chain losses. When glutamic acid is located at the N-terminus in Figure 6.4(a),  $c_n''$ ,  $n = 2-6$ ,  $z_n'$ ,  $n = 4-6$ ,  $[z_n'-18]^+$ ,  $n = 4-6$ ,  $b_n$ ,  $n = 3-6$ ,  $[b_n+H-17]^+$ ,  $n = 4-6$ ,  $a_n'$ ,  $n = 5-6$ ,  $y_n$ ,  $n = 3-6$ ,  $[M+2H-17-59]^+$ ,  $[M+2H-17-18]^+$  and  $[M+2H-17]^+$  are produced. Figure 6.4(b) has glutamic acid at the fourth



**Figure 6.1.** ETD mass spectra of  $[M+2H]^{2+}$  from (a) EAAAEA, (b) AAARAAA, and (c) AAAAAAA.

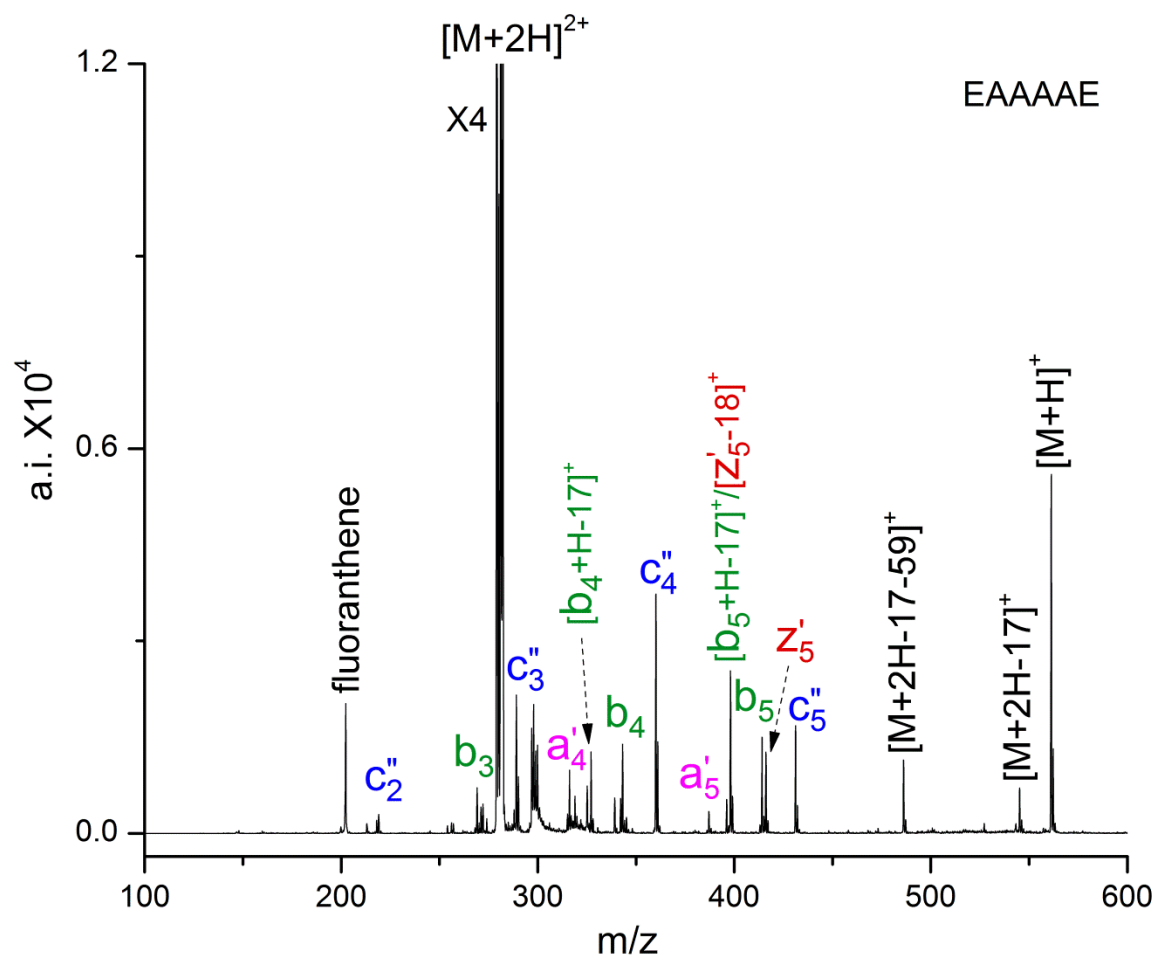


**Figure 6.2.** ETD mass spectrum of  $[M+2H]^{2+}$  from EAAAAE.

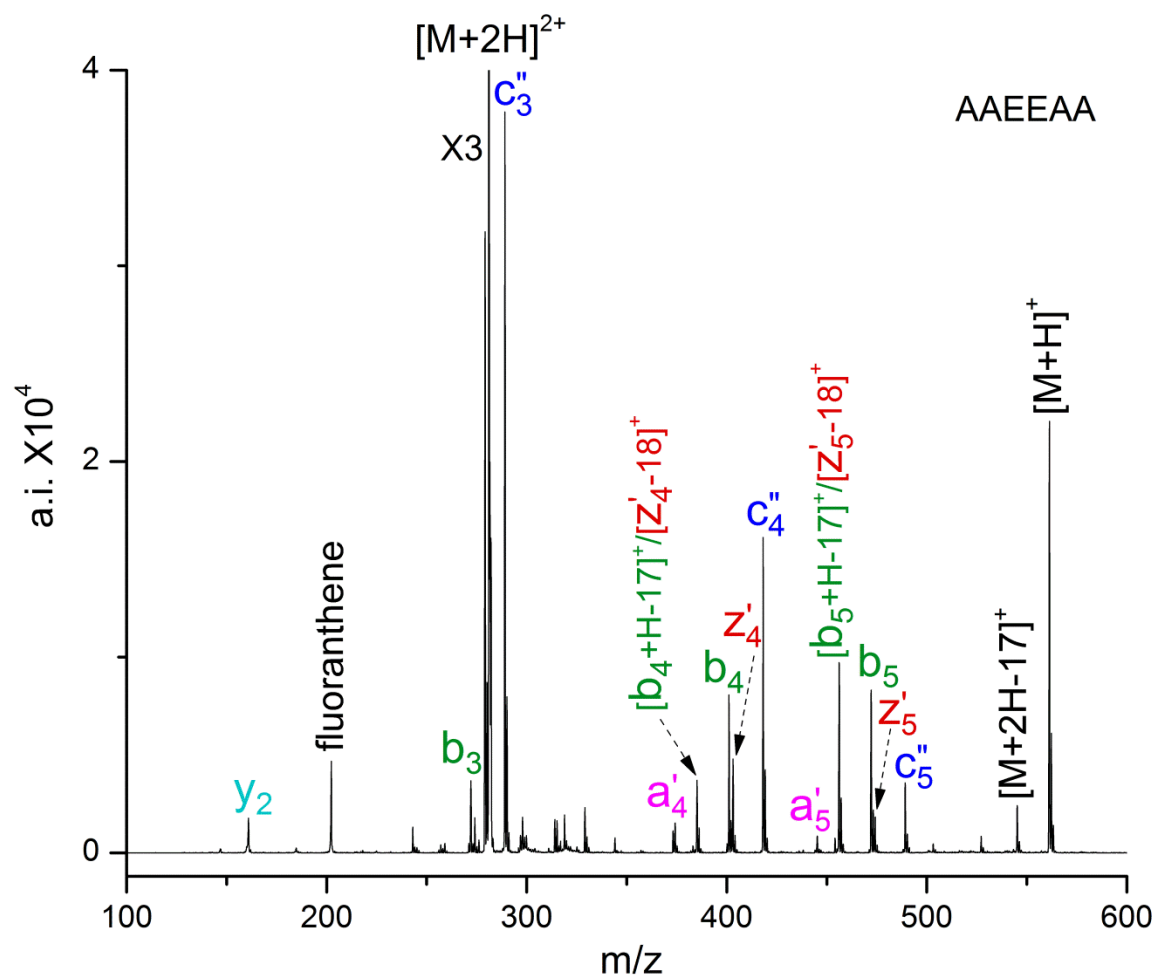


**Figure 6.3.** ETD mass spectrum of  $[M+2H]^{2+}$  from AAEEAA.

**Table 6.1.** Product ions produced by ETD on  $[M+2H]^{2+}$  of peptides with acidic side chains.<sup>a</sup>

Peptides	n =	a <sub>n</sub> '	b <sub>n</sub>	[b <sub>n</sub> +H-17]	c <sub>n</sub> ''	y <sub>n</sub>	z <sub>n</sub> '	z <sub>n</sub> '-18
EAAAAAA		5-6	3-6	4-6	2-6	3-6	4-6	4-6
AAAEAAA		4-6	4-6	4-6	3-6		4-6	4-6
AAAAAAE		4-6	4-6	4-6	3-6	2,4,5	4-6	
EAAAEA		4	3-5	3-5	2-5		4-5	4
EAAAAE		4-5	3-5	4-5	2-5		5	5
AAEEAA		4-5	3-5	4-5	3-5	2	4-5	4-5
DAAAAAA			3-6	4-6	3-6	4-5	4-6	4-6
AAADAAA		4-6	3-6	4-6	3-6		5-6	5-6
AAAAAAD		4-6	3-6	4-6	3-6	4-5	4-6	
AAAADD		4	3-5	5	3-5	2-4	4	
DAAADA		4	3-5	3-5	3-5		4-5	4-5
D7			5-6	5-6	3-6		5-6	5-6
E7					3-6		5-6	
EEEEGDD					2-6	4-5	6	

<sup>a</sup> Numerical values in the table indicate the range of n values (position of cleavage sites) observed in the ETD spectra.

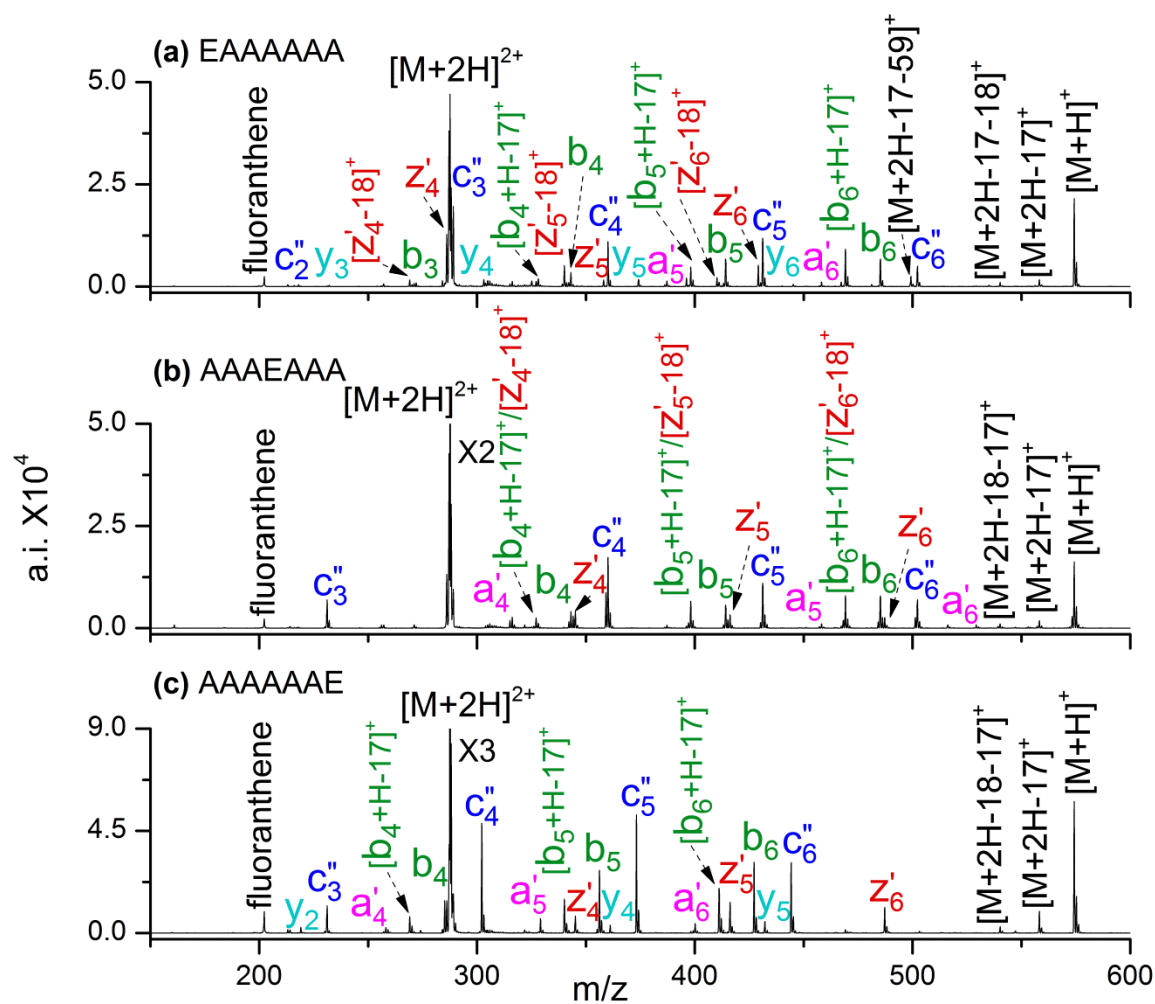


**Figure 6.4.** ETD mass spectra of  $[M+2H]^{2+}$  from (a) EAAAAAA, (b) AAAEAAA, and (c) AAAAAAE.



position, where  $c_n''$ ,  $n = 3-6$ ,  $z_n'$ ,  $n = 4-6$ ,  $[z_n'-18]^+$ ,  $n = 4-6$ ,  $b_n$ ,  $n = 4-6$ ,  $[b_n+H-17]^+$ ,  $n = 4-6$ ,  $a_n'$ ,  $n = 4-6$ ,  $[M+2H-17-18]^+$  and  $[M+2H-17]^+$  form. Figure 6.4(c) gives the spectrum of ETD of glutamic acid at the C-terminus where  $c_n''$ ,  $n = 3-6$ ,  $z_n'$ ,  $n = 4-6$ ,  $b_n$ ,  $n = 4-6$ ,  $[b_n+H-17]^+$ ,  $n = 4-6$ ,  $a_n'$ ,  $n = 4-6$ ,  $y_n$ ,  $n = 2, 4, 5$ ,  $[M+2H-17-18]^+$  and  $[M+2H-17]^+$  are produced. When the position of glutamic acid changes, there are very few effects on the major product ions. All of these peptides form members of the b-, c- and z-ion series.

### 6.3.2 Effects of Aspartic Acid Residues on ETD

The ETD product ions from all aspartic acid-containing peptide are summarized in Table 6.1. Figure 6.5 shows the ETD spectra of  $[M+2H]^{2+}$  from DAAADA and AAAADD. The aspartic acid containing peptides mainly produce b-, c- and z-ions. In Figure 6.5(a), the acidic peptide DAAADA gives  $c_n''$ ,  $n = 3-5$ ,  $z_n'$ ,  $n = 4-5$ ,  $[z_n'-18]^+$ ,  $n = 4-5$ ,  $b_n$ ,  $n = 3-5$ ,  $[b_n+H-17]^+$ ,  $n = 3-5$ ,  $a_4'$ , and  $[M+H-59]^+$ . AAAADD in Figure 6.5(b) produces  $c_n''$ ,  $n = 3-5$ ,  $z_4'$ ,  $b_n$ ,  $n = 3-5$ ,  $[b_5+H-17]^+$ ,  $y_n$ ,  $n = 2-4$ ,  $a_4'$ , and  $[M+H-59]^+$ . The two peptides produce mainly the b-, c- and z-ion series.  $[M+H-59]^+$  is the side chain loss of  $CH_2COOH$  from aspartic acid. In CID, peptides containing aspartic acid residues show selective cleavage adjacent to aspartic acid.<sup>37-39</sup> In ETD, no preferential cleavage adjacent to aspartic acid is observed. The product ions do not always contain an acidic residue.

To further study the effects of aspartic acid residues on dissociation, ETD was performed on DAAAAAA, AAADAAA, and AAAAAAD as seen in Figure 6.6. The product ions are also mainly b-, c- and z-series ions. With aspartic acid at the N-terminus, Figure 6.6(a), produces  $c_n''$ ,  $n = 3-6$ ,  $z_n'$ ,  $n = 4-6$ ,  $[z_n'-18]^+$ ,  $n = 4-6$ ,  $b_n$ ,  $n = 3-6$ ,  $[b_n+H-17]^+$ ,  $n = 4-6$ ,  $y_n$ ,  $n = 4-5$ ,  $[M+H-59]^+$ , and  $[M+2H-17]^+$ . Aspartic acid at the fourth position, of the heptapeptide in Figure 6.6(b),

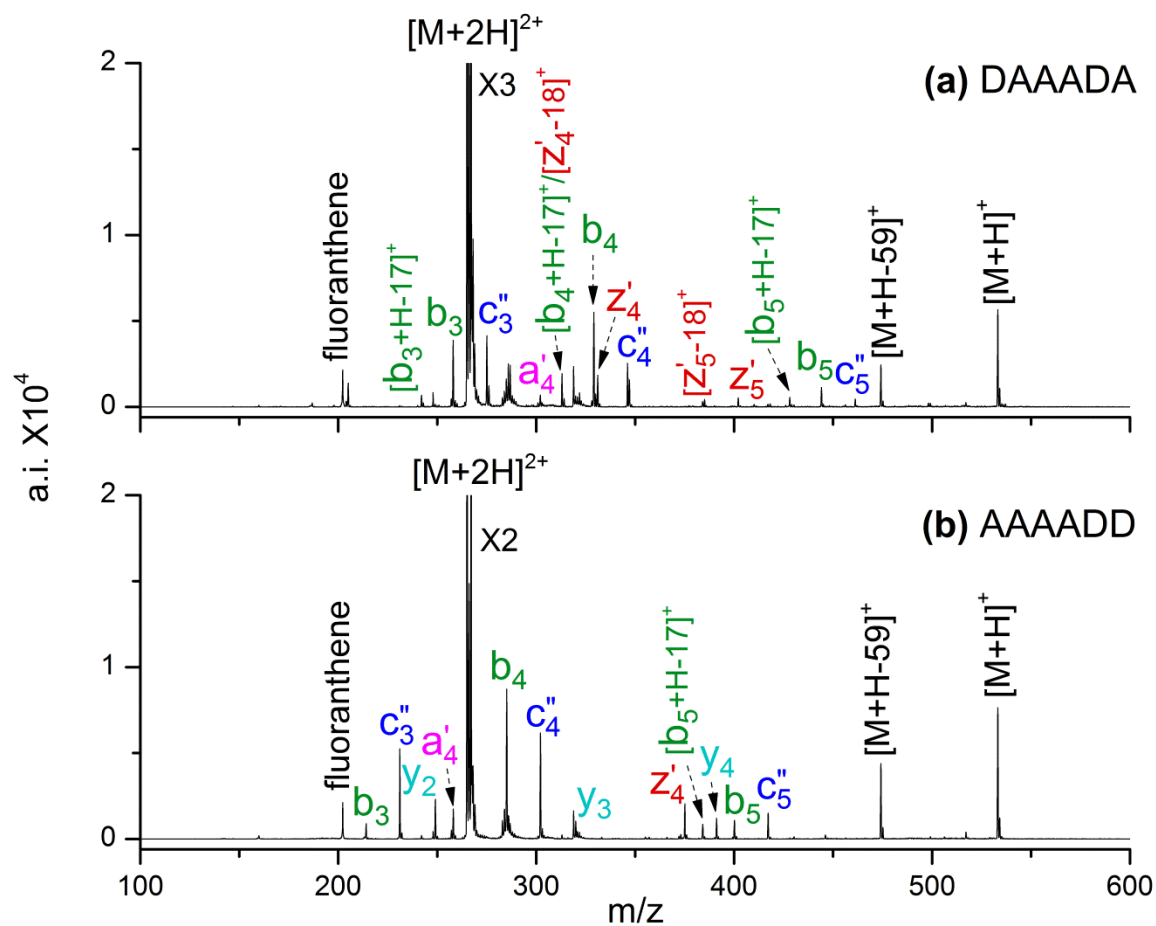


**Figure 6.5.** ETD mass spectra of  $[M+2H]^{2+}$  from (a) DAAADA and (b) AAAADD.

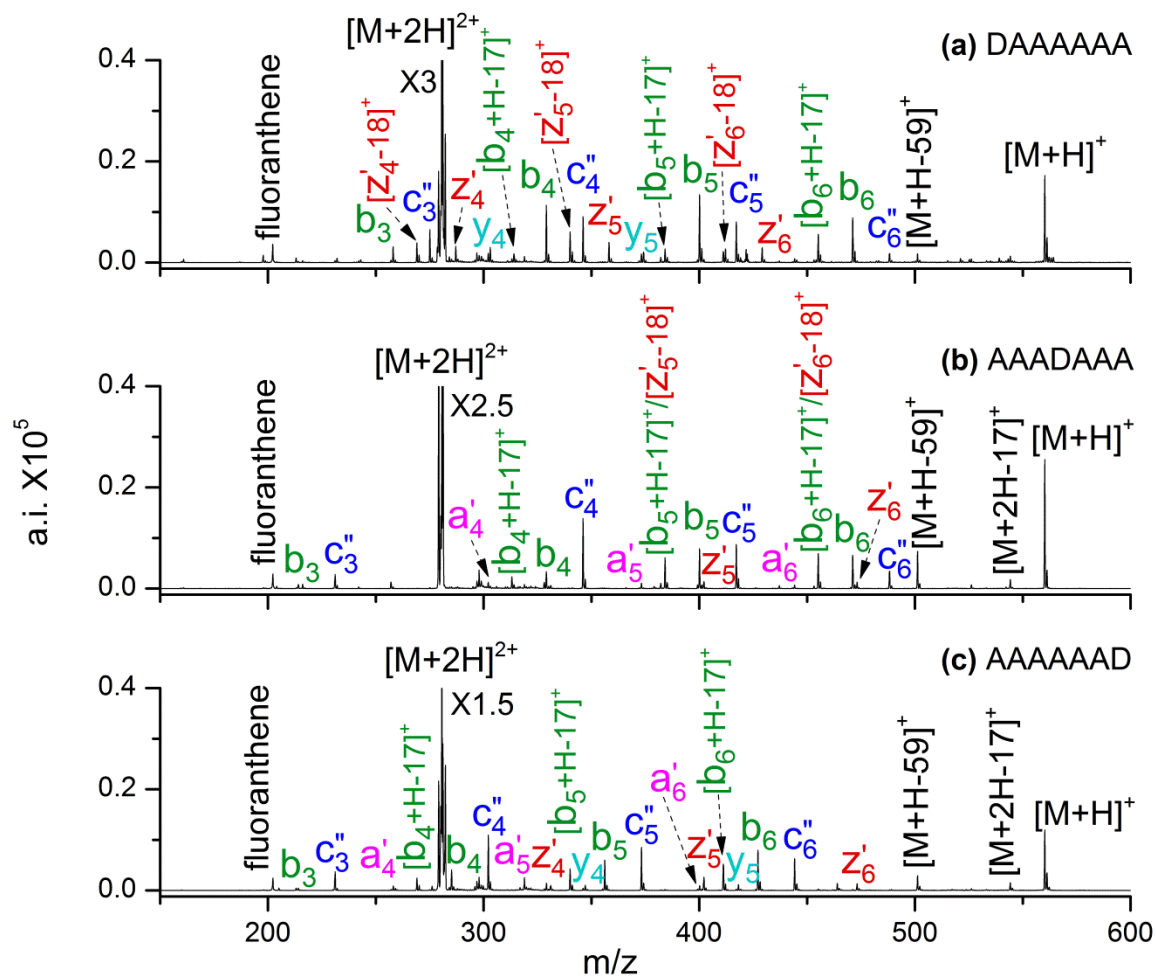


**Figure 6.6.** ETD mass spectra of  $[M+2H]^{2+}$  from (a) DAAAAAA, (b) AAADAAA, and (c) AAAAAAD.

yields  $c_n''$ ,  $n = 3-6$ ,  $z_n'$ ,  $n = 5-6$ ,  $[z_n'-18]^+$ ,  $n = 5-6$ ,  $b_n$ ,  $n = 3-6$ ,  $[b_n+H-17]^+$ ,  $n = 4-6$ ,  $a_n'$ ,  $n = 4-6$ ,  $[M+H-59]^+$  and  $[M+2H-17]^+$ . Figure 6.6(c) gives the spectrum of aspartic acid at the C-terminus where  $c_n''$ ,  $n = 3-6$ ,  $z_n'$ ,  $n = 4-6$ ,  $b_n$ ,  $n = 3-6$ ,  $[b_n+H-17]^+$ ,  $n = 4-6$ ,  $a_n'$ ,  $n = 4-6$ ,  $y_n$ ,  $n = 4-5$ ,  $[M+H-59]^+$  and  $[M+2H-17]^+$  are produced. Like glutamic acid, the position of aspartic acid has little effect on the ETD product ions.

All of the ETD spectra of acidic peptides show that the product ions do not have to contain an acidic residue. Preferential cleavage adjacent to an acidic residue is not observed. There is no noticeable difference for the ETD spectra of peptides containing glutamic acid and aspartic acid.

### 6.3.3 Effects of Overall Peptide Acidity on ETD

Figure 6.7 is the ETD spectra of  $[M+2H]^{2+}$  from highly acidic peptides containing multiple E and D residues. The peptides give primarily  $c''$  and  $z'$  ions like basic peptides in ETD, as discussed in Chapter 3. Figure 6.7(a) displays the spectrum of EEEEGDD where  $c_n''$ ,  $n = 2-6$ ,  $z_6'$ ,  $y_n$ ,  $n = 4-5$ ,  $[M+2H-59]^+$  and  $[M+2H-17]^+$  are produced. Figure 6.7(b) shows the ETD spectrum of  $[M+2H]^{2+}$  for the peptide DDDDDDD where  $c_n''$ ,  $n = 3-6$ ,  $z_n'$ ,  $n = 5-6$ ,  $[z_n'-18]^+$ ,  $n = 5-6$ ,  $b_n$ ,  $n = 5-6$ ,  $[b_n+H-17]^+$ ,  $n = 5-6$ ,  $[M+H-59]^+$ ,  $[M+2H-17-18]^+$  and  $[M+2H-17]^+$  are produced. Figure 6.7(c) is the ETD spectrum of  $[M+2H]^{2+}$  from peptide EEEEEEE, which yields  $c_n''$ ,  $n = 3-6$ ,  $z_n'$ ,  $n = 5-6$ ,  $[M+H-59]^+$  and  $[M+H-17]^+$ . When the peptide is highly acidic, only a few low intensity b- and y-ions are produced and c-ions dominate. The dissociation mechanism seems to change to the radical mechanism yielding mainly c- and z-ions. The lone pairs of oxygen atoms at the side chains of acidic residues probably take part in the mechanism.

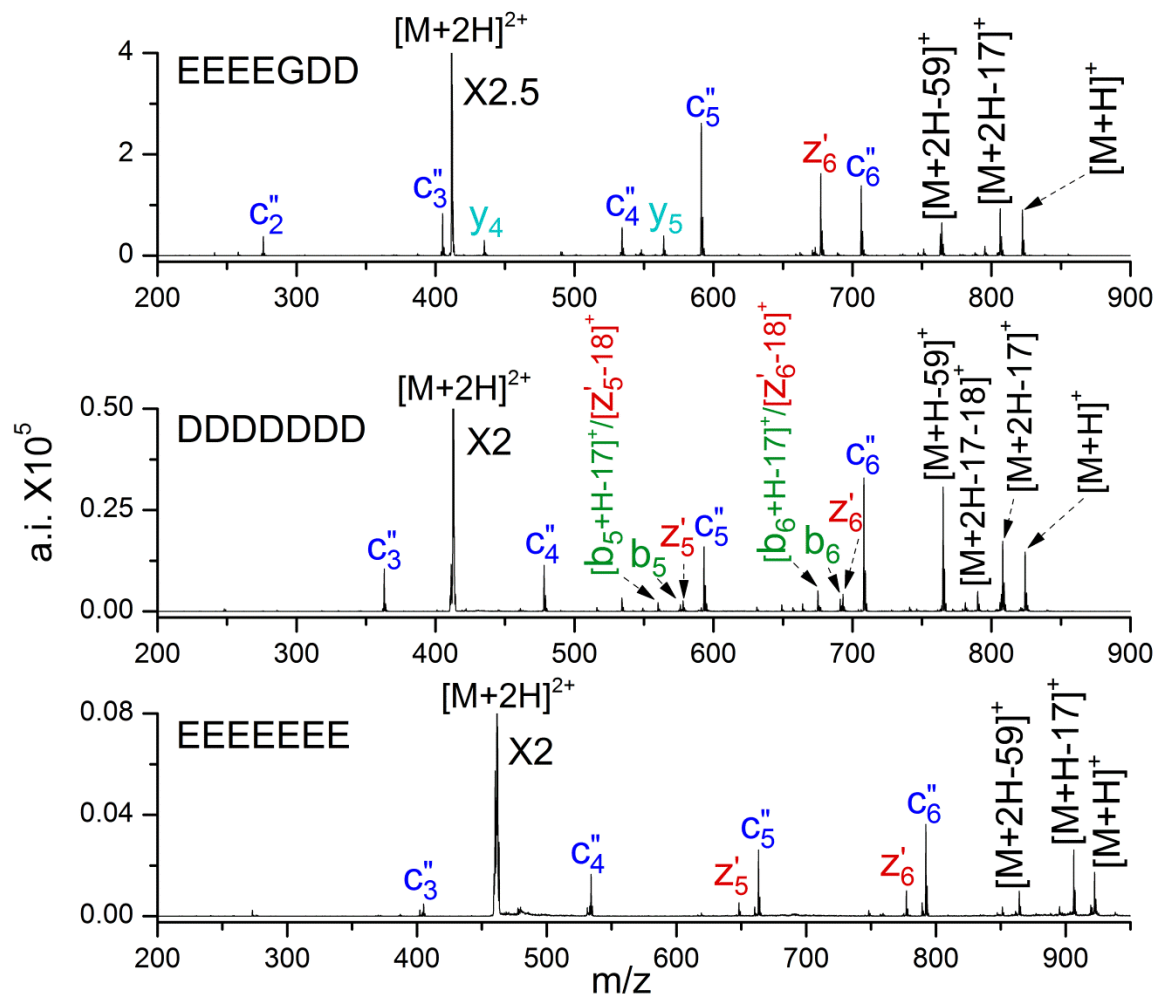


**Figure 6.7.** ETD mass spectra of  $[M+2H]^{2+}$  from (a) EEEEGDD, (b) DDDDDDD, and (c) EEEEEEE.

## 6.4 Conclusions

Electron transfer dissociation experiments have been performed for the first time on acidic peptides lacking residues with basic side chains. These peptides produce members of the b-, c- and z-ion series. The c- and z-ion series are also found in the spectra of basic peptides, while b-ions are prominent in the spectra of acidic peptides. The identity of the glutamic acid and aspartic acid residues has minimal effect on ETD. Unlike basic peptides, the ETD product ions of acidic peptides do not always contain an acidic residue. Compared to the aspartic acid effect in CID, no preferential cleavage is found adjacent to acidic residues in ETD. The position of acidic residues along the peptide chain has no effect in the ETD fragmentation. Glutamic acid and aspartic acid both exhibit a  $\bullet\text{CH}_2\text{COOH}$  (59 Da) loss from their side chains. For highly acidic peptides, the ETD product ions were mainly from the c- and z-ion series. Lone pairs on oxygen atoms of the carboxylic acid groups at the side chains probably take part in the mechanism for ion formation.

## References

1. Pierotti, A. R.; Prat, A.; Chesneau, V.; Gaudoux, F.; Leseney, A. M.; Foulon, T.; Cohen, P. N-Arginine Dibasic Convertase, a Metalloendopeptidase as a Prototype of a Class of Processing Enzymes. *Proc. Natl. Acad. Sci. USA* **1994**, *91*, 6078-6082.
2. Lemaire, S.; Yamashiro, D.; Rao, A. J.; Li, C. H. Synthesis and Biological Activity of Beta-Melanotropins and Analogs. *J. Med. Chem.* **1977**, *20*, 155-158.
3. Tatemoto, K. Neuropeptide Y: Complete Amino Acid Sequence of the Brain Peptide. *Proc. Natl. Acad. Sci. USA* **1982**, *79*, 5485-5489.
4. Ebert, R. F.; Bell, W. R. Assay of Human Fibrinopeptides by High-Performance Liquid Chromatography. *Anal. Biochem.* **1985**, *148*, 70-78.
5. Voet, D.; Voet, J. G. *Biochemistry*; John Wiley & Sons: New York, 1995.
6. Nelson, D. L.; Cox, M. M., Eds. In *Lehninger Principles of Biochemistry*; W. H. Freeman: New York, 2004.
7. Carroll, J.; Ding, S.; Fearnley, I. M.; Walker, J. E. Post-translational Modifications near the Quinone Binding Site of Mammalian Complex I. *J. Biol. Chem.* **2013**, *288*, 24799-24808.
8. Guo, X.; Trudgian, D. C.; Lemoff, A.; Yadavalli, S.; Mirzaei, H. Confetti: A Multi-protease Map of the HeLa Proteome for Comprehensive Proteomics. *Mol. Cell Proteomics* **2014**, *13*, 1573-1584.
9. O'Brien, J. A.; Taylor, J. A.; Bellamy, A. R. Probing the Structure of Rotavirus NSP4: a Short Sequence at the Extreme C Terminus Mediates Binding to the Inner Capsid Particle. *J. Virol.* **2000**, *74*, 5388-5394.
10. Gupta, N.; Hixson, K. K.; Culley, D. E.; Smith, R. D.; Pevzner, P. A. Analyzing Protease Specificity and Detecting in Vivo Proteolytic Events Using Tandem Mass Spectrometry. *Proteomics* **2010**, *10*, 2833-2844.
11. Jai-nhuknan, J.; Cassady, C. J. Negative Ion Postsource Decay Time-of-Flight Mass Spectrometry of Peptides Containing Acidic Amino Acid Residues. *Anal. Chem.* **1998**, *70*, 5122-5128.
12. Ewing, N. P.; Cassady, C. J. Dissociation of Multiply-charged Negative Ions for Hirudin (54-65), Fibrinopeptide B, and Insulin A (Oxidized). *J. Am. Soc. Mass Spectrom.* **2001**, *12*, 105-116.
13. Vinh, J.; Loyaux, D.; Redeker, V.; Rossier, J. Sequencing Branched Peptides with CID/PSD MALDI-TOF in the Low-picomole Range: Application to the Structural Study of the Posttranslational Polyglycylation of Tubulin. *Anal. Chem.* **1997**, *69*, 3979-3985.

14. Lapko, V. N.; Jiang, X. Y.; Smith, D. L.; Song, P. S. Posttranslational Modification of Oat Phytochrome A: Phosphorylation of a Specific Serine in a Multiple Serine Cluster. *Biochemistry* **1997**, *36*, 10595-10599.
15. Yagami, T.; Kitagawa, K.; Futaki, S. Liquid Secondary-ion Mass Spectrometry of Peptides Containing Multiple Tyrosine-O-sulfates. *Rapid Commun. Mass Spectrom.* **1995**, *9*, 1335-1341.
16. Ishihama, Y.; Wei, F. Y.; Aoshima, K.; Sato, T.; Kuromitsu, J.; Oda, Y. Enhancement of the Efficiency of Phosphoproteomic Identification by Removing Phosphates after Phosphopeptide Enrichment. *J. Proteome Res.* **2007**, *6*, 1139-1144.
17. Marcantonio, M.; Trost, M.; Courcelles, M.; Desjardins, M.; Thibault, P. Combined Enzymatic and Data Mining Approaches for Comprehensive Phosphoproteome Analyses: Application to Cell Signaling Events of Interferon-gamma-stimulated Macrophages. *Mol. Cell. Proteomics* **2008**, *7*, 645-660.
18. Svoboda, M.; Meister, W.; Kitas, E. A.; Vetter, W. The Influence of Strongly Acidic Groups on the Protonation of Peptides in Electrospray MS. *J. Mass Spectrom.* **1997**, *32*, 1117-1123.
19. Speetjens, J. K.; Parand, A.; Crowder, M. W.; Vincent, J. B.; Woski, S. A. Low-molecular Weight Chromium-binding Substance and Biomimetic  $[\text{Cr}_3\text{O}(\text{O}_2\text{CH}_2\text{CH}_3)_6(\text{H}_2\text{O})_3]^+$  Do Not Cleave DNA Under Physiologically-relevant Conditions. *Polyhedron* **1999**, *18*, 1821, 2617-2624.
20. Chen, Y.; Watson, H. M.; Gao, J.; Sinha, S. H.; Cassady, C. J.; Vincent, J. B. Characterization of the Organic Component of Low-Molecular-Weight Chromium-Binding Substance and Its Binding of Chromium. *J. Nutr.* **2011**, *141*, 1225-1232.
21. Syka, J. E. P.; Coon, J. J.; Schroeder, M. J.; Shabanowitz, J.; Hunt, D. F. Peptide and Protein Sequence Analysis by Electron Transfer Dissociation Mass Spectrometry. *Proc. Natl. Acad. Sci. USA* **2004**, *101*, 9528-9533.
22. Zubarev, R. A.; Kruger, N. A.; Fridriksson, E. K.; Lewis, M. A.; Horn, D. M.; Carpenter, B. K.; McLafferty, F. W. Electron Capture Dissociation of Gaseous Multiply-charged Proteins is Favored at Disulfide Bonds and Other Sites of High Hydrogen Atom Affinity. *J. Am. Chem. Soc.* **1999**, *121*, 2857-2862.
23. Axelsson, J.; Palmblad, M.; Håkansson, K.; Håkansson, P. Electron Capture Dissociation of Substance P Using a Commercially Available Fourier Transform Ion Cyclotron Resonance Mass Spectrometer. *Rapid Commun. Mass Spectrom.* **1999**, *13*, 474-477.
24. Robinson, N. E.; Robinson, A. B. *Molecular Clocks: Deamidation of Asparaginyl and Glutaminyl Residues in Peptides and Proteins*; Althouse Press: Cave Junction, OR, 2004.



25. Wright, H. T. Nonenzymatic Deamidation of Asparaginy and Glutaminy Residues in Proteins. *Crit. Rev. Biochem. Mol. Biol.* **1991**, *26*, 1-52.
26. Chan, W. Y. K.; Chan, T. W. D.; O'Connor, P. B. Electron Transfer Dissociation with Supplemental Activation to Differentiate Aspartic and Isoaspartic Residues in Doubly Charged Peptide Cations. *J. Am. Soc. Mass Spectrom.* **2010**, *21*, 1012-1015.
27. Schindler, P.; Müller, D.; Märki, W.; Grossenbacher, H.; Richter, W. J. Characterization of a  $\beta$ -Asp33 Isoform of Recombinant Hirudin Sequence Variant 1 by Low-energy Collision-induced Dissociation. *J. Mass Spectrom.* **1996**, *31*, 967-974.
28. Ni, W.; Dai, S.; Karger, B. L.; Zhou, Z. S. Analysis of Isoaspartic Acid by Selective Proteolysis with Asp-N and Electron Transfer Dissociation Mass Spectrometry. *Anal. Chem.* **2010**, *82*, 7485-7491.
29. Sargaeva, N. P.; Lin, C.; O'Connor, P. B. Differentiating N-Terminal Aspartic and Isoaspartic Acid Residues in Peptides. *Anal. Chem.* **2011**, *83*, 6675-6682.
30. O'Connor, P. B.; Cournoyer, J. J.; Pitteri, S. J.; Chrisman, P. A.; McLuckey, S. A. Differentiation of Aspartic and Isoaspartic Acids Using Electron Transfer Dissociation. *J. Am. Soc. Mass Spectrom.* **2006**, *17*, 15-19.
31. Cournoyer, J. J.; Lin, C.; O'Connor, P. B. Detecting Deamidation Products in Proteins by Electron Capture Dissociation. *Anal. Chem.* **2006**, *78*, 1264-1271.
32. Li, X.; Lin, C.; O'Connor, P. B. Glutamine Deamidation: Differentiation of Glutamic Acid and gamma-Glutamic Acid in Peptides by Electron Capture Dissociation. *Anal. Chem.* **2010**, *82*, 3606-3615.
33. Creese, A. J.; Cooper, H. J. The Effect of Phosphorylation on the Electron Capture Dissociation of Peptide Ions. *J. Am. Soc. Mass Spectrom.* **2008**, *19*, 1263-1274.
34. Cooper, H. J.; Hudgkins, R. R.; Hakansson, K.; Marshall, A. G. Characterization of Amino Acid Side Chain Losses in Electron Capture Dissociation. *J. Am. Soc. Mass Spectrom.* **2002**, *13*, 241-249.
35. Savitski, M. M.; Nielsen, M. L.; Zubarev, R. A. Side-chain Losses in Electron Capture Dissociation to Improve Peptide Identification. *Anal. Chem.* **2007**, *79*, 2296-2302.
36. Xia, Q.; Lee, M.; Rose, C.; Marsh, A.; Hubler, S.; Wenger, C.; Coon, J. Characterization and Diagnostic Value of Amino Acid Side Chain Neutral Losses Following Electron-Transfer Dissociation. *J. Am. Soc. Mass Spectrom.* **2011**, *22*, 255-264.
37. Tsaprailis, G.; Nair, H.; Somogyi, A.; Wysocki, V. H.; Zhong, W.; Futrell, J. H.; Summerfield, S. G.; Gaskell, S. J. Influence of Secondary Structure on the Fragmentation of Protonated Peptides. *J. Am. Chem. Soc.* **1999**, *121*, 5142-5154.

38. Yu, W.; Vath, J. E.; Huberty, M. C.; Martin, S. A. Identification of the Facile Gas-Phase Cleavage of the Asp-Pro and Asp-Xxx Peptide Bonds in Matrix-Assisted Laser Desorption Time-of-Flight Mass Spectrometry. *Anal. Chem.* **1993**, *65*, 3015-3023.
39. Qin, J.; Chait, B. Preferential Fragmentation of Protonated Gas-Phase Peptide Ions Adjacent to Acidic Amino Acid Residues. *J. Am. Chem. Soc.* **1995**, *117*, 5411-5412.
40. Paizs, B.; Suhai, S. Fragmentation Pathways of Protonated Peptides. *Mass Spectrom. Rev.* **2005**, *24*, 508-548.
41. Liu, H.; Håkansson, K. Abundant b-Type Ions Produced in Electron Capture Dissociation of Peptides Without Basic Amino Acid Residues. *J. Am. Soc. Mass Spectrom.* **2007**, *18*, 2007-2013.
42. Chan, W. C.; White, P. D. *Fmoc Solid Phase Peptide Synthesis A Practical Approach*; Oxford University Press Inc., New York: 2000.
43. Wada, O.; Wu, G. Y.; Yamamoto, A.; Manabe, S.; Ono, T. Purification and Chromium-Excretory Function of Low-Molecular-Weight, Chromium-Binding Substances from Dog Liver. *Environ. Res.* **1983**, *32*, 228-239.
44. Bakken, V.; Helgaker, T.; Uggerud, E. Models of Fragmentations Induced by Electron Attachment to Protonated Peptides. *Eur. J. Mass Spectrom.* **2004**, *10*, 625-638.
45. Cooper, H. J. Investigation of the Presence of b Ions in Electron Capture Dissociation Mass Spectra. *J. Am. Soc. Mass Spectrom.* **2005**, *16*, 1932-1940.

## CHAPTER 7: CONCLUDING REMARKS

Electron transfer dissociation (ETD) is becoming an important analytical technique in the Human Proteome Project. ETD produces c- and z-type fragment ions by random backbone N-C $\alpha$  bond cleavages and is a very promising dissociation technique in peptide and protein sequencing, but still has limitations. A big problem for ETD is that only basic peptides can be studied. Non-basic peptides usually produce only singly protonated precursor ions by electrospray ionization (ESI) and addition of an electron to the precursor ion in ETD makes the charge neutral, which cannot be detected by mass spectrometry. The other problem is that the intensity of doubly protonated precursor ions,  $[M+2H]^{2+}$ , may be too low to be studied in ETD. This dissertation is focused on the mechanism of ETD for basic peptides, the supercharging of the non-basic peptides, and the fragmentation pathways and mechanisms for the dissociation of non-basic peptides by ETD.

The effects of the position and identity of basic residues on ETD were explored using a series of model peptides. ETD on  $[M+2H]^{2+}$  produces almost exclusively c''- and z'-ions. As the basic residue position is changed from the N-terminus to the C-terminus, fewer c-ions and more z-ions are formed. Almost all of the ETD product ions contain the basic residue. For peptides containing histidine residues, an electron transfer without dissociation ion product,  $[M+2H+e]^+$ , also forms; in contrast, peptides containing arginine and lysine residues exhibit very little electron transfer without dissociation. All peptides studied show a side chain loss of NH<sub>3</sub> (17 Da), while arginine has additional side chain losses of CH<sub>5</sub>N<sub>3</sub> (59 Da) and CH<sub>3</sub>N<sub>2</sub> $\cdot$  (43 Da). In ETD, enhanced fragmentation occurs on the C-terminal side of basic residues. In addition, an

enhanced formation of  $c_{n-1}^{+}$  ion is observed, where  $n$  is the number of residues in the peptide. The heptapeptides with N-terminal basic residues contain the entire  $c_{1-6}^{+}$  product ion distribution. ETD is particularly useful for sequencing peptides that have a basic residue at the N-terminus.

The addition of Cr(III) nitrate to solutions of peptides with seven or more residues greatly increases the formation of  $[M+2H]^{2+}$  by ESI. The test compound heptaalanine has only one highly basic site (the N-terminal amino group) and undergoes almost exclusive single protonation using standard solvents. When Cr(III) is added to the solution, abundant  $[M+2H]^{2+}$  forms, which must involve protonation of the peptide backbone. Salts of Al(III), Mn(II), Fe(III), Fe(II), Cu(II), Zn (II), Rh(III), La(III), Ce(IV), and Eu(III) were also studied. While several metal ions slightly enhance protonation, Cr(III) has by far the greatest ability to generate  $[M+2H]^{2+}$ . Cr(III) does not supercharge peptide methyl esters, which suggests that the mechanism involves interaction of Cr(III) with a carboxylic acid group on the peptide. Other significant factors include the high acidity of hexaaquochromium(III) and the resistance of Cr(III) to reduction. Nitrate salts enhance protonation more than chloride salts and a molar ratio of 10:1 Cr(III):peptide produces the most intense  $[M+2H]^{2+}$ . Cr(III) also supercharges numerous other small peptides, including highly acidic species. For basic peptides, Cr(III) increases the charge state distribution (2+ versus 1+) and causes the number of peptide molecules being protonated to double. However, Cr(III) does not supercharge the protein cytochrome c. The use of Cr(III) to enhance  $[M+2H]^{2+}$  intensity may prove useful in tandem mass spectrometry because of the resulting overall increase in signal-to-noise ratio, the fact that 2+ ions generally dissociate more readily than 1+ ions, and the ability to produce  $[M+2H]^{2+}$  precursors for electron-based dissociation techniques. A future application is that Cr(III) can be used in a mixture of biological peptides to enhance the ion intensity of multiply protonated ions so that ETD

experiments can be performed. With the use of Cr(III) to supercharge, ETD will not be limited to tryptic peptides in protein sequencing. Cr(III) could also be added to the mobile phase of liquid chromatography (LC) to enhance the intensity of multiply protonated ions to perform ETD.

Electron transfer dissociation (ETD) has been performed on doubly protonated ions from a series of small neutral peptides with alkyl side chains. The peptides produce b- and c-ion series, which is different from basic peptides that mainly produce c- and z-ion series. The addition of Cr(III) nitrate to the peptide solutions was used to generate  $[M+2H]^{2+}$  by ESI. The b-ions produced in ETD of neutral peptides are also found in collision-induced dissociation (CID) experiments. The MS/MS/MS spectra of b-ions in ETD of  $[M+2H]^{2+}$  and CID of  $[M+H]^+$  are very similar. These results indicate the b-ions produced in ETD have the same structure as b-ions produced by CID. One explanation is that the first hydrogen ion attaches to the N-terminus and the second hydrogen ion attaches to the amide nitrogen backbone to produce the b-ions. Another explanation is that there is a  $H\bullet$  loss after  $[M+2H]^{2+}$  to produce vibrationally excited  $[M+H]^+$ . The singly protonated ion undergoes mobile proton pathways to produce b-ions similar to CID. When peptide size increases, there are fewer b-ions and more c-ions produced. With the increase of the chain length of a peptide, the internal solvation of the charge bearing group and the increase of internal hydrogen bonds may lead to a decrease in  $H\bullet$  loss. The lower abundance of  $[M+H]^+$  produces fewer b-ions and the higher abundance of  $[M+2H]^{2+}$  produces more c-ions. Peptide size can change the fragmentation pathways from a vibrational excitation to a radical-initiated process. The identity of the alanine, glycine, valine, leucine, and isoleucine residues has minimal effect on ETD, which is due to their similar side chain structures and basicities.

The effects of the position and identity of acidic residues on ETD of peptides were explored using a series of model peptides. The acidic residues involved were aspartic acid and

glutamic acid. Cr(III) nitrate was added to the peptide solutions to produce  $[M+2H]^{2+}$  by ESI. This dissertation is the first report of the use of ETD to study acidic peptides containing no residues with basic side chains. ETD on acidic peptides mainly produces members of the b-, c-, and z-ion series. The c- and z-ions formed are also found in the spectra of basic peptides, while b-ions occur in the spectra of neutral peptides. The location of the acidic residue along the peptide chain has no effect in ETD and the identity of the acidic residue has minimal effect. The ETD product ions from acidic peptides do not always contain an acidic residue. No preferential cleavage is found adjacent to acidic residues in ETD, which is different from the acidic residue effect in CID. Glutamic acid and aspartic acid both exhibit a  $\bullet\text{CH}_2\text{COOH}$  (59 Da) loss from their side chain. For highly acidic peptides such as EEEEEEE (E7), the ETD product ions are primarily members of the c and z-ion series. This suggests that the b-ions found in peptides with one acidic residue and multiple alanine (A) residues result from the presence of the neutral residues. Radical sites on the carboxylic acid side chains of aspartic acid and glutamic acid residues may take part in the mechanism. Suggested further research is methyl esterification of the carboxylate groups of the side chains of aspartic acid and glutamic acid to probe the mechanism. In addition, longer chain peptides such as AAAAAAEEEEEEEE (A7E7) can be used to test if the size of acidic peptide could affect the fragmentation.

In general, ETD breaks the N-C $\alpha$  bond to produce c- and z-ion series, which is complementary to CID cleavages at C-N amide bonds to produce b- and y-ion series. Peptide sequencing using CID and ETD together can greatly facilitate sequencing. A basic residue at the N-terminus is especially useful in peptide and protein sequencing as a complete series of c"-ions are made. The characteristic side chain loss of 59 Da and 43 Da can be used to identify arginine residues in sequencing. The extended use of ETD on neutral peptides produces b-, c- and z-ion

series with the ion series formed being dependent on the lengths of peptide chain. When the length of peptide chain increases, the product ions are mainly c- and z-ion series. ETD on acidic peptides mainly produces b-, c- and z-ion series depends on the acidity of peptides. For highly acidic peptides, c- and z-ions are predominant ions, while for peptides with one or two acidic residues, the major product ions are b- and c-ions. The use of ETD on neutral and acidic peptides provides novel tools to analyze non-basic peptides.

In this dissertation research, all the tested peptides are synthesized simple peptides. However, most of the biological peptides in nature are a combination of basic, neutral, and acidic residues. In addition, the side chains of peptides or proteins may be modified and no longer simple alkyl side chains in post-translational modifications (PTM). The future work can be the addition of Cr(III) to digested biological peptide or protein mixtures to perform ETD on these species and investigate the fragmentation. An uncertainty is that adding Cr(III) to the modified peptides or proteins may result in interactions with the modified side chains. Although ETD of peptides or proteins with PTM has widely been reported, these peptides or proteins are limited to at least doubly protonated in ESI. ETD of the peptides or proteins with PTM that is hard to be doubly protonated in ESI has not been reported. The fragmentation mechanism of these biological peptides in ETD needs to be investigated. The real biological peptides and proteins are much more complicated than custom synthesized peptides, but the works in this dissertation gives a promising start of extending ETD on non-basic peptides.